FINAL REPORT

Validation of Stable Isotope Ratio Analysis to Document the Biodegradation and Natural Attenuation of RDX

ESTCP Project ER-201208

APRIL 2018

Dr. Paul Hatzinger
Dr. Mark Fuller
Aptim Federal Services LLC

Dr. Neil C. Sturchio
University of Delaware

Dr. J.K. Böhlke
U.S. Geological Survey

Distribution Statement A
This document has been cleared for public release

Page Intentionally Left Blank

This report was prepared under contract to the Department of Defense Environmental Security Technology Certification Program (ESTCP). The publication of this report does not indicate endorsement by the Department of Defense, nor should the contents be construed as reflecting the official policy or position of the Department of Defense. Reference herein to any specific commercial product, process, or service by trade name, trademark, manufacturer, or otherwise, does not necessarily constitute or imply its endorsement, recommendation, or favoring by the Department of Defense.

Page Intentionally Left Blank

REPORT DOCUMENTATION PAGE	Form Approved OMB No. 0704-0188

The public reporting burden for this collection of information is estimated to average 1 hour per response, including the time for reviewing instructions, searching existing data sources, gathering and maintaining the data needed, and completing and reviewing the collection of information. Send comments regarding this burden estimate or any other aspect of this collection of information, including suggestions for reducing the burden, to the Department of Defense, Executive Services and Communications Directorate (0704-0188). Respondents should be aware that notwithstanding any other provision of law, no person shall be subject to any penalty for failing to comply with a collection of information if it does not display a currently valid OMB control number.
PLEASE DO NOT RETURN YOUR FORM TO THE ABOVE ORGANIZATION.

1. REPORT DATE *(DD-MM-YYYY)*	2. REPORT TYPE	3. DATES COVERED *(From - To)*
04-03-2018	ESTCP Final Report	April 2012 - March 2018

4. TITLE AND SUBTITLE	5a. CONTRACT NUMBER
Validation of Stable Isotope Ratio Analysis to Document the Biodegradation and Natural Attenuation of RDX	W912-HQ-12-C-0019
	5b. GRANT NUMBER: NA
	5c. PROGRAM ELEMENT NUMBER: NA
6. AUTHOR(S) Hatzinger, Paul B.(APTIM) Fuller, Mark E. (APTIM) Sturchio, Neil C. (Univ. of Delaware) Böhlke, J.K. (USGS)	5d. PROJECT NUMBER: ER-201208
	5e. TASK NUMBER: NA
	5f. WORK UNIT NUMBER: NA

7. PERFORMING ORGANIZATION NAME(S) AND ADDRESS(ES)	8. PERFORMING ORGANIZATION REPORT NUMBER
APTIM Federal Services 17 Princess Road Lawrenceville, NJ 08648	ER-201208
9. SPONSORING/MONITORING AGENCY NAME(S) AND ADDRESS(ES)	10. SPONSOR/MONITOR'S ACRONYM(S): ESTCP
Environmental Security Technology Certification Program 4800 Mark Center Drive, Suite 17D08 Alexandria, VA 22350-3605	11. SPONSOR/MONITOR'S REPORT NUMBER(S): ER-201208

12. DISTRIBUTION/AVAILABILITY STATEMENT

Distribution Statement A: Approved for Public Release, Distribution is Unlimited

13. SUPPLEMENTARY NOTES

None

14. ABSTRACT

The objective of this project was to validate a stable isotope method that can be utilized by DoD to quantify aerobic and anaerobic biodegradation of RDX at field sites. Combined analysis of $\delta^{15}N$ and $\delta^{13}C$ in RDX was used to clearly document anaerobic RDX biodegradation in groundwater at a DOD range where a biobarrier was installed to promote this process. Documenting aerobic RDX biodegradation in the field proved to be more difficult because the expected fractionation of N is low (~ 2.4 ‰ based on pure culture studies) and no fractionation of C is expected. $\delta^{15}N$ measurements provided supporting data for aerobic RDX biodegradation in a push-pull test conducted at a DoD site, but results from other similar tests were inconclusive. In support of the field studies with RDX, a column method was developed to collect and concentrate RDX from wells with low concentrations for isotope analysis, and the $\delta^{15}N$ and $\delta^{18}O$ values in NO_2^- and NO_3^- generated from RDX during biodegradation were assesed as a potential second isotopic measure of RDX biodegradation.

15. SUBJECT TERMS

RDX, munitions, nitrate, nitrite, stable isotope, carbon-13, nitrogen-15, oxygen-17, groundwater, CSIA, MNA

16. SECURITY CLASSIFICATION OF:			17. LIMITATION OF ABSTRACT	18. NUMBER OF PAGES	19a. NAME OF RESPONSIBLE PERSON
a. REPORT	b. ABSTRACT	c. THIS PAGE			Dr. Paul B. Hatzinger
U	U	U	UU	145	19b. TELEPHONE NUMBER *(Include area code)*: 609-895-5356

Standard Form 298 (Rev. 8/98)
Prescribed by ANSI Std. Z39.18

Page Intentionally Left Blank

FINAL REPORT
Project: ER-201208

TABLE OF CONTENTS

Page

EXECUTIVE SUMMARY ES-1
1.0 INTRODUCTION 1
1.1 BACKGROUND 1
1.2 OBJECTIVES OF THE DEMONSTRATION 2
1.3 REGULATORY DRIVERS 2
2.0 TECHNOLOGY 3
2.1 TECHNOLOGY DESCRIPTION AND DEVELOPMENT 3
2.1.1 Compound-specific stable isotope analysis (CSIA) 3
2.1.2 Method for analysis of C and N stable isotopes in RDX 3
2.1.3 Isotopic fractionation of N in RDX during biodegradation 3
2.1.4 Isotopic fractionation of C in RDX during biodegradation 5
2.1.5 Isotopic analysis of N and O in RDX degradation products NO_3^- and NO_2^- 5
2.1.6 Implications for nitrate detected in groundwater at RDX contaminated sites. 6
2.1.7 Conclusions from pure culture studies 6
2.1.8 Overview of research approach 7
2.2 ADVANTAGES AND LIMITATIONS OF THE TECHNOLOGY 7
3.0 PERFORMANCE OBJECTIVES 17
3.1 MEASURE $\varepsilon^{15}N$ FOR RDX *IN SITU* UNDER AEROBIC CONDITIONS 18
3.1.1 Data requirements for measuring $\varepsilon^{15}N$ for RDX in situ under aerobic conditions 18
3.1.2 Success criteria for measuring $\varepsilon^{15}N$ for RDX in situ under aerobic conditions 18
3.2 MEASURE $\varepsilon^{15}N$ AND $\varepsilon^{13}C$ FOR RDX *IN SITU* UNDER ANAEROBIC CONDITIONS 18
3.2.1 Data requirements for measuring $\varepsilon^{15}N$ and $\varepsilon^{13}C$ for RDX for RDX in situ under anaerobic conditions 18
3.2.2 Success criteria for measuring $\varepsilon^{15}N$ and $\varepsilon^{15}C$ for RDX in situ under anaerobic conditions 18
3.3 MEASURE $\delta^{15}N$ AND/OR $\delta^{18}O$ IN NO_3^- OR NO_2^- *IN SITU* UNDER AEROBIC CONDITIONS 19
3.3.1 Data requirements for measuring $\delta^{15}N$ and $\delta^{18}O$ in NO_3^- or NO_2^- in situ under aerobic conditions 19
3.3.2 Success criteria for measuring $\delta^{15}N$ and $\delta^{18}O$ in NO_3^- or NO_2^- under aerobic conditions 19
3.4 VERIFICATION OF COLUMN COLLECTION METHOD FOR RDX STABLE ISOTOPE ANALYSIS 19

TABLE OF CONTENTS (Continued)

Page

3.4.1 Data requirements for verifying the column collection method for RDX stable isotope analysis 19
3.4.2 3.4.2 Success criteria for verifying the column collection method for RDX stable isotope analysis 19
3.5 EFFICIENT SAMPLE COLLECTION 20
3.5.1 Data requirements for efficient sample collection. 20
3.5.2 Success criteria for efficient sample collection. 20
4.0 SITE DESCRIPTION 21
4.1 SITE 1: NAVAL SURFACE WARFARE CENTER, DAHLGREN, VA 22
4.1.1 Demonstration site geology and hydrogeology 22
4.1.2 Site characterization during ESTCP ER-201028 28
4.2 SITE 2: UMATILLA CHEMICAL DEPOT 40
4.2.1 UMCD site characteristics 41
4.2.2 In Situ bioremediation study at UMCD 42
5.0 TEST DESIGN 47
5.1 CONCEPTUAL EXPERIMENTAL DESIGN 47
5.2 BASELINE CHARACTERIZATION ACTIVITIES 47
5.2.1 C and N stable isotope values in RDX from different sources 47
5.2.2 Dahlgren NSWC biobarrier – column study 48
5.2.3 UMCD Field Study 59
5.3 DESIGN AND LAYOUT OF TECHNOLOGY COMPONENTS 63
5.4 FIELD TESTING 63
5.4.1 Sample collection in the field using SPE columns 64
5.4.2 Comparison of stable isotope values between field and laboratory SPE samples 65
5.4.3 Development and testing of an SPE column for field application 66
5.4.4 Dahlgren NSWC – Natural attenuation testing 66
5.4.5 Dahlgren NSWC – Isotopic fractionation during anaerobic RDX biodegradation 69
5.4.6 UMCD push pull tests 71
5.5 SAMPLING PLAN 73
5.5.1 Dahlgren NSWC sampling plan 73
5.5.2 UMCD sampling plan 76
5.5.3 Compound specific isotope analysis of RDX 78
5.5.4 Compound specific isotope analysis of NO3- 80
5.6 DATA ANALYSIS AND SAMPLING RESULTS 80
5.6.1 Determination and analysis of isotope fractionation factors 80
5.6.2 Corrections to RDX and isotope data based on mixing with background RDX 81
5.6.3 Dahlgren NSWC - Natural attenuation sampling 83
5.6.4 Dahlgren NSWC - Biobarrier sampling 88
5.6.5 UMCD - Push-pull test sampling 92
6.0 PERFORMANCE ASSESSMENT 101

TABLE OF CONTENTS (Continued)

Page

6.1 MEASURE $\varepsilon^{15}N$ FOR RDX *IN SITU* UNDER AEROBIC CONDITIONS 101
6.1.1 Dahlgren NSWC 101
6.1.2 UMCD 101
6.2 MEASURE $\varepsilon^{15}N$ AND $\varepsilon^{13}C$ FOR RDX *IN SITU* UNDER ANAEROBIC CONDITIONS 102
6.2.1 Dahlgren NSWC 102
6.2.2 UMCD 103
6.3 MEASURE $\delta^{15}N$ AND/OR $\delta^{18}O$ IN NO_3^- OR NO_2^- *IN SITU* UNDER AEROBIC CONDITIONS 103
6.4 VERIFICATION OF COLUMN COLLECTION METHOD FOR RDX STABLE ISOTOPE ANALYSIS 104
6.5 EFFICIENT SAMPLE COLLECTION 104
7.0 COST ASSESSMENT 105
8.0 IMPLEMENTATION ISSUES 107
8.1 TECHNOLOGY AVAILABILITY 107
8.2 APPROPRIATE APPLICATION OF THE TECHNOLOGY AT DOD SITES 107
8.3 INTERPRETATION OF CSIA DATA 108
9.0 REFERENCES 109
APPENDIX A POINTS OF CONTACT A-1
APPENDIX B SELECTED DATA FOR NITRATE AND NITRITE ISOTOPIC STUDIES B-1

LIST OF FIGURES

Page

Figure 2.1. Biodegradation Pathways for RDX. 9

Figure 2.2. Isotopic Fractionation of $^{12}C/^{13}C$ and $^{14}N/^{15}N$ during Biodegradation of RDX by Different Pathways..... 11

Figure 2.3. Isotopic Fractionation of N by Two Aerobic RDX Degraders. 12

Figure 2.4. Production ofNnitrite (NO_2^-) during Aerobic Biodegradation of RDX by *Rhodococcus* Strain 11Y. 12

Figure 2.5. $\delta^{15}N$ and $\delta^{18}O$ in NO_3^- Collected from RDX-contaminated Wells (Alpha/Bravo and Shaver) Compared to Uncontaminated Wells (Deep Confined Aquifer). 13

Figure 2.6. Concentrations of NO_2^- (closed symbols) during Aerobic Degradation of RDX by *Rhodococcus* DN22 and *R. rhodocrous* 11Y and Anaerobic RDX Degradation by *P. putida* II-B and *P. fluorescens* I-C. 14

Figure 2.7. Comparison of $\delta^{15}N$ Values of RDX (closed symbols) and NO_2^- (open symbols) during (A) Aerobic RDX Degradation by *Rhodococcus* DN22 and *R. rhodocrous* 11Y and (B) Anaerobic RDX Degradation by *P. putida* II-B and *P. fluorescens* I-C. 15

Figure 4.1. Location of the Dahlgren NSWC Site (URS, 2010). 23

Figure 4.2. Map Showing the Main Areas of Dahlgren NSWC (URS, 2007). 24

Figure 4.3. Map showing the Churchill Range of Dahlgren NSWC. 25

Figure 4.4. Schematic of the Geologic and Hydrogeologic Units of the EEA (Bell, 1996). .. 26

Figure 4.5. Map Showing the Well Locations on the Churchill Range of Dahlgren NSWC circa 2007 (modified from URS, 2007). 27

Figure 4.6. Sampling Locations for Preliminary Site Assessment in the Plume Emanating from the Fast Cookoff Area. 30

Figure 4.7. Map Showing the Well and Piezometer Locations on the Churchill Range of Dahlgren NSWC (November 2011)..... 31

Figure 4.8. Potentiometric Surface Map of the Churchill Range in May 2011. 32

Figure 4.9. Potentiometric Surface Map of the Churchill Range in October 2011. 32

Figure 4.10. Dissolved Oxygen Contours in the Southeast Area of the Churchill Range in October 2011..... 34

Figure 4.11. pH Contours in the Southeast Area of the Churchill Range in October 2011. 35

Figure 4.12. RDX, HMX and Perchlorate Data from Piezometers Installed During the May 2011 Site Investigation. 37

Figure 4.13. Plume Map for RDX in the Southeast Area of the Churchill Range. 38

Figure 4.14. Plume Map for HMX in the Southeast Area of the Churchill Range. 39

LIST OF FIGURES

Page

Figure 4.15. Schematic of Biobarrier Demonstration Plot Layout..... 40

Figure 4.16. Map Showing the Umatilla Ordnance Depot and Boardman Bombing Range in Northeastern OR. 42

Figure 4.17. Photo of Ammunition Igloos at UMCD (circa 2006). 43

Figure 4.18. RDX Plume Map at UMCD as of October 2008 (73). 44

Figure 4.19. Top: Location of the Push-pull Test Plots on UMCD and Inset of test plot configuration. Bottom: A closer view of the wells within the test plot area. 45

Figure 5.1. Column Design for Laboratory Treatability Testing. 52

Figure 5.2. Perchlorate in the Influent Groundwater and the Effluent of the Three Flow-through Columns..... 53

Figure 5.3. HMX in the Influent Groundwater and the Effluent of the Three Flow-through Columns. 53

Figure 5.4. RDX in the Influent Groundwater and the Effluent of the Three Flow-through Columns. 54

Figure 5.5. MNX, DNX, and TNX in the Influent Groundwater and the Effluent of the Three Flow-through Columns. 55

Figure 5.6. Nitrate and Sulfate in the Influent Groundwater and the Effluent of the Three Flow-through Columns. 56

Figure 5.7. Profile of One Geoprobe Core (7.5 to 10 ft, saturated zone) from the Dahlgren Site Showing Significant Amounts of Iron Minerals (orange). 57

Figure 5.8. Profiles of RDX and Perchlorate as a Function of Distance from the Influent End of the Columns. 58

Figure 5.9. Fractionation of N in RDX as a Function of Fraction Remaining (ln f), which Decreases with Distance from Influent End of Column (Col 2)..... 59

Figure 5.10. RDX Concentrations in UMCD Microcosms in Both Uninoculated (control) and Inoculated with Strains KTR9 Kan^R, RHA1 pGKT2, and *P. fluorescens* I-C..... 60

Figure 5.11. Breakthrough Curves for Bromide, Cells, and RDX for Column Experiment with UMCD Site Samples..... 62

Figure 5.12. Fractionation of C (left panel) and N (right panel) isotopes by *Gordonia* sp. KTR9 in A) liquid culture and B) column experiments. 63

Figure 5.13. Design and Photograph of Field Sampling Column for RDX Isotopes..... 66

Figure 5.14. Plume Map for RDX in the Southeast Area of the Churchill Range with Locations Demarcated (yellow well markers) for the First Round of Stable Isotope Sampling. 68

LIST OF FIGURES

Page

Figure 5.15. Collection of RDX for Stable Isotope Analysis on a Small SPE Column at the Dahlgren Site. 69

Figure 5.16. Map (top) and Layout (bottom) of the Dahlgren NSWC Passive *in situ* Emulsified Oil Biobarrier. 70

Figure 5.17. RDX Concentrations Along the Centerline of the Biobarrier Monitoring Well Network. 71

Figure 5.18. Well layout for UMCD push-pull tests. 72

Figure 5.19. Overview of Field Push-pull Test in Bioaugmentation and Biostimulation Test Plots. 72

Figure 5.20. Example Groundwater Parameter Stabilization Form for Low Flow Sampling... 74

Figure 5.21. $\delta^{15}N$ isotope Data from RDX Extracted from Dahlgren NSWC Groundwater in the Laboratory and the Field. 86

Figure 5.22. Plot of $\delta^{15}N$ (RDX) vs RDX Concentration Across the Churchill Range at Dahlgren NSWC. 86

Figure 5.23. Plot of $\delta^{18}O$ vs $\delta^{15}N$ in NO_3^- Across the Churchill Range at Dahlgren NSWC Compared to Common Sources and NO_2^- Generated by Aerobic and Anaerobic RDX Biodegradation. 87

Figure 5.24. RDX Concentrations Along the Centerline of the Biobarrier before (October 2012) and After (June 2013) Oil Injection. 89

Figure 5.25. $\delta^{13}C$ and $\delta^{15}N$ of RDX Collected from Sampled Along the Centerline of the Biobarrier before (October 2012) and after (June 2013) Oil Injection. 90

Figure 5.26. Plot of $\delta^{15}N$ and $\delta^{13}C$ and versus RDX Concentration Expressed as ln (f) for Samples Collected Along the Centerline of the Dahlgren Biobarrier in June 2013. 91

Figure 5.27. RDX Degradation during Aerobic Bioaugmentation (top) and Anaerobic Biostimulation (bottom) Push Pull Testing at UMCD Under the Mixing During Injection Scenario. 93

Figure 5.28. RDX Degradation During Aerobic Bioaugmentation (top) and Anaerobic Biostimulation (bottom) Push Pull Testing at UMCD Under the Mixing during Sampling Scenario. 94

Figure 5.29. Fractionation of ^{15}N During RDX Degradation During Aerobic Bioaugmentation (left) and Anaerobic Biostimulation (right) Push Pull Testing at UMCD Under the Mixing During Injection Scenario. 95

Figure 5.30. Fractionation of ^{15}N During RDX Degradation During Aerobic Bioaugmentation (left) and Anaerobic biostimulation (right) Push Pull Testing at UMCD under the Mixing During Sampling Scenario. 96

LIST OF FIGURES

Page

Figure 5.31. Fractionation of ^{15}N in RDX Degradation During Aerobic Bioaugmentation (top panel) and Anaerobic Biostimulation (bottom panel) Push Pull Testing at UMCD Compared with Pure Culture Data (Mixing during Injection Scenario)..... 97

Figure 5.32. Fractionation of ^{15}N in RDX Degradation During Aerobic Bioaugmentation (top panel) and Anaerobic Biostimulation (bottom panel) Push Pull Testing at UMCD Compared with Pure Culture Data (Mixing During Sampling Scenario)..... 98

LIST OF TABLES

Page

Table 2.1. Summary of Bulk ^{13}C and ^{15}N Fractionation Factors (ε) via Different RDX Degradation Pathways. 10
Table 3.1. Performance Objectives. 17
Table 4.1. Site Selection Criteria. 21
Table 4.2. Initial Water Quality Data from Four Permanent Wells on the Churchill Range. 30
Table 5.1. $\delta^{15}N$ and $\delta^{13}C$ Values of Neat RDX from Different Sources. 48
Table 5.2. Treatment Assignments for the Column Experiment. 49
Table 5.3. Apparent Steady State Degradation Rates of Target Compounds. 50
Table 5.4. Adsorption and Recovery of RDX Using Two Different SPE Media. 64
Table 5.5. Influence of Flow Rate on the Adsorption and Recovery of RDX Using ENVI-Chrom P Media. 64
Table 5.6. Influence of Sorbent Mass on the Adsorption and Recovery of RDX Using ENVI-Chrom P Media. 65
Table 5.7. Comparison of Adsorption and Recovery of RDX from Distilled Water and Groundwater. 65
Table 5.8. Comparison of $\delta^{15}N$ in RDX from a Standard, with that Extracted from Distilled Water or Groundwater via SPE. 65
Table 5.9. Analytical Methods and Total Samples Collected During Field Sampling at Dahlgren NSWC. 75
Table 5.10. UMCD Phase III Push-pull Testing Sampling Preservation. 76
Table 5.11. Phase III Push-pull Testing Sampling Plan. 77
Table 5.12. Natural Attenuation Sampling Data Obtained Using Field and Laboratory Collection of RDX from Groundwater. 85
Table 5.13. $\delta^{13}C$ and $\delta^{15}N$ from RDX in Biobarrier Wells at Dahlgren NSWC. 89
Table 5.14. Compiled ^{13}C and ^{15}N RDX Fractionation Factors from Dahlgren NSWC Biobarrier Sampling. 91
Table 5.15. Compiled ^{15}N Enrichment Factors (ε) from UMCD Push-Pull Testing (Mixing During Injection). 99
Table 5.16. Compiled ^{15}N Enrichment Factors (ε) from UMCD Push-Pull Testing (Mixing During Sampling). 100
Table B.1. Concentrations and Isotopic Compositions of RDX, Nitrate+Nitrite ($NO_{[3+2]}$), and Nitrite (NO_2^-) from Selected RDX Degradation Experiments (data used in Figures 2.6, 2.7, and 5.23). B-1
Table B.2. Concentration and Isotopic Composition of Nitrate in Groundwater Samples from the Dahlgren Site (data used in Figure 5.23). B-2

ACRONYMS AND ABBREVIATIONS

amsl	above mean sea level
bgs	below ground surface
^{13}C	carbon-13
Cl^-	chloride
^{37}Cl	chlorine-37
CCL-3	USEPA Contaminant Candidate List-3
CO_2	carbon dioxide
cm	centimeter
CSIA	compound-specific isotope analysis
d	day
1,2-DNT	1,2-dinitrotoluene
DNAN	2,4-dinitroanisole
2,4-DNT	2,4-dinitrotoluene
2,6-DNT	2,6-dinitrotoluene
DNX	hexahydro-1,3-dinitroso-5-nitro-1,3,5-triazine
DO	dissolved oxygen
DoD	Department of Defense
DPT	direct push technology
EDB	1,2-dibromoethane
EEA	Explosives Experimental Area
EIGL	Environmental Isotope Geochemistry Laboratory
EOD	explosives ordnance disposal
EOS	emulsified oil substrate
EPA	US Environmental Protection Agency
ESTCP	Environmental Security Technology Certification Program
Fe	iron
ft	feet
GAC	granular activated carbon
GC	gas chromatograph
GC-IRMS	gas chromatography-isotope –ratio mass-spectrometry
GPM	gallons per minute
GPS	Groundwater Protection Standard
H	Hour
HAAP	Holsten Army Ammunition Plant
HMX	octahydro-1,3,5,7-tetranitro-1,3,5,7-tetrazocine
HPLC	high performance liquid chromatography

ID	inner diameter
ITRC	Interstate Technology & Regulatory Council
K	hydraulic conductivity
K_{ow}	octanol water partitioning coefficient
KIE	kinetic isotope effect
L	liter
MEDINA	methylenedinitramine
mL	milliliter
MNA	monitored natural attenuation
MNX	hexahydro-1-nitroso-3,5-dinitro-1,3,5-triazine
NBK	Naval Base Kitsap-Bangor, Poulsbo, WA
^{14}N	nitrogen-14
^{15}N	nitrogen-15
NDAB	4-nitro-2,4-diazabutanal
NO_3^-	nitrate
NO_2^-	nitrite
NSWC	Naval Surface Warfare Center
^{18}O	oxygen-18
OB/OD	open burn/open detonation
ORP	oxidation-reduction potential
PI	principal investigator
PZ	piezometer
RDX	hexahydro-1,3,5-trinitro-1,3,5-triazine
RPM	remedial project manager
RTD&E	research, development, test & evaluation
RITS	Remediation Innovative Technology Seminar
SERDP	Strategic Environmental Research & Development Program
SIP	stable isotope probing
SO_4^{2-}	sulfate
Sp. Cond.	specific conductance
SPE	solid phase extraction
TNT	2,4,6-trinitrotoluene
TOC	total organic carbon
TNX	hexahydro-1,3,5-trinitroso-1,3,5-triazine
µg	microgram
UDel	University of Delaware

UIC	University of Illinois at Chicago
UMCD	Umatilla Chemical Depot, Umatilla, OR
USACE	U.S. Army Corps of Engineers
USEPA	United States Environmental Protection Agency
USGS	United States Geological Survey
VOC	volatile organic compound
VPDB	Vienna Peedee Belemnite
‰	per mil
δ	delta; relative differences in isotope ratios
ε	epsilon; isotope fractionation factor

Page Intentionally Left Blank

ACKNOWLEDGEMENTS

The project team includes Drs. Paul B. Hatzinger and Mark E. Fuller (APTIM Federal Services; formerly CB&I), who were responsible for project coordination, field and laboratory experiments, interpretation, and reporting; Dr. Neil C. Sturchio (University of Delaware; formerly at University of Illinois at Chicago), who was responsible for RDX isotopic analyses and interpretation; and Dr. J.K. Böhlke, (U.S. Geological Survey, USGS), who was responsible for nitrate and nitrite isotopic analyses and interpretations. Our research team gratefully acknowledges the financial and technical support provided for this project by the Environmental Security Technology Certification Program (ESTCP). We thank Dr. Andrea Leeson, the Environmental Restoration Program Manager from ESTCP, for her guidance and the support staff at Noblis for their administrative assistance. Major contributors to this work included Janet Hannon (USGS), Linnea Heraty (University of Delaware), Paul Hedman and Charles Condee (APTIM). Views, opinions, and/or findings contained in this report are those of the authors and should not be construed as an official Department of Defense position or decision unless designated by other official documentation. Any use of trade, firm, or product names is for descriptive purposes only and does not imply endorsement by the U.S. Government.

Page Intentionally Left Blank

EXECUTIVE SUMMARY

1.0 INTRODUCTION

Hexahydro-1,3,5-trinitro-1,3,5-triazine (RDX) is a common soil contaminant at current and former military facilities, which impacts groundwater and drinking water at numerous locations. RDX contamination often occurs over expansive areas, making *in situ* or *ex situ* treatment technologies difficult to implement. One potential alternative for managing RDX sites is monitored natural attenuation (MNA), in which contaminantss are controlled by natural processes, including biodegradation. However, one limitation of this approach for RDX is that biodegradation rates can be relatively slow under field conditions, making accurate rate measurements difficult. Compound-specific stable isotope analysis (CSIA) may overcome this limitation, because it allows measurements of slow degradation rates by measuring changes in the ratios of the stable isotopes of present in RDX, specifically the ratios of $^{15}N/^{14}N$ and $^{13}C/^{12}C$.

CSIA relies on the fact that bacteria biodegrade heavier isotopes (e.g., RDX with ^{15}N rather than ^{14}N in its structure) more slowly than lighter ones, due to the greater bond stability of the heavier molecules. As a result, the residual parent molecules become increasingly enriched in the heavier isotopes as biodegradation proceeds. Analyzing stable isotope ratios of RDX along the flow path of a plume, in a single well over time, and/or in contaminated groundwater compared to the contaminant source material can therefore document degradation and natural attenuation *in situ* (as opposed to losses due to dilution, volatilization or other nondestructive mechanisms). In addition, CSIA can provide information on specific reaction mechanisms, particularly if isotopes of multiple elements are evaluated, since the breaking of specific bonds is typically associated with characteristic kinetic isotope effects (KIE), resulting in different isotopic enrichment factors for elements when different degradation pathways occur. Thus, CSIA is a powerful tool to detect, understand, and in some cases, quantify contaminant degradation in the environment.

2.0 OBJECTIVES

The objective of this project was to validate a CSIA method to confirm and constrain rates of aerobic and anaerobic biodegradation of RDX at field sites. If successful, this method can be used by DoD to provide critical data to support MNA as a remedy for RDX in groundwater, and also to confirm the effectiveness of *in situ* enhanced aerobic or anaerobic bioremediation. The stable isotopic composition of NO_3^- and NO_2^- were also measured when these anions co-occurred with RDX, to evaluate whether these potential degradation products from RDX could be used to further demonstrate MNA in the field.

3.0 TECHNOLOGY DESCRIPTION

A CSIA method was developed that utilizes gas-chromatography coupled to isotope-ratio mass-spectrometry (GC-IRMS) to quantify C and N isotope ratios in RDX. In summary, RDX collected from groundwater is concentrated via solid-phase extraction (SPE) either in the field using a

column developed during this project (primarily for wells with low RDX concentrations) or in the laboratory. The RDX is then eluted from the SPE columns into acetonitrile, concentrated, and analyzed for $\delta^{15}N$ and $\delta^{13}C$ in RDX using GC-IRMS. To evaluate the use of CSIA to document anaerobic biodegradation of RDX, $\delta^{15}N$ and $\delta^{13}C$ in RDX were measured in a series of wells along a groundwater flow path at Dahlgren Naval Surface Warfare Center, MD (Dahlgren NSWC) before and after injection of emulsified oil into a biobarrier to promote RDX biodegradation. To evaluate aerobic biodegradation of RDX via CSIA, $\delta^{15}N$ in RDX was measured in groundwater samples collected both (1) during a series of push-pull tests in which a culture capable of aerobically degrading RDX was bioaugmented into an aquifer at Umatilla Chemical Depot, OR (UCMD) along with a low dose of carbon substrate, and (2) from the bulk aerobic aquifer at Dahlgren NSWC along the flowpath of two RDX plumes. $\delta^{13}C$ values were not measured for RDX during these field tests because previous studies with pure cultures indicated no measurable fractionation of C during aerobic RDX biodegradation.

4.0 PERFORMANCE ASSESSMENT

At Dahlgren NSWC, the calculated $\varepsilon\ ^{13}C$ and $\varepsilon\ ^{15}N$ values downgradient of the biobarrier were -2.2 ‰ and -6.8 ‰, respectively. These results compare favorably to pure culture data for strains degrading RDX under anaerobic conditions (which averaged -4.7 ‰ and -9.9 ‰ for C and N respectively, and included individual strains whose ε values were as low as -2.0 ‰ and -5.8 ‰, respectively). The marginal depression in the $\varepsilon\ ^{13}C$ and $\varepsilon^{15}N$ values in the field compared to laboratory studies has been observed during the degradation of other compounds and is commonly attributed to abiotic effects (e.g., dispersion, dilution, incomplete mixing). The isotope fractionation factor ratio ($\varepsilon^{15}N$ / $\varepsilon^{13}C$) for the samples was ~ 3.0, which falls well within the range determined from anaerobic cultures (1.5 to 5.5), and most closely matches that determined for a *Clostridium* sp. at ~ 2.9. The range most likely reflects the differing or mixed anaerobic pathways of RDX degradation. To our knowledge this project represents the first field study clearly showing dual-element CSIA can be used to document RDX biodegradation under anaerobic conditions.

At UMCD, under bulk aerobic conditions, the fractionation of ^{15}N during one of the push-pull tests provided a clear indication of aerobic RDX biodegradation, with an $\varepsilon^{15}N$ value of -1.5 to -1.6 ‰, irrespective of the modeled mixing between the added and background groundwater. Results from the additional tests at the site, however, were less conclusive and varied with the interpretation of the mixing scenario. The relatively small $\varepsilon^{15}N$ value for aerobic RDX biodegradation (averaging -2.4 ‰ for four different pure cultures) made documenting this process more difficult than for anaerobic biodegradation, where $\varepsilon^{15}N$ is much larger and $\varepsilon^{13}C$ can also be evaluated. While documenting aerobic RDX biodegradation in the field is certainly possible at this ε value, the precision of N isotope measurements in RDX as well as the effects of field heterogeneity will make it more difficult.

$\delta^{15}N$ values were also measured for RDX from 11 different wells at Dahlgren NSWC. The field-collected $\delta^{15}N$ data along assumed transects through two RDX plumes did not provide an indication of natural attenuation via aerobic RDX biodegradation. While laboratory tests suggested the potential for natural biodegradation of RDX at this site, field data revealed no detectable NDAB (an aerobic degradation product of RDX) or MNX, DNX, or TNX (common anaerobic degradation

products) in groundwater from the site. Taken together ($\delta^{15}N$ in RDX and absence of intermediates), the data indicate a lack of measurable biological attenuation of RDX plume at this location.

$\delta^{15}N$ and $\delta^{18}O$ in nitrate (NO_3^-) were also measured at the Dahlgren NSWC site as a potential indication of RDX biodegradation. With the exception of one sample, the combined $\delta^{15}N$ and $\delta^{18}O$ data fell within the range of biogenic NO_3^- on a dual isotope plot, typically a result of NO_3^- produced via nitrification in soils. The $\delta^{18}O$ values for most of the Dahlgren NSWC samples were in the general range of those of nitrite (NO_2^-) produced during aerobic degradation of RDX, but the $\delta^{15}N$ values were appreciably higher. The one NO_3^- sample that did not fall within this range had a very high value of $\delta^{15}N$ (> +30 ‰) and a somewhat elevated value of $\delta^{18}O$ (nearly +20 ‰), which could be consistent with N isotope fractionation during biological degradation of biogenic NO_3^-. Thus, it is likely that most of the NO_3^- that was analyzed from Dahlgren NSWC did not originate from RDX, a conclusion that is consistent with the absence of evidence for MNA of RDX at this site (no measurable metabolites or ^{15}N enrichment, as previously described).

This study demonstrated that $\delta^{15}N$ and $\delta^{18}O$ in NO_2^- and/or NO_3^- can be a useful marker of aerobic or anaerobic RDX biodegradation, provided that the amounts of these anions generated from RDX are not overwhelmed by those generated from other sources. Further, the combination of RDX and NO_2^-/NO_3^- stable isotope analyses can be used to confirm natural degradation processes, particularly under anaerobic conditions.

5.0 COST ASSESSMENT

Stable isotope analysis of N and O in nitrate is currently estimated at $149 per sample (for 6 to 20 samples) from the USGS Reston, VA Stable Isotope Laboratory and C and N isotope analysis in RDX at $500 per sample by the University of Delaware EIGL Laboratory of Dr. Neil Sturchio, which is currently the only laboratory performing this method on a per sample basis. The estimated total cost for sampling and analysis of 20 wells to support a natural attenuation evaluation of RDX was just over $21,000.

6.0 IMPLEMENTATION ISSUES

The primary end-users of this technology are expected to be DoD site managers and their contractors, consultants, and engineers. The general concerns of these end users are likely to include: (1) technology availability and cost; (2) appropriate application of the technology at DoD sites; and (3) interpretation of CSIA data. The C and N stable isotope analyses described herein are not currently available in commercial laboratories to our knowledge. However, the analyses are currently being conducted at the University of Delaware, Environmental Isotope Geochemistry Laboratory (EIGL) under the supervision of Dr. Neil Sturchio on a per sample basis. Analyses of N and O stable isotopes in NO_3^- are available on a routine per sample basis from various laboratories including the USGS in Reston, VA. Isotopic analyses of NO_2^- may be available by special arrangement at some laboratories.

The CSIA technology described herein is applicable for documenting the biological degradation of RDX in groundwater by both aerobic and anaerobic mechanisms. However, when RDX is degraded aerobically via the typical denitration pathway, the extent of N fractionation is expected to be low (ε= ~ -2.4 ‰) and C is not expected to fractionate measurably based on pure culture studies. Thus, for the method to be useful for field samples, losses of RDX in groundwater either over distance (e.g., along a groundwater flowpath) or time (e.g., in an individual well) must be substantial, on the order of 80% or higher from initial concentrations. In many instances, and given the observed variability in this measurement, it is unlikely that aerobic biodegradation of RDX in the field will be definitively proven by N isotope fractionation. It is recommended that additional lines of evidence of RDX biodegradation under aerobic conditions be assessed along with N isotope analysis of RDX, including: (1) measurements of NDAB as a possible degradation intermediate; (2) molecular analysis of aquifer samples for the presence of *xplA/xplB* genes, which encode key enzymes involved in aerobic RDX biodegradation; (3) analysis of N and O stable isotopes in NO_2^- and/or NO_3^- that co-occur with RDX (particularly if initial RDX concentrations are in the mg/L range or higher); (4) laboratory microcosms or columns incubated aerobically to document RDX biodegradation under controlled conditions; and (5) application of stable isotope probing (SIP) in laboratory microcosms or mesocosms to identify organisms that aerobically degrade RDX. The combination of one or more of these techniques in conjunction with N stable isotope analysis of RDX at a field site is recommended to clearly document aerobic RDX biodegradation or confirm the absence of this process.

When RDX is biodegraded via anaerobic mechanisms, C and N stable isotopes are both applicable to document this process, due to the relatively large fractionation factors measured in culture studies (ε= ~ -4.7 ‰ for C and ε= ~ -9.9 ‰ for N). Dual isotope plots can be used to confirm biodegradation, as was done for Dahlgren NSWC field samples downgradient of an emulsified oil biobarrier. Many of the general lines of evidence previously suggested for evaluating aerobic RDX biodegradation are also applicable for anaerobic biodegradation, including: (1) evaluation of degradation intermediates, but in this case MNX, DNX and TNX rather than NDAB; (2) analysis of N and O stable isotopes in NO_2^- and/or NO_3^- that co-occur with RDX; (3) laboratory microcosms or columns incubated anaerobically; and (4) application of SIP in laboratory microcosms or mesocosms to identify anaerobic RDX degraders. As previously noted for evaluating aerobic biodegradation, a combination of one or more of these techniques in conjunction with C and N stable isotope analyses of RDX is recommended to document anaerobic RDX biodegradation.

Page Intentionally Left Blank

1.0 INTRODUCTION

1.1 BACKGROUND

Hexahydro-1,3,5-trinitro-1,3,5-triazine (RDX) is a common soil contaminant at current and former military facilities, including many training and testing ranges. Because RDX is readily transported through soils to the subsurface, this nitramine explosive now also impacts groundwater and drinking water at numerous locations across the country (17, 80). For example, according to a report from the US Army Corps of Engineers, the US Army has 583 sites at 82 installations that have explosives in groundwater, and 87 additional locations with suspected contamination (76). Although there is currently no federal drinking water standard for RDX, the USEPA has established a health advisory level of 2 μg/L, and military facilities sometimes must meet more stringent state requirements for offsite discharges. For example, the Virginia Groundwater Protection Standard (GPS) for the US Navy Churchill Range in Dahlgren, VA is 1.08 μg/L. The long-term sustainability of many military ranges depends on meeting environmental objectives.

Techniques to remove explosives from surface soils, including soil washing, soil bioreactors, iron addition, and enhanced *in situ* bioremediation, are well established (e.g., (19, 28, 33, 82)), and increasingly, biological treatment technologies are also being tested for field application to groundwater (26, 30, 41, 65). However, a significant issue with RDX contamination on ranges and at other military installations is that it often occurs over expansive areas, where *in situ* or *ex situ* treatment technologies are difficult to implement.

One potential alternative for military ranges and other facilities is monitored natural attenuation (MNA), in which contaminant losses by natural physical, chemical, and biological processes are evaluated. When intrinsic loss rates are sufficient, these processes alone can be utilized to meet groundwater protection standards for a contaminant without human intervention. MNA is now commonly implemented as a remedy for chlorinated solvents (e.g., (23, 77)), and this approach has been evaluated for various other contaminants, including the explosive 2,4,6-trinitrotoluene (TNT) (81). However, one limitation of this approach for RDX is the inability to accurately evaluate whether the nitramine is biodegrading under field conditions, particularly in aerobic or anaerobic environments where rates may be relatively slow (see Section 2.1.3 for further discussion of RDX biodegradation). The USEPA has issued a guidance document for using compound-specific isotope analysis (CSIA) for biodegradation rate determinations, wherein they confirm the unique value of this method for MNA (47).

The goal of this ESTCP effort was to field test stable isotope methods to quantify the microbial fractionation of C and N isotopes in RDX as a measure of biodegradation. The stable isotopic composition of NO_3^- and NO_2^- was also measured when these anions co-occurred with RDX to evaluate whether these potential degradation products from RDX could be used to further demonstrate MNA in the field.

1.2 OBJECTIVES OF THE DEMONSTRATION

This ESTCP project was a joint effort among Drs. Paul Hatzinger and Mark Fuller at APTIM Federal Services (formerly CB&I Federal Services), Dr. J.K. Böhlke at U.S. Geological Survey (USGS), and Dr. Neil Sturchio at the University of Delaware (UD). The objective of this project was to validate a CSIA method that could be utilized by DoD to quantify aerobic and anaerobic biodegradation of RDX at field sites. This technique would provide critical data to support MNA as a remedy for treating this energetic in groundwater at DoD sites, and to confirm the effectiveness of *in situ* enhanced bioremediation remedies.

1.3 REGULATORY DRIVERS

There is currently no federal drinking water standard for RDX. However, the compound is listed under the current USEPA Contaminant Candidate List -3 (CCL-3), which is used to select potential compounds for regulation under the Safe Drinking Water Act (http://water.epa.gov/scitech/drinkingwater/dws/ccl/ccl3.cfm). In addition, the USEPA has established a Health Advisory level of 2 μg/L, and military facilities sometimes must meet more stringent state requirements for offsite discharges. For example, the Virginia Groundwater Protection Standard (GPS) for the US Navy Churchill Range in Dahlgren, VA is 1.08 μg/L. Most importantly, this technique will provide DoD range and site managers with a means to document the natural attenuation or RDX or to confirm the effectiveness of aerobic or anaerobic biostimulation or bioaugmentation technologies.

2.0 TECHNOLOGY

2.1 TECHNOLOGY DESCRIPTION AND DEVELOPMENT

2.1.1 Compound-specific stable isotope analysis (CSIA)

CSIA is increasingly being applied as an analytical tool to quantify the biodegradation and environmental fate of industrial and military pollutants, including chlorinated solvents (68, 70), gasoline oxygenates (52) perchlorate (39, 69, 70), TNT (18, 36), and most recently, RDX (4, 5, 27). This technique relies on the fact that bacteria biodegrade heavier isotopocules (e.g., RDX with ^{15}N rather than ^{14}N in its structure) more slowly than lighter ones due to the greater bond stability of the heavier molecules. This leads to relative enrichment in the heavier isotopes within the residual parent molecules as biodegradation proceeds. An analysis of stable isotope ratios of a contaminant along the flow path of a plume, in a single well over time, and/or in contaminated groundwater compared to the contaminant source material can be utilized to document degradation and natural attenuation *in situ* (as opposed to losses due to dilution, volatilization or other nondestructive mechanisms). In addition, CSIA can provide information on specific reaction mechanisms, particularly if isotopes of multiple elements are evaluated, since the breaking of specific bonds is typically associated with characteristic kinetic isotope effects (KIE), resulting in different isotopic enrichment factors for elements when different degradation pathways occur (e.g., (36, 38, 47). Thus, CSIA is a powerful tool to detect, understand, and in some cases, quantify contaminant degradation in the environment.

2.1.2 Method for analysis of C and N stable isotopes in RDX

During SERDP Project ER-1607, a CSIA method was developed that utilizes gas-chromatography coupled to isotope-ratio mass-spectrometry (GC-IRMS) to quantify C and N isotope ratios in RDX. Improvements and modifications to this initial method have been made during this ESTCP effort. In summary, groundwater samples with RDX are initially collected in the field either as aqueous samples in 950-ml amber bottles or using a solid-phase extraction (SPE) column specifically developed for this project (Section 5.4.1-5.4.3). Aqueous samples are concentrated via SPE in the laboratory, and the RDX is extracted and concentrated in acetonitrile. For the SPE field columns, the same basic elution procedure is used. The concentration of RDX and intermediates in the samples is then measured by HPLC according to a modified EPA 8330 protocol, and the samples are then analyzed for $\delta^{15}N$ and $\delta^{13}C$ in RDX using a GC-IRMS technique developed for this process. The method details are provided in Section 5.5.3 and in (27).

2.1.3 Isotopic fractionation of N in RDX during biodegradation

The biodegradation of RDX occurs under aerobic, microaerophilic, and anaerobic conditions, and pathways for its catabolism by various bacteria have been described. A summary of different potential degradative pathways is provided in **Figure 2.1**. The results from SERDP Project ER-1607 clearly indicate that there is significant N isotope fractionation during RDX biodegradation by pure cultures and different extents of N fractionation (measured as a ^{15}N enrichment factor [ε]) depending on the bacterial degradation pathway. These data and more detailed interpretations were published previously (27). A summary of the three pathways, and relevant isotope results are provided in **Figure 2.2**, and compiled isotope data are provided in **Table 2.1**.

For aerobic degradation of RDX via the XplA/B enzyme system (Pathway C; (49)), the $\varepsilon^{15}N$ value averaged -2.4 ± 0.2 ‰ for four separate strains (compiled data in **Figure 2.2** and **Table 2.1**). Data from replicate studies with two of the strains are provided in **Figure 2.3** to demonstrate experimental and analytical reproducibility. The isotopic fractionation of N during degradation of RDX by strains with XenA/XenB enzymes under low oxygen/anaerobic conditions (Pathway B; (29)) was significantly higher than for aerobic degradation, with an average $\varepsilon^{15}N$ value of -12.7 ± 0.8 ‰ observed for two strains. The most widely studied pathway of anaerobic RDX biodegradation, which proceeds through mono-, di-, and tri-nitroso derivatives of RDX (Pathway A; (42)) resulted in N fractionation ranging from -5.8‰ for a *Klebsiella* sp. to -10.9‰ for a *Desulfovibrio* sp, with a mean of -9.9 ± 0.7 ‰ for four strains tested. Some of this variability may reflect the fact that cultures follow mixed pathways or that there are different initial reaction mechanisms as detailed below.

For the seven anaerobic cultures tested, we attempted to obtain cultures that degraded RDX exclusively via Pathway A or Pathway B in **Figure 2.1**. We measured total nitroso-intermediates to evaluate the extent to which the organisms reduced nitro ($N–NO_2$) groups in RDX to the corresponding nitroso (N–NO) groups resulting in the initial formation of MNX, followed by DNX and TNX, and then possibly ring cleavage. In the absence of these intermediates, we assumed that cultures were following Pathway B1/B2 in **Figure 2.1**, which entails one of several different initial reactions followed by ring cleavage to the intermediate MEDINA, which is labile in water (61) and was not measured during this study. Interpretations of isotope effects were complicated in some cases by incomplete knowledge of reaction mechanisms; for example: (1) with one exception, cultures that were presumed to degrade RDX primarily via Pathway A (nitro reduction) did not produce stoichiometric amounts of NXs during degradation, leaving the possibility that either both pathways were operating at the same time, or that the NXs were being degraded rapidly to something beyond TNX; (2) some of the cultures that were reported to degrade RDX via a ring cleavage mechanism were observed to produce some NXs, indicating that organisms degraded RDX via both pathways; and, (3) the reactions that initiate ring cleavage in RDX (and the enzymes catalyzing those reactions) may differ by species, and entail direct ring cleavage by α-hydroxylation of a CH_2 group, N-denitration followed by ring cleavage, or other initial reaction mechanisms (6), potentially resulting in different isotopic fractionation effects. These different considerations are addressed on a culture-by-culture basis (27).

Most importantly, however, significant N fractionation was observed under each specific set of conditions, as evidenced in **Figure 2.2** and detailed previously**.** For aerobic degradation with the well-known XplA/B enzyme system, $\varepsilon^{15}N$ value averaged -2.4 ± 0.2 ‰. These data are reasonably consistent with those reported recently from studies at a heavily contaminated military site in Israel (Bernstein et al., 2008) where the $\varepsilon^{15}N$ value during aerobic biodegradation was calculated to be -2.1 ‰. For anaerobic strains, several pathways/mechanisms are possible, and these may be mixed in the field, but the composited $\varepsilon^{15}N$ for all strains tested was -11.9 ± 0.7 ‰.

2.1.4 Isotopic fractionation of C in RDX during biodegradation

The isotopic fractionation of C in RDX has not been widely studied, in part due to difficulties in quantifying C isotopes for this molecule. However, the GC-IRMS method developed during ER-1607 generally overcomes this limitation. Significant C isotope fractionation is not expected during aerobic RDX degradation via the XplA/B enzyme system because the initial enzymatic attack results in denitration of the molecule, and a C-N bond is not broken (**Figure 2.1**; Pathway C). Our initial isotope data for C during aerobic RDX degradation support this hypothesis, as the fractionation factor ($\varepsilon^{13}C$) was < 1‰ (-0.8 ± 0.5 ‰) (**Table 2.1**). Similar results were reported by Bernstein et al., 2013 (5), who observed $\varepsilon^{13}C$ < 1 ‰ for three aerobic organisms that degrade RDX via denitration. In contrast, for strains that initiate RDX degradation via direct ring cleavage to methylenedinatrimine (MEDINA) under microaerophilic conditions (**Figure 2.1**; Pathway B), enrichment in ^{13}C can be reasonably anticipated because the initial step in this process is the cleavage of a C-N bond. For example, for two *Pseudomonas* spp. strains degrading RDX anaerobically via XenA/XenB enzymes (29), a $\varepsilon^{13}C$ value of -2.7 ± 0.7 ‰ was observed, with a corresponding $\varepsilon^{15}N$ value -12.7 ‰ as previously noted. Fractionation of C under anaerobic Pathway A by four strains averaged -4.7 ± 1.1 ‰, with strain-to-strain variation ranging from -2.0 to -6.0 ‰. Because the degradative intermediates in this reaction, such as MEDINA, are short-lived, stable isotope evidence ($\varepsilon^{13}C$ and $\varepsilon^{15}N$) for biodegradation via this route may be the only evidence obtainable that this process is occurring *in situ*.

2.1.5 Isotopic analysis of N and O in RDX degradation products NO_3^- and NO_2^-

In addition to evaluating N and C in RDX, we also quantified stable isotope ratios of N and O in NO_3^- at one field site that had historical contamination with RDX. NO_2^- and NO_3^- (which is derived from released NO_2^- via oxidation) are common degradation products of aerobic RDX biodegradation (see **Figure 2.1** and **Figure 2.4**). Although NO_2^- is released by aerobic RDX degraders and some anaerobes, this compound tends to be labile in the environment and may be either oxidized to NO_3^- under aerobic conditions or reduced to N_2O and N_2 gas under anaerobic conditions in groundwater. Isotopic analyses of any or all of these constituents could be useful for detecting RDX degradation products. Importantly, recent papers suggest that the N and O isotope ratios in NO_3^- derived from the degradation of nitramine and nitroaromatic explosives may differ from those from other sources such as atmospheric production and nitrification (10, 22) (**Figure 2.5**), although there were no pure culture data to support this assertion.

In order to more thoroughly evaluate the N and O isotope effects, $\delta^{15}N$ and $\delta^{18}O$ were measured on NO_2^- released during aerobic degradation of RDX by *Rhodococcus* DN22 and *R. rhodocrous* 11Y (Pathway C in **Figure 2.1**) and during anaerobic degradation by *P. putida* II-B and *P. fluorescens* I-C (Pathway B in **Figure 2.1**) (27). $\delta^{15}N$ values for NO_2^- produced by the two *Pseudomonas* cultures under anaerobic conditions were approximately -36 to -24 ‰ for *P. putida* II-B (XenA) and -42 to -29 ‰ for *P. fluorescens* I-C (XenB). Compared to the measured bulk RDX isotope effects, these data indicate substantially larger intrinsic N isotope fractionations associated with release of NO_2^- during degradation (**Figures 2.6** and **2.7**). $\delta^{18}O$ values of NO_2^- ranged from -17 ‰ to +1 ‰ (data not shown), generally somewhat lower than those expected from equilibrium between NO_2^- and H_2O (13). $\delta^{18}O$ and $\delta^{15}N$ were positively correlated with $\Delta\delta^{18}O/\Delta\delta^{15}N$ = 0.8 to 0.9.

During experiments with the aerobic *Rhodococcus* cultures (XplA), $\delta^{15}N$ values for NO_2^- ranged from -7 to +2 ‰ for *Rhodococcus* DN22 and -6 to 0 ‰ for *R. rhodochrous* 11Y, consistent with kinetic fractionation effects, but smaller than those of the anaerobic *Pseudomonas* cultures (**Figure 2.6**). $\delta^{15}N$ values for [NO_2^- + NO_3^-] generally were higher than those for NO_2^- alone. Relatively high $\delta^{15}N$ of NO_3^- could be qualitatively consistent with an "inverse" isotope effect of NO_2^- oxidation (12), or it could indicate another production mechanism separate from the one producing most of the NO_2^-. However, NO_3^- concentrations were too low and uncertain to permit accurate estimation of NO_3^- isotopic composition. $\delta^{18}O$ values of NO_2^- ranged from +9 ‰ to +14 ‰ (data not shown), approximately equal to or slightly higher than those expected from equilibrium between NO_2^- and H_2O. $\delta^{18}O$ and $\delta^{15}N$ were relatively weakly correlated ($\Delta\delta^{18}O/\Delta\delta^{15}N$ = 0.3 to 0.8), possibly because of partial O exchange accompanying fractionation (11, 13).

2.1.6 Implications for nitrate detected in groundwater at RDX contaminated sites.

In typical field situations (e.g., soil, groundwater, surface water), processes such as nitrification, denitrification, anammox, or nitrite ammonification are likely to prevent NO_2^- accumulation and may or may not yield detectable anomalies in N_2, N_2O, NO_3^-, or NH_4^+. Small concentrations of N_2 produced locally from NO_2^- reduction in anaerobic systems might be difficult to quantify in the presence of ubiquitous N_2 from the atmosphere. However, if the large isotope effect observed in NO_2^- from anaerobic experiments with *Pseudomonas* strains were transferred to N_2 or N_2O during denitrification in a system relatively closed to atmospheric exchange, then N_2 or N_2O isotopic analyses might reveal anomalies related to RDX degradation. In aerobic systems, excess NO_3^- from RDX degradation (e.g., from oxidation of released NO_2^-) could be detectable by relatively low $\delta^{15}N$ where other NO_3^- sources were not overwhelming. Based on our results, $\delta^{15}N$ values of NO_3^- derived from oxidation of the NO_2^- product of RDX degradation in aerobic conditions (-7 to +2 ‰) might not be much different from those of NO_3^- derived from natural soils and artificial fertilizers, but they could be significantly lower than those of NO_3^- derived from wastewater and manure sources, which are typically > +6 ‰ (1, 43, 45), 48, (79). $\delta^{15}N$ values of NO_3^- derived from oxidation of the NO_2^- product of anaerobic RDX degradation (-42 to -24 ‰) (e.g., in soils with heterogeneous redox conditions) could be substantially lower than those of most common NO_3^- sources. Additional laboratory and/or field data are required to improve confidence in this approach.

2.1.7 Conclusions from pure culture studies

In summary, significant and consistent fractionation of N isotopes occurred in anaerobic conditions for all of the different cultures tested, representing multiple mechanisms of RDX degradation (□15N = -11.9 ‰), and lesser but consistent enrichment occurred during aerobic degradation (□15N = -2.4 ‰). These data are in general concurrence with the few previous reports using different microbial cultures or mixed cultures, although our $\varepsilon^{15}N$ values for anaerobic degradation are significantly more negative (3, 4). In contrast, there was no measurable fractionation of C isotopes in RDX during aerobic degradation, which is consistent with the proposed mechanism of degradation by the XplA/B cytochrome P450 system. Interestingly, there was significant C isotopic fractionation during anaerobic RDX degradation for all of the cultures for which data were available, although the extent of fractionation was highly variable. This variability most likely reflects the fact that (1) cultures appear to degrade RDX by multiple pathways in many instances; and, (2) the initial degradative step for RDX as it breaks down to MEDINA (which may be a multi-step process) may vary by culture, and reflect differential attack by different enzymes.

It would be informative to obtain more reliable $\varepsilon^{13}C$ values for RDX degraded by cultures or pure enzymes that catalyze nitro-reduction reactions on RDX, forming MNX as an initial product (**Figure 2.1**; Pathway A). We were not able to obtain such values either because we could not confirm that this was the only reaction that was occurring or, in the one case where this was the only reaction based on NX production, due to unresolved analytical interference from other compounds in the growth medium. For any experimental conditions, techniques for measuring separately the isotope ratios of non-equivalent sites within the RDX (e.g., ring-N versus nitro-N), or for measuring the isotope ratios in various reaction products, could provide valuable information about underlying causes of bulk isotope effects during degradation.

Isotopic analyses of NO_2^- that accumulated during RDX degradation were consistent with a simple denitration model for aerobic degradation and they implied more complex (and uncertain) models for anaerobic degradation (27). Despite uncertainty about the details, both the RDX data and the NO_2^- data indicated larger N isotopic fractionation effects in the anaerobic experiments than in the aerobic experiments; while stoichiometry and isotope data from both the anaerobic and aerobic experiments were consistent with a fractionating mechanism involving only a subset of the N atoms in the RDX to produce NO_2^- .

Overall, the data indicate that N stable isotope ratio analysis can be useful for documenting both aerobic and anaerobic biodegradation of RDX, and may be suitable for discerning which pathways are operating in the environment. C stable isotopic analysis may be useful for documenting anaerobic biodegradation, but may not be useful in the field for aerobic degradation due to the relatively small fractionation. Combined C and N isotope data may be useful for distinguishing aerobic vs. anaerobic degradation in the absence of daughter product data. Further work is required to better understand fractionation of C and N isotopes in RDX at an enzymatic and mechanistic level. Nonetheless, the data presented herein indicate that CSIA may have broad application for documenting RDX biodegradation in the environment. In addition, combined isotopic analyses of RDX and reaction products such as NO_2^- may provide useful information about possible reaction pathways, as well as potential secondary environmental contaminants derived from RDX degradation.

2.1.8 Overview of research approach

In summary, the focus of this ESTCP Project was to develop currently available stable isotope techniques for RDX into a technology that can be applied at field sites to support MNA remedies, and to document degradation during biostimulation/bioaugmentation applications at military ranges and other DoD facilities. Isotopic analysis of NO_3^- and NO_2^- was included as a potentially important supporting technique for RDX stable isotope analysis. The isotope data gained from our SERDP studies with pure and mixed cultures (more than 10 pure cultures and various microcosms have now been tested) provided a strong fundamental basis for this approach, as detailed in Sections 2.1.3 to 2.1.7 and described in detail in (27).

2.2 ADVANTAGES AND LIMITATIONS OF THE TECHNOLOGY

The key advantage of this technology is that it provides a means to document the biological or abiotic degradation of RDX in groundwater that is independent of chemical concentration.

Moreover, the approach also provides a technique to estimate or constrain *in situ* degradation rates when applied to several wells along a groundwater flow path or at the same well over time.

Potential limitations of this approach included the following: (1) the relatively low isotopic fractionation factor for N (~ 2.4 ‰), and minimal isotopic fractionation for C under aerobic conditions could have somewhat limited its usefulness in the field to document aerobic processes (although the fractionation was very consistent among strains); (2) no laboratories offered this technique commercially, although University of Delaware is capable of conducting the analysis as a pay for sample service in their Environmental Isotope Geochemistry Laboratory (EIGL); and, (3) recent studies suggest that there may be some analytical interference issues with fatty acids or other compounds under highly reducing conditions. The latter interferences only impacted a small set of the samples analyzed during this project, but further method refinements for sample cleanup may be necessary.

Figure 2.1. Biodegradation Pathways for RDX.

Aerobic conditions via the anaerobic conditions via nitroreductases or other enzymes (Pathway A); anaerobic conditions via XenA and XenB enzymes (Pathway B); via the XplA/B enzyme system (Pathway C). Pathways reproduced from (27), as derived from (4, 6, 24, 34, 42, 83).

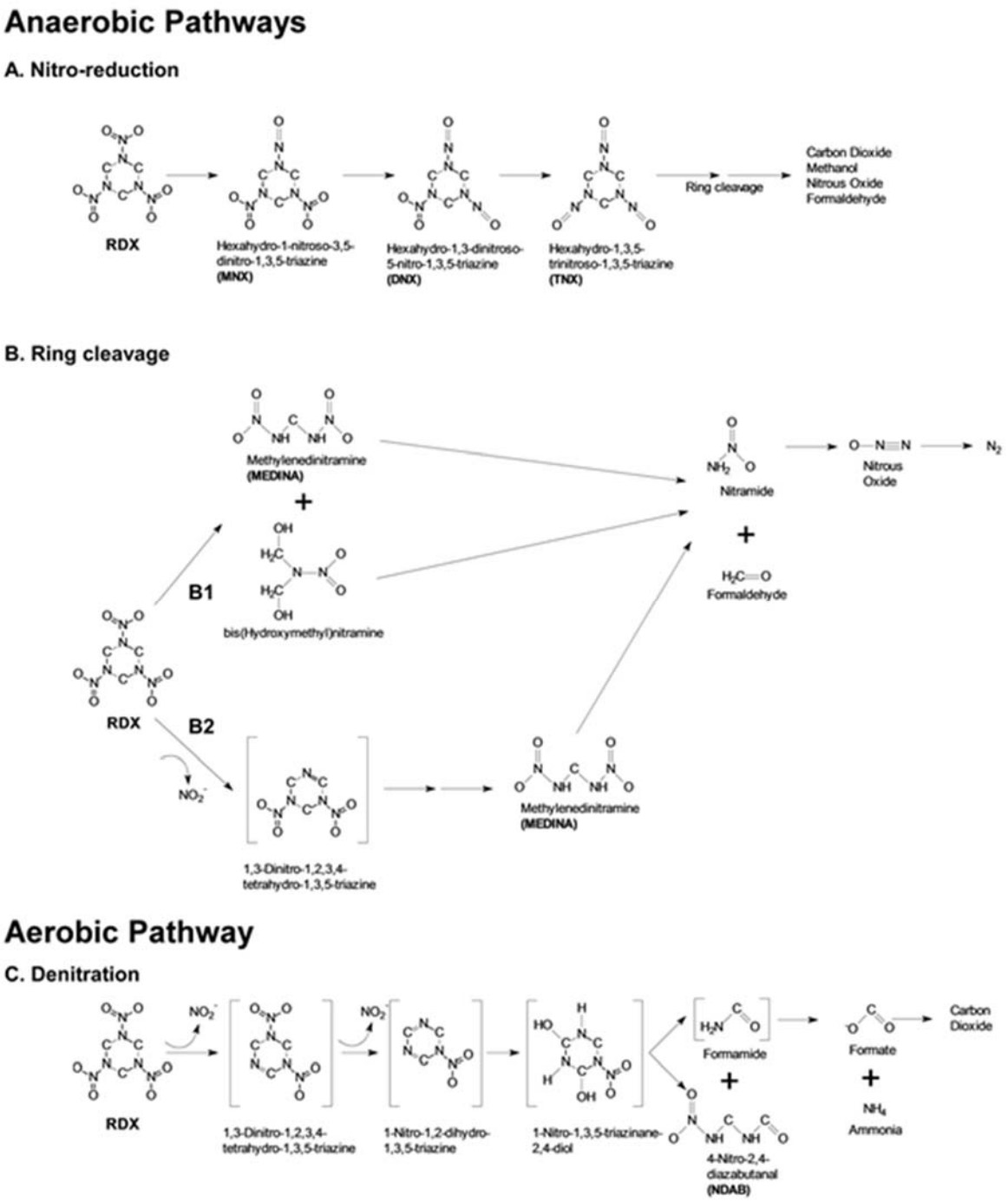

Table 2.1. Summary of Bulk ^{13}C and ^{15}N Fractionation Factors (ε) via Different RDX Degradation Pathways.

Values represent the slope of the linear regression of the combined data for duplicate fractionation experiments of each culture ± the 95 % confidence interval of the slope. P-values represent the probability that the observed slope is different from zero. Data from (27).

	ε ^{13}C			ε ^{15}N		
Strain	‰	±	**P-value**	‰	±	**P-value**
Anaerobic Pathway A						
Shewanella oneidensis MR-1	-6.0	2.6	2.0E-04	-9.6	1.3	5.6E-12
Klebsiella pneumoniae SCZ-1	-4.1	1.6	4.7E-05	-5.8	2.6	6.3E-04
Desulfovibrio sp.	-2.0	0.5	2.8E-06	-10.9	1.2	5.2E-10
Clostridium acetobutylicum ATCC 824	-2.8	1.6	2.7E-03	-8.0	5.5	1.9E-02
Composited Pathway A data[a]	**-4.7**	**1.1**	**1.8E-11**	**-9.9**	**0.7**	**1.8E-32**
Anaerobic Pathway B						
Pseudomonas putida II-B	-3.1	1.0	1.3E-05	-13.3	1.5	6.0E-12
Pseudomonas fluorescens I-C	-2.1	1.3	6.2E-03	-12.7	1.1	1.7E-12
Composited Pathway B data[a]	**-2.7**	**0.7**	**8.7E-08**	**-12.7**	**0.8**	**9.0E-26**
Composited Pathway A and B data[a]	**-4.0**	**0.8**	**3.4E-15**	**-11.9**	**0.7**	**7.5E-52**
Aerobic Pathway C						
Rhodococcus sp. DN22	-1.3	2.3	2.2E-01	-2.8	0.5	7.1E-09
Rhodococcus rhodocrous 11Y	0.3	0.8	4.0E-01	-2.6	0.3	2.3E-10
Rhodococcus sp. Strain A	-0.7	0.3	2.1E-04	-2.3	0.4	2.6E-06
Gordonia sp. KTR9	-0.9	0.6	7.2E-03	-2.3	0.5	2.0E-06
Composited Pathway C data[a]	**-0.8**	**0.5**	**1.2E-03**	**-2.4**	**0.2**	**3.3E-25**

[a] All data from the strains associated with designated pathway included in a single regression analysis.

Figure 2.2. Isotopic Fractionation of $^{12}C/^{13}C$ and $^{14}N/^{15}N$ during Biodegradation of RDX by Different Pathways.

Dashed lines represent 95% confidence intervals around the best fit solid lines with slopes as reported in Table 2.1. Refer to Figure 2.1 for pathways.

A

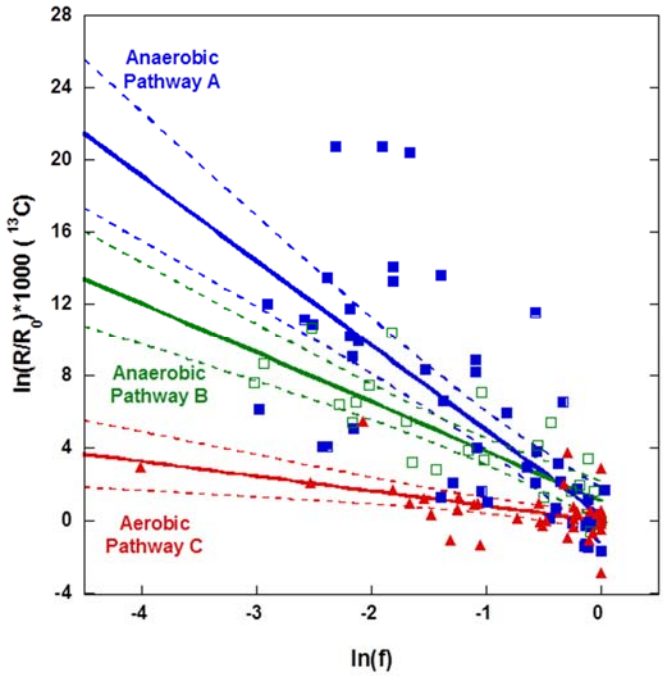

B

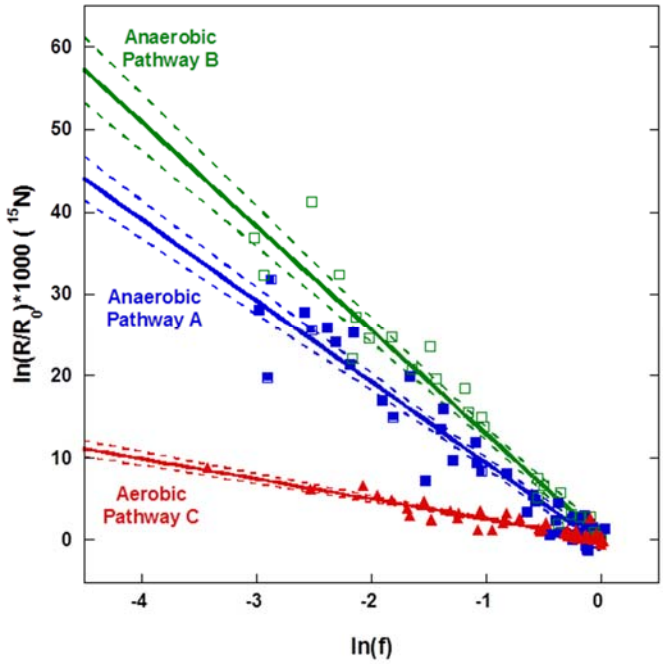

Figure 2.3. Isotopic Fractionation of N by Two Aerobic RDX Degraders.

Analysis of replicate experiments for each strain are provided to show reproducibility of analysis.

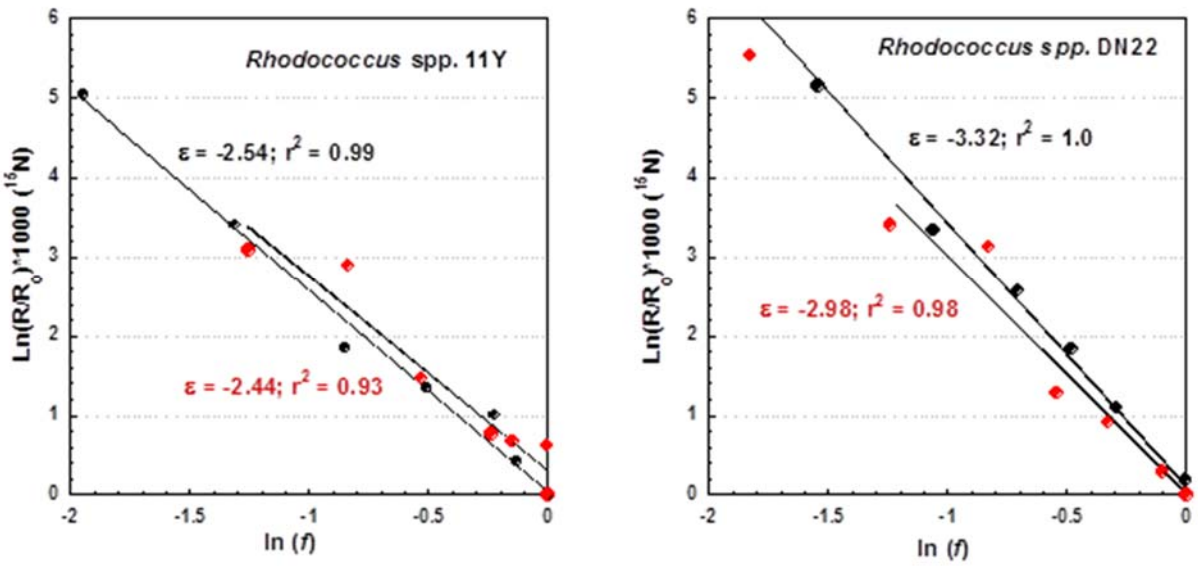

Figure 2.4. Production ofNnitrite (NO_2^-) during Aerobic Biodegradation of RDX by *Rhodococcus* Strain 11Y.

Unpublished data from SERDP Project ER-1607. Nitrite analyses were done by ion chromatography (EPA 300).

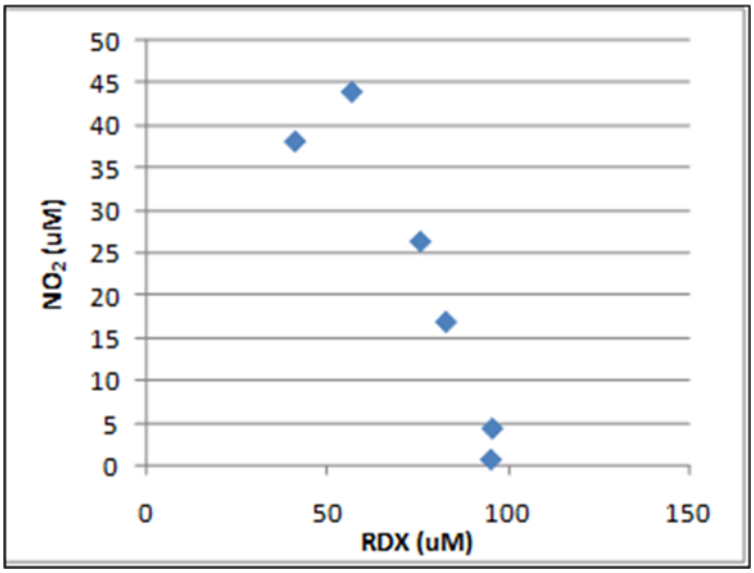

Figure 2.5. $\delta^{15}N$ and $\delta^{18}O$ in NO_3^- Collected from RDX-contaminated Wells (Alpha/Bravo and Shaver) Compared to Uncontaminated Wells (Deep Confined Aquifer).

Large differences in $\delta^{15}N$ and $\delta^{18}O$ were noted among samples with and without historical RDX contamination (figure from Bordeleau et al., 2008)

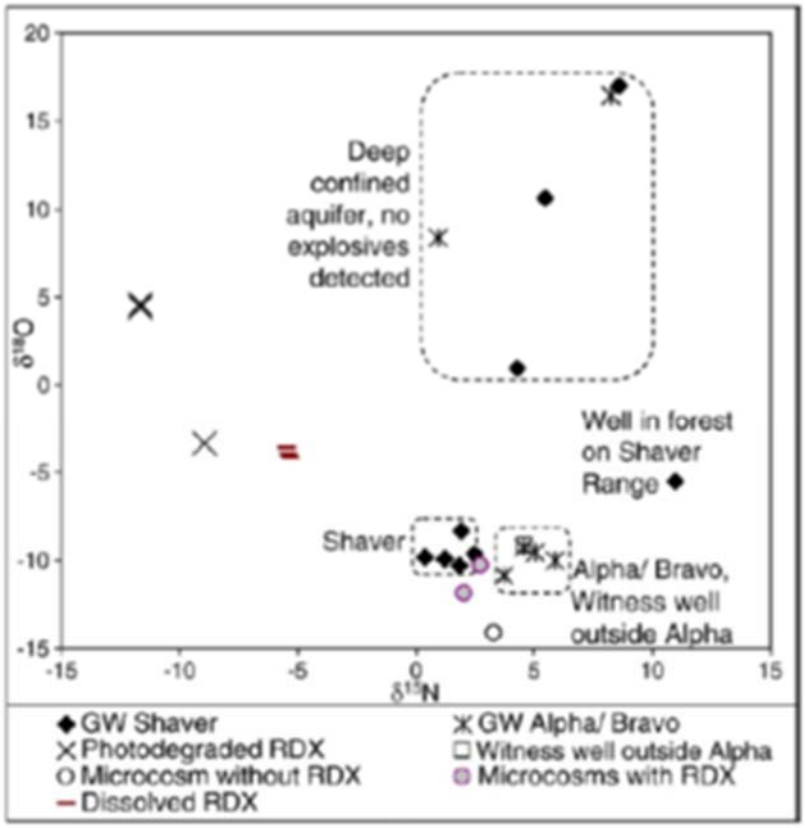

Figure 2.6. Concentrations of NO_2^- (closed symbols) during Aerobic Degradation of RDX by *Rhodococcus* DN22 and *R. rhodocrous* 11Y and Anaerobic RDX Degradation by *P. putida* II-B and *P. fluorescens* I-C.

An "x" next to a plot symbol indicates that NO_3^- (calculated by difference) was detected at greater than 10 µM. Nitrite analyses were done by IRMS (8). Data from (27) and also provided in Appendix B, Table B-1.

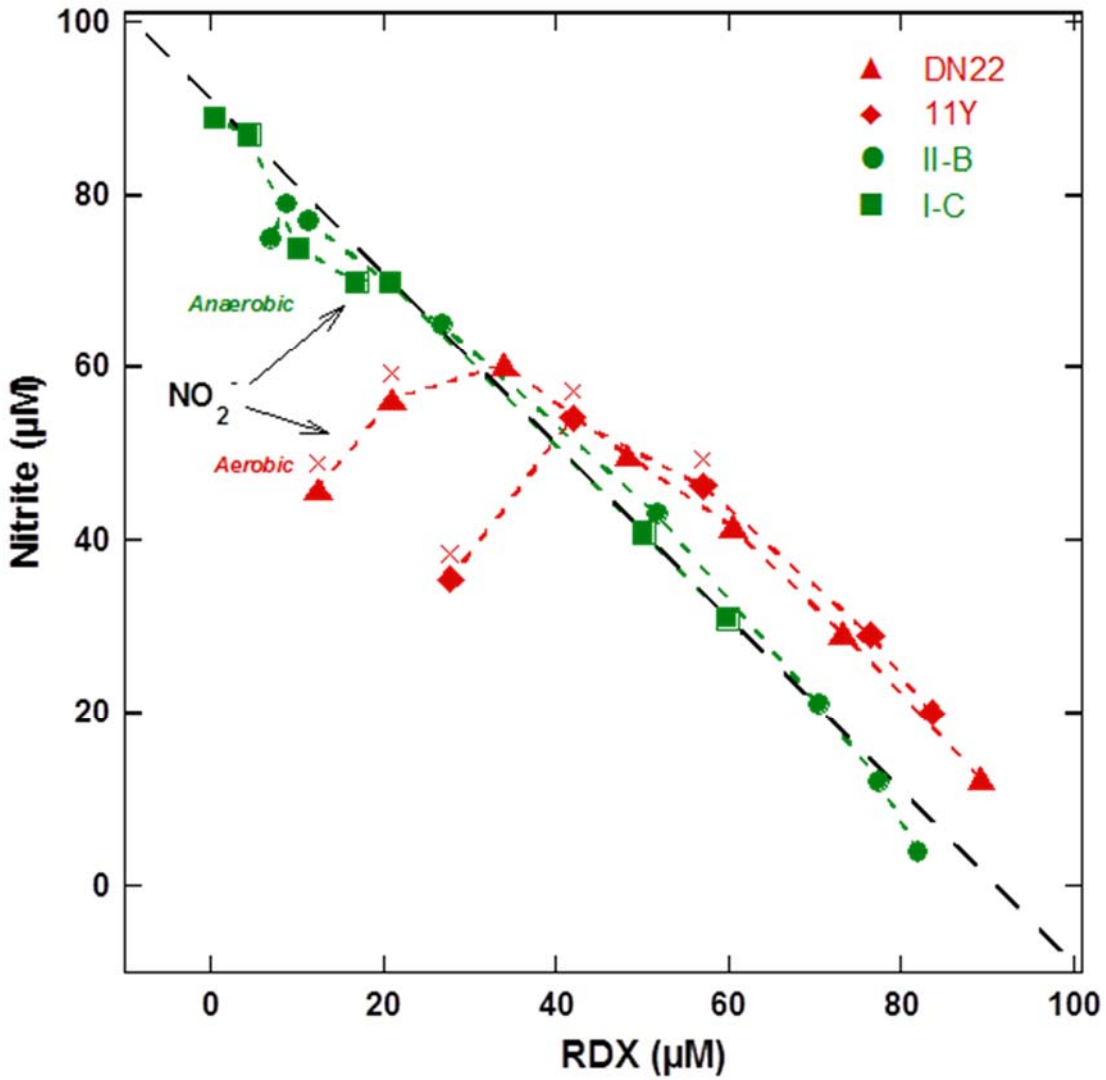

Figure 2.7. Comparison of $\delta^{15}N$ Values of RDX (closed symbols) and NO_2^- (open symbols) during (A) Aerobic RDX Degradation by *Rhodococcus* DN22 and *R. rhodocrous* 11Y and (B) Anaerobic RDX Degradation by *P. putida* II-B and *P. fluorescens* I-C.

Curves indicate results of numerical isotopic fractionation models in which bulk isotope effects in residual RDX (solid curve) are attributed to single-stage total breakdown to bulk products consistent with Rayleigh fractionation (Model 1) or to larger intrinsic isotope effects of reactions at subsets of N sites in the RDX yielding NO_2^- (Model 2, Model 3). Data from (27) and also provided in Appendix B, Table B-1. NOTE: different y-axis scales.

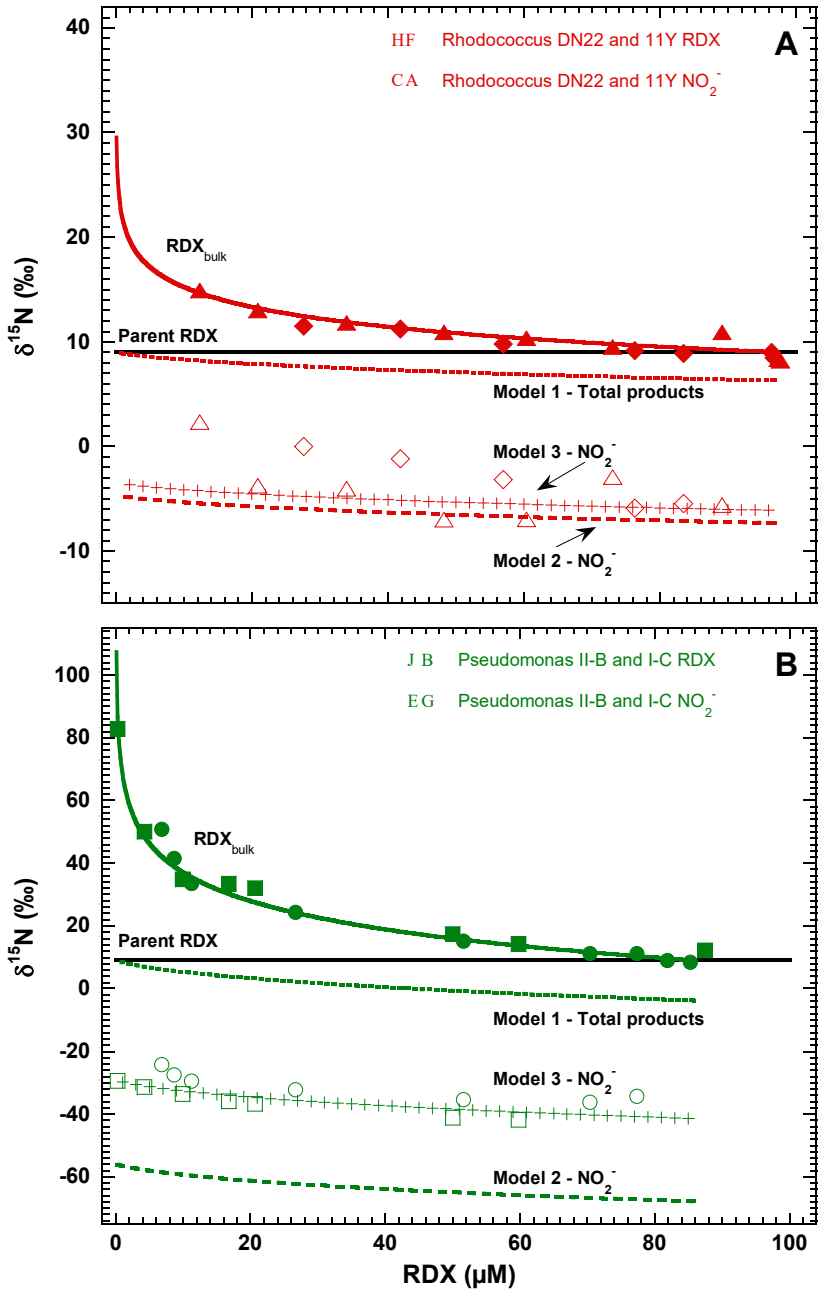

Page Intentionally Left Blank

3.0 PERFORMANCE OBJECTIVES

The performance objectives for this project are summarized in **Table 3.1**, and details are provided in Sections 3.1-3.5.

Table 3.1. Performance Objectives.

Performance Objective	Data Requirements	Success Criteria	Results
Quantitative Performance Objectives			
Measure $\varepsilon^{15}N$ for RDX *in situ* under aerobic conditions.	CSIA analysis of N in RDX from field sites as a function of (A) distance from a source area in downgradient wells and/or (B) time in a single well (i.e., push-pull test).	• Reproducibility of individual isotopic measurements at precision of ± 1 ‰ or better (1-sigma) • Enrichment in $\delta^{15}N$ in RDX as a function of distance or time as evidenced by significant positive trends of $\delta^{15}N$. • Data allow estimate of *in situ* RDX biodegradation based on known ε values of N for pure culture or microcosm studies.	Method reproducibility for $\delta^{15}N$ achieved ± 1 ‰ but fractionation was not sufficient during aerobic Umatilla or Dahlgren NSWC studies to consistently document *in situ* RDX degradation.
Measure $\delta^{15}N$ and $\delta^{13}C$ for RDX *in situ* under anaerobic conditions.	CSIA analysis of C and N in RDX from field sites a(A) downgradient from an emulsified oil biobarrier and (B) as a function of time/RDX concentration in a single well (i.e., push-pull type test).	• Reproducibility of individual isotopic measurements at precision of ± 1 ‰ or better (1-sigma). • Enrichment in ^{15}N and/or ^{13}C in RDX as a function of declining RDX concentration, as evidenced by significant positive trend of $\delta^{15}N$ and/or $\delta^{13}C$ values. • Data allow estimate of *in situ* RDX biodegradation based on known ε values of C and N for pure culture or microcosm studies.	Method reproducibility for $\delta^{15}N$ achieved ± 1 ‰ and trends for Dahlgren NSWC biobarrier and Umatilla study allowed documentation of *in situ* biodegradation of RDX.
Measure $\delta^{15}N$ and $\delta^{18}O$ in NO_3^- or NO_2^- *in situ* under aerobic conditions.	CSIA analysis of N and O in NO_3^- or NO_2^- in field samples where RDX is undergoing aerobic biodegradation.	• Reproducibility of individual isotopic measurements at precision of ± 0.6 ‰ or better (1-sigma) • Unique $\delta^{15}N$ and/or $\delta^{18}O$ values in NO_3^- or NO_2^- derived from RDX, such that these anions can be distinguished from the same anions derived from other sources (e.g., nitrification) outside of 2-sigma analytical uncertainties.	Analysis of $\delta^{15}N$ $\delta^{15}N$ and $\delta^{18}O$ in NO_3^- was completed at Dahlgren NSWC. Isotope data did not show unique signature indicative of RDX biodegradation but aerobic biodegradation of RDX also was not indicated
Verification of column collection method for RDX stable isotope analysis.	CSIA analysis of C and N in RDX collected in bottles vs. columns in the field.	• < 2‰ difference in measured $\delta^{15}N$ and $\delta^{13}C$ between column-collected and bottle-collected samples. • Yield of RDX reproducible to within ± 25 % in replicate samples	Objective was achieved
Qualitative Performance Objectives			
Efficient sample collection.	Total time and effort for sample collection using field columns. Feedback from field technician on ease of use.	• Columns used properly. • Field technician having no significant issues with sample collection such as column clogging.	Objective was achieved

3.1 MEASURE $\varepsilon^{15}N$ FOR RDX *IN SITU* UNDER AEROBIC CONDITIONS

The objective was to quantify $\varepsilon^{15}N$ for RDX *in situ* under aerobic conditions either by measuring isotopic fractionation as a function of distance from a source area (with biodegradation occurring along the flowpath) or as a function of time during a push-pull test, where aerobic RDX biodegradation was occurring. Based on pure culture studies, no significant C fractionation was expected.

3.1.1 Data requirements for measuring $\varepsilon^{15}N$ for RDX in situ under aerobic conditions

The data required were measurements of $\delta^{15}N$ in RDX collected (1) from a series of wells along a groundwater flow path at Dahlgren NSWC and (2) from a time series of samples from a single well during aerobic RDX biodegradation conducted at UMCD via push-pull tests. $\delta^{15}N$ in RDX was measured by methods described in Section 5.5.3.

3.1.2 Success criteria for measuring $\varepsilon^{15}N$ for RDX in situ under aerobic conditions

The objective was considered to be met if (1) $\delta^{15}N$ values obtained from a series of groundwater samples containing RDX in a flow path and/or during a push-pull test had a reproducibility of individual isotopic measurements at a precision of ± 1 ‰ or better (1-sigma) and (2) $\varepsilon^{15}N$ values could subsequently be calculated from those $\delta^{15}N$ values and used to document aerobic RDX biodegradation.

3.2 MEASURE $\varepsilon^{15}N$ AND $\varepsilon^{13}C$ FOR RDX *IN SITU* UNDER ANAEROBIC CONDITIONS

The objective was to quantify $\varepsilon^{13}C$ and $\varepsilon^{15}N$ for RDX *in situ* under anaerobic conditions by measuring isotopic fractionation as a function of distance downgradient of an emulsified oil biobarrier at Dahlgren NSWC and as a function of time during a push-pull test at UMCD in which fructose was added to an aquifer to promote anaerobic RDX biodegradation.

3.2.1 Data requirements for measuring $\varepsilon^{15}N$ and $\varepsilon^{13}C$ for RDX for RDX in situ under anaerobic conditions

The data requirements were measurements of $\delta^{15}N$ and $\delta^{13}C$ in RDX collected (1) from a series of wells downgradient from an emulsified oil biobarrier and (2) from a time series of samples from a single well during anaerobic RDX biodegradation via push-pull testing. $\varepsilon^{15}N$ and $\varepsilon^{13}C$ were calculated from the $\delta^{15}N$ and $\delta^{13}C$ values. $\delta^{15}N$ and $\delta^{13}C$ in RDX were measured by methods described in Section 5.5.3.

3.2.2 Success criteria for measuring $\varepsilon^{15}N$ and $\varepsilon^{15}C$ for RDX in situ under anaerobic conditions

The objective was considered to be met if (1) $\delta^{15}N$ and $\delta^{13}C$ values could be obtained from a series of groundwater samples containing RDX downgradient of a biobarrier and/or or during a push-pull test with reproducibility of individual isotopic measurements at a precision of ± 1‰ or better (1-sigma) and (2) $\varepsilon^{15}N$ and $\varepsilon^{13}C$ could subsequently be calculated from those values.

3.3 MEASURE $\delta^{15}N$ AND/OR $\delta^{18}O$ IN NO_3^- OR NO_2^- *IN SITU* UNDER AEROBIC CONDITIONS

The objective was to quantify $\delta^{15}N$ and $\delta^{18}O$ in NO_3^- or NO_2^- *in situ* under aerobic conditions at a site where RDX was biodegrading. Ideally, the $\delta^{15}N$ and/or $\delta^{18}O$ values in the NO_3^- or NO_2^- derived from RDX during biodegradation would differ isotopically from those of NO_3^- or NO_2^- present in groundwater from other sources (e.g., nitrification). Sampling and analysis were done during MNA sampling at Dahlgren NSWC.

3.3.1 Data requirements for measuring $\delta^{15}N$ and $\delta^{18}O$ in NO_3^- or NO_2^- in situ under aerobic conditions

The data required were measurements of $\delta^{15}N$ and $\delta^{18}O$ in NO_3^- or NO_2^- collected from the field. These samples were taken in conjunction with RDX samples as described in Section 4.1. Sample analyses were conducted by the Reston USGS lab by established methods (13, 14).

3.3.2 Success criteria for measuring $\delta^{15}N$ and $\delta^{18}O$ in NO_3^- or NO_2^- under aerobic conditions

The objective was considered to be met (1) if $\delta^{15}N$ and $\delta^{18}O$ values can be obtained from NO_3^- or NO_2^- generated during *in situ* RDX degradation, either along a flow path or during the push-pull test at UMCD had a reproducibility of individual isotopic measurements at precision of ± 0.6 ‰ or better (1-sigma) and (2) if those isotope values allowed NO_3^- or NO_2^- generated from RDX to be distinguished from that generated from other processes *in situ*.

3.4 VERIFICATION OF COLUMN COLLECTION METHOD FOR RDX STABLE ISOTOPE ANALYSIS

The main objective was to develop an efficient means to collect RDX from groundwater where low concentrations exist (e.g., < 10 µg/L) to avoid shipping multiple liters of groundwater to the laboratory for processing. SPE columns were evaluated for this purpose. Verification of this technique was both qualitative (see Section 5.4) and quantitative. The quantitative aspect was to ensure that the collection process did not fractionate N or C isotopes in RDX to a significant extent.

3.4.1 Data requirements for verifying the column collection method for RDX stable isotope analysis

The data required were measurement of $\delta^{13}C$ and $\delta^{15}N$ in RDX in groundwater collected in bottles vs. RDX concentrated on SPE columns in the field from multiple wells. $\delta^{15}N$ and $\delta^{13}C$ in RDX was measured by methods described in Section 5.5.3.

3.4.2 3.4.2 Success criteria for verifying the column collection method for RDX stable isotope analysis

The objective was considered to be met if the mean deviation in $\delta^{13}C$ or $\delta^{15}N$ in RDX was < 2 ‰ from samples collected from the same well in bottles vs. concentrated in the field on SPE columns. Also, the objective was considered met if the yield of RDX was reproducible to within ± 25 % in replicate samples.

3.5 EFFICIENT SAMPLE COLLECTION

Small SPE columns were developed for field use. The qualitative performance objective for these columns was to determine if they could be used efficiently in the field for sample collection.

3.5.1 Data requirements for efficient sample collection.

The data required was an assessment of the total time required for sample collection using SPE columns in the field, and any feedback from field personnel identifying any issues with the SPE column procedure or apparatus (e.g., plugging, slow flow, etc).

3.5.2 Success criteria for efficient sample collection.

The objective was considered to be met if collection of RDX on SPE columns was performed successfully by field personnel (e.g., no significant plugging or other issues).

4.0 SITE DESCRIPTION

Site selection for this ESTCP Project entailed contacting DoD environmental managers and/or other personnel associated with four sites known to have RDX in groundwater. Discussions were held with personnel from the US Navy's Potomac River Test Range and Explosives Experimental Area in Dahlgren, VA (Dahlgren NSWC), the Naval Weapons Station, Earle in Colts Neck, NJ (Earle NSWC), the Umatilla Chemical Depot (UMCD; Umatilla OR), and US Navy Operable Unit 1, Site A, at Naval Base Kitsap-Bangor, Poulsbo, WA (NBK). Site data evaluated for each candidate location included the following: (1) basic aquifer conditions (e.g., geochemistry, hydrology, etc.); (2) RDX and co-contaminant concentrations and plume characteristics; (3) evidence for RDX degradation; (4) extent of historical data; (5) interest of base environmental personnel and potential for technology to assist with regulatory considerations; and (6) existing SERDP/ESTCP projects assessing RDX biodegradation at each location.

Site selection criteria and the corresponding information from potential demonstration sites are provided in **Table 4.1.**

Table 4.1. Site Selection Criteria.

Parameter	Relative Importance (1-5, with 1 being highest)	Dahlgren NSWC	UMCD	NBK	Earle NSWC
Interest from site personnel	1	Yes	Yes	Yes	Yes
Sufficient historical data for explosive concentrations and site geochemistry	1	Yes	Yes	Yes	No
Evidence of RDX degradation	2	Yes	Yes*	No	No
Sufficient well network	1	Yes	Yes*	Yes	No
Significant site assessment work complete – plume maps	1	Yes	Yes	Yes	No
Preliminary laboratory biodegradation data	3	Yes	Yes	No	No
Ongoing ESTCP Project	3	Yes	Yes	No	No

*For UMCD, a push-pull test was conducted to evaluate RDX degradation by aerobic bacteria (bioaugmented) and by anaerobic biostimulation. The well network and lab data support this design (ESTCP Project ER-201207).

Based on the parameters listed above, two sites were selected for evaluation during this project: (1) Dahlgren NSWC and (2) UMCD.

The hydrogeological conditions and contaminant concentrations at Dahlgren NSWC have been extensively investigated during ESTCP Project ER-201028 "Passive Biobarrier for Treating Co-mingled Perchlorate and RDX in Groundwater at an Active Range". In addition, preliminary column data conducted during this project suggest the potential for natural attenuation occurring at the site (see Section 5.2.1).

The UMCD site was used as a demonstration site under ESTCP Project ER-201207 "Bioaugmentation for Aerobic Bioremediation of RDX-Contaminated Groundwater" led by Dr. Mandy Michalsen at USACE, Seattle District. During this project, *in situ* studies were performed to evaluate the potential to stimulate *in situ* RDX biodegradation by injecting aerobic RDX-degrading cultures in one plot, and by adding carbon source to stimulate anaerobic degradation in a second plot (see Sections 5.2.2 and 5.4.6). Some of the data from this project were published previously (55). This project provided a unique opportunity to conduct N stable isotope analysis of RDX for each of the *in situ* treatments, subsequently documenting isotopic enrichment as RDX biodegrades under aerobic and anaerobic conditions. Thus, UMCD was selected as a second demonstration site for this project.

4.1 SITE 1: NAVAL SURFACE WARFARE CENTER, DAHLGREN, VA

The Naval Surface Warfare Center, Dahlgren was one of two sites selected for this ESTCP demonstration. This site is located in King George County, VA along the Potomac River approximately 40 miles south of downtown Washington, DC and 28 miles east of Richmond, VA (**Figure 4.1**; from (72)). Dahlgren NSWC, which was originally established in 1918 as a testing site for naval ordnance, is presently focused on research, development, test, and evaluation (RDT&E) of ordnance, integrated warfare systems, weapons and ammunition, sensors and directed energy, and force protection. Apart from testing and disposal activities associated with their RTD&E mission, Dahlgren NSWC accepts obsolete and/or waste munitions from other military facilities for treatment and serves as a center for emergency Explosives Ordnance Disposal (EOD) for the public sector. The explosives requiring disposal are thermally treated at the Open Burn (OB) or the open detonation (OD) units located at the Churchill Range of the Explosives Experimental Area (EEA) at Dahlgren.

The EEA, which is commonly referred to as "Pumpkin Neck", is one of the two main areas comprising Dahlgren NSWC. The Upper Machodoc Creek passes through Dahlgren NSWC, cutting the facility into these two areas, the Mainside which consists of 2677 acres and the EEA which comprises 1614 acres (**Figure 4.2**; Bell, 1996). The EEA is composed of > 60% forest and marshland, with two open areas (Churchill Range and Harris Range) for munitions testing and disposal activities (**Figure 4.3**). The Churchill Range includes OB and OD areas as well as a fast cook-off area, and other facilities for ordnance and energetics testing, including drop test towers, static thrust stands, and other facilities. This ESTCP demonstration will be conducted on the Churchill Range.

4.1.1 Demonstration site geology and hydrogeology

4.1.1.1 Basic geology

The geology of the EEA was studied by the U.S. Geologic Survey in the mid-1990's (2), and has been the subject of additional investigative work by the URS Group Inc. (71, 72) and APTIM under ESTCP Project ER-201028. The surface of the EEA varies in elevation from ~ 0 to 30 ft above mean sea level (amsl), and the surface topography is basically flat. The geology of the site consists of two sequences of fluvial-estuarine deposits (Pleistocene) that overlie marine deposits (Pleistocene-Eocene) of the Nanjemoy-Marlboro confining unit (Bell, 1996; **Figure 4.4**).

The surficial water bearing unit is the Columbia aquifer, which is the unit within which the demonstration will be conducted. The Columbia aquifer unconformably overlies the upper confining unit (clay with significant organic deposits) across most of the EEA and ranges from < 8 ft to ~ 34 ft thick. The Columbia aquifer consists of sand, silt and clay with a pebble deposit at the bottom (on top of the underlying confining layer). The upper confining layer was observed to be absent in the central region of the OB/OD area; rather the Columbia aquifer appears to directly overlie the Nanjemoy-Marlboro confining unit in this region, which consists of glauconitic fine grained sands of the Nanjemoy formation (2, 72).

Figure 4.1. Location of the Dahlgren NSWC Site (URS, 2010).

Figure 4.2. Map Showing the Main Areas of Dahlgren NSWC (URS, 2007).

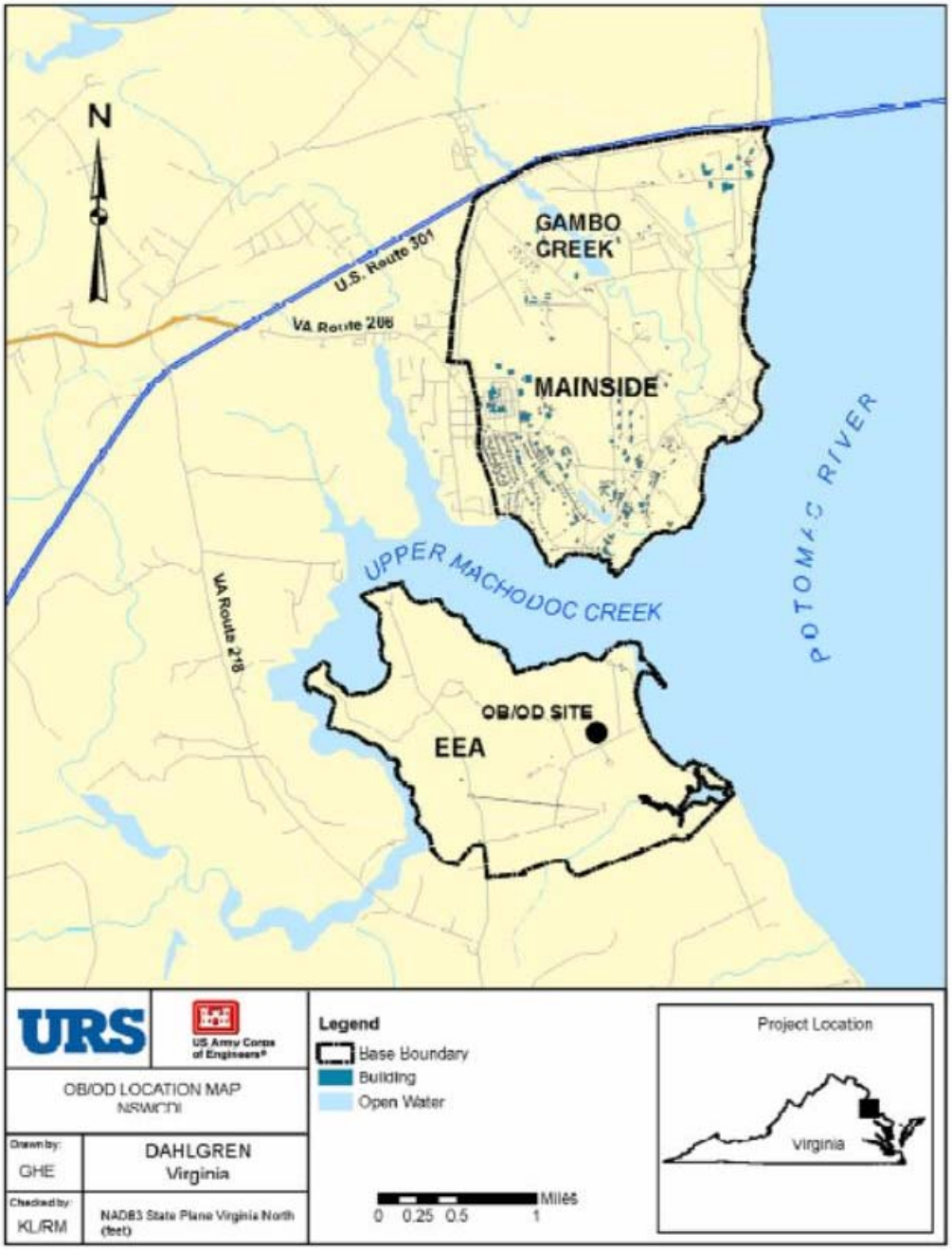

Figure 4.3. Map showing the Churchill Range of Dahlgren NSWC.

The inset provides the location of the Range within the EEA (URS, 2010).

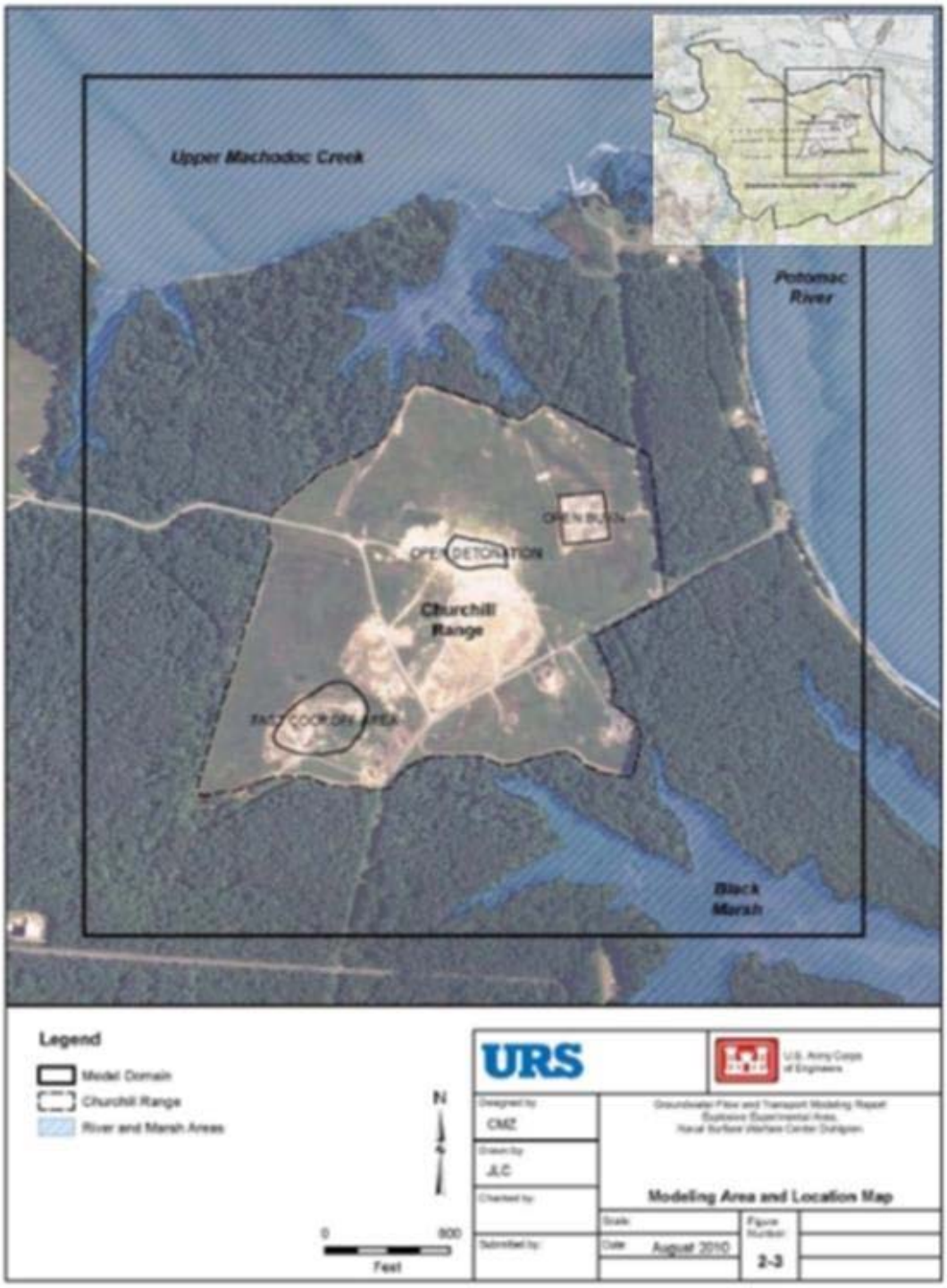

Figure 4.4. Schematic of the Geologic and Hydrogeologic Units of the EEA (Bell, 1996).

<table>
<tr><th colspan="3">GEOLOGIC UNIT</th><th>HYDROGEOLOGIC UNIT</th></tr>
<tr><td rowspan="3">QUATENRARY</td><td>HOLOCENE</td><td colspan="2">Alluvial, paludal, and fill deposits</td><td rowspan="2">Columbia aquifer</td></tr>
<tr><td rowspan="2">PLEISTOCENE</td><td colspan="2">Tabb Formation (Sedgefield Member)</td></tr>
<tr><td colspan="2">Pleistocene deposits, undifferentiated</td><td>upper confining unit</td></tr>
<tr><td colspan="3"></td><td>upper confined aquifer</td></tr>
<tr><td rowspan="3">TERITIARY</td><td rowspan="2">EOCENE</td><td rowspan="2">Nanjemoy Formation</td><td>Woodstock Member</td><td rowspan="3">Nanjemoy-Marlboro confining unit</td></tr>
<tr><td>Potapaco Member</td></tr>
<tr><td>PALEOCENE</td><td colspan="2">Marlboro Clay</td></tr>
</table>

NOT TO SCALE

Figure 4.5. Map Showing the Well Locations on the Churchill Range of Dahlgren NSWC circa 2007 (modified from URS, 2007).

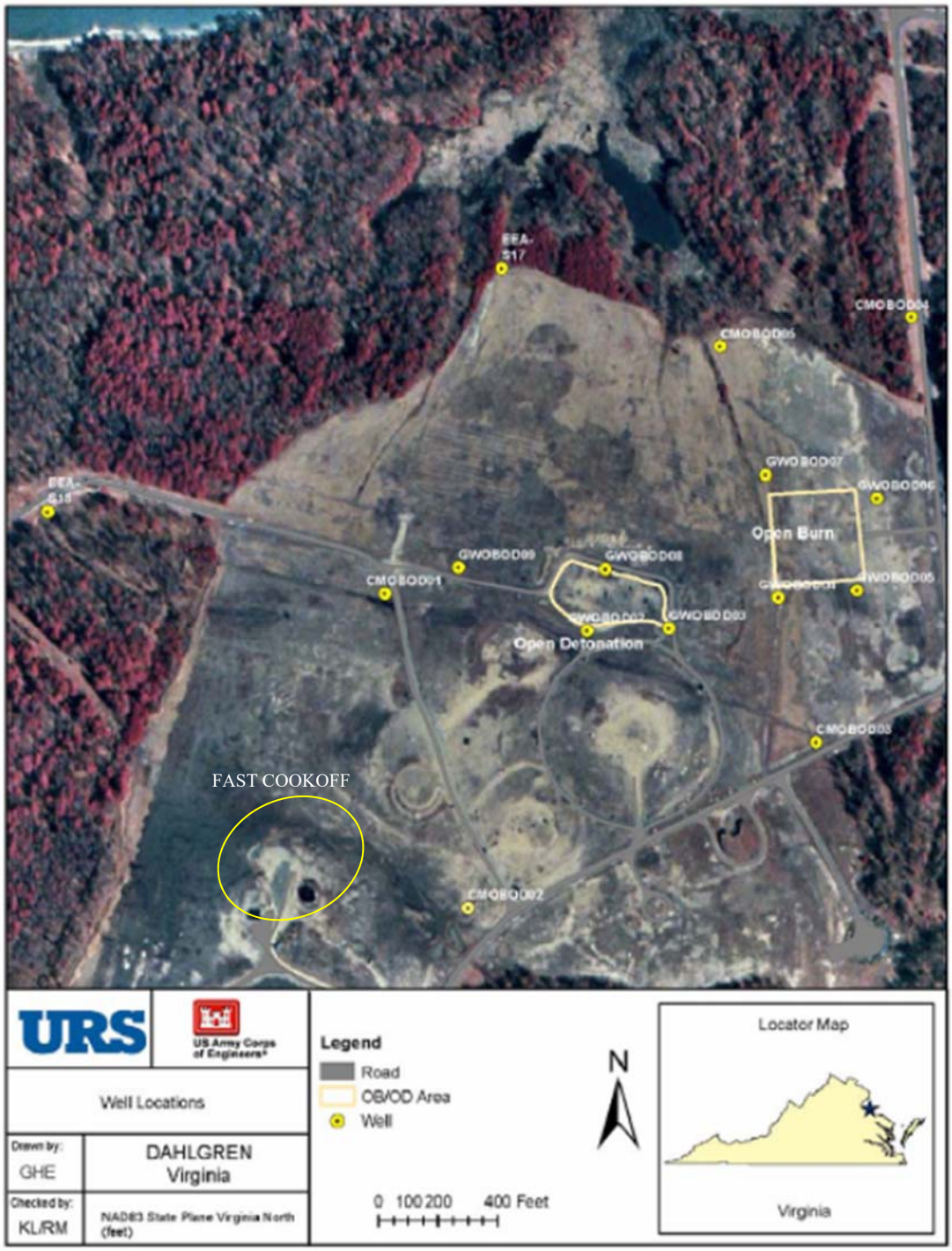

4.1.1.2 Groundwater monitoring wells

A total of 15 groundwater monitoring wells were present in the Churchill Range Area prior to the initiation of project ESTCP Project ER-201028 (**Figure 4.5**). Two of these wells were installed by USGS in 1993 as part of the overall site investigation work (EEA-S17, EEA-S18), during which time a total of 28 wells were drilled across the entire EEA (Bell 1996 #12). Eight (8) additional wells were installed by USGS in the Churchill Range area in 1998 (GWOBOD02-GWOBOD09), and five (5) wells were subsequently installed in 2007 by URS during site assessment studies (CMOBOD01-CMOBOD05). All of these wells are screened in the Columbia Aquifer.

4.1.2 Site characterization during ESTCP ER-201028

A total of 27 piezometers were installed during three separate events in support of project ER-201028. The installation and sampling of these piezometers was conducted primarily to assess site geochemistry, to characterize RDX (and perchlorate) plumes in the area, and to determine the optimal location to place an *in situ* biobarrier. The wells for that barrier were subsequently installed and an initial injection of emulsified oil was conducted in February, 2013. Further details are provided in (40). In general, the assessment focused on a location east of the Fast Cookoff area (see **Figure 4.5**). The initial RDX stable isotope work to evaluate MNA of RDX in an aerobic aquifer along a flowpath (Section 3.1) utilized the piezometers installed in the area. The details of the site geology, well installation, and all other characterization work were provided in the Project Final Report for ESTCP ER-201028 (40). The data that were important for the implementation of this project are provided in the subsequent subsections.

Site characterization work was performed during 2010 and 2011 to (1) better define the extent of contamination in the region; and (2) to confirm the local hydrogeology, including lithology, hydraulic conductivity, and the estimated velocity and direction of groundwater flow (see below). In addition, a series of treatability studies using sediment and groundwater from the area around CMOBOD02 were performed, including microcosms and flow-through columns. Relevant details of these studies are provided in Section 5.2.1.

During initial site assessment work during October 2010, four piezometers were installed using a direct-push technology (DPT) rig to gather water chemistry data to determine the local extent of the plume of RDX and perchlorate intersected by monitoring well CMOBOD02. Continuous soil core samples were collected and logged for each of the boring locations (Dahlgren 01 through Dahlgren 04). Upon completion of each of the borings, 1" piezometers were installed in the open boreholes. The locations of these borings and piezometers are provided in **Figure 4.6** (borings became piezometers Dahlgren 01-04) and **Figure 4.7**.

An additional investigation was performed in May 2011 based on the results from October 2010. The purpose of this investigation was to confirm the previously reported groundwater potentiometric surface and likely flow direction, and to determine the approximate extent of groundwater contamination in the vicinity of monitoring well CMOBOD02. This contamination is presumed to originate from the Fast Cookoff Area (**Figure 4.5**). Thirteen (13) soil boring locations were selected east of the Fast Cookoff area, in and around a surficial swale feature that appeared to be directly affecting the groundwater flow direction and energetics plume migration at the site. Continuous soil cores were collected through the first encountered water bearing layer to the confining clay unit using DPT. Upon the completion of the soil borings and review of the boring logs, 1" piezometers were installed at each location.

The piezometers were surveyed and site-wide groundwater levels and groundwater chemistry parameters (e.g. DO, pH, etc.) were measured at the end of the investigation. Groundwater samples were collected from the piezometers and analyzed for perchlorate, explosives, and additional groundwater chemistry parameters at APTIM's laboratory in Lawrenceville, NJ.

Due to discrepancies discovered in the contaminant plumes compared to historical mapping and modeling at the site, along with the need to further our understanding of the groundwater flow regime east of the Fast Cookoff area, an additional subsurface investigation was performed in October 2011. The focus of this investigation was the area south of the OB/OD area (**Figure 4.5**), where the majority of the groundwater plume was detected during the previous sampling events. Ten additional piezometers were installed following the same construction criteria used during the May 2011 investigation. These piezometers were similarly installed with the screened portion of the piezometer contained within the upper water bearing unit overlying the clay. The piezometers were pumped continuously for approximately 10 to 30 minutes to remove any suspended sediments in the groundwater prior to sample collection. Site-wide groundwater levels were collected at the end of the investigation.

4.1.2.1 Groundwater flow direction and rate

Groundwater was typically encountered between 1.5 and 5.8 ft bgs during the May 2011 groundwater survey, and 0.5 to 3.8 ft bgs in October 2011. The average depth to groundwater across the Churchill Range was 3.8 ft bgs in May 2011 and 2.1 ft bgs in October 2011 indicating a seasonal fluctuation of approximately 1.5 to 2 ft. It should be noted that the October site characterization event occurred following an exceptionally wet fall season (including passage of Hurricane Irene and Tropical Storm Lee), which caused widespread inundation of the Churchill Range site. Groundwater measurements compiled during the two characterization events were used to create potentiometric surface maps (**Figure 4.8** and **Figure 4.9**, respectively). The figures confirm previous site data which identifies a general groundwater gradient to the south-southeast. Using an estimated aquifer porosity of 0.30, calculated K values of 4.3 to 4.4 ft/day from slug and pump tests in well CMOBOD02, and a localized hydraulic gradient of 0.004 over the 900 ft study area for the potential biobarrier, the expected horizontal flow velocity in this area is approximately 0.059 ft/day or 21.4 ft/year. The K value and horizontal flow rate calculated based on the slug test data falls within the ranges reported in previous groundwater reports for the area (2, 70).

4.1.2.2 Groundwater chemistry

In November 2008, we sampled several wells on the Churchill Range to conduct studies for SERDP Project ER-1607. Basic geochemistry was collected for wells GWOBOD02, GWOBOD03, CMOBOD02, and EEA-S17 (as an uncontaminated control well), along with analysis of metals, explosives, anions and cations. The basic geochemical parameters for these Churchill Range wells in 2008 are provided in **Table 4.2**. During the 2010 and 2011 sampling events, pH and dissolved oxygen measurements were collected from each of the piezometers prior to collecting groundwater samples using a field meter and in-line flow cell. These measurements were used to create maps depicting geochemical conditions at the Churchill Range. The pH measurements east of the Fast Cookoff area ranged from 3.9 to 6.4, averaging approximately 4.9. Dissolved oxygen measurements ranged from 0 to 9.6 mg/L, averaging approximately 5.3 mg/L. Maps showing the October, 2011 pH and dissolved oxygen concentrations are presented in **Figure 4.10** and **Figure 4.11**, respectively.

Table 4.2. Initial Water Quality Data from Four Permanent Wells on the Churchill Range.

	Parameter						
Well ID	**pH (SU)**	**ORP (mV)**	**DO (mg/L)**	**Sp. Cond. (µS/cm)**	**Cl^- (mg/L)**	**NO_3^- (mg/L)**	**SO_4^- (mg/L)**
GWOBOD02	4.20	289	1.5	0.079	8.4	1.2	9.5
GWOBOD03	4.45	236	3.7	0.073	6.7	0.9	6.4
CMOBOD02	4.76	424	4.1	0.052	3.8	<0.1	4.3
EEA-S17	4.02	293	1.9	0.039	2.2	0.3	8.5

Figure 4.6. Sampling Locations for Preliminary Site Assessment in the Plume Emanating from the Fast Cookoff Area.

Concentration of perchlorate and RDX in groundwater taken from each borehole are provided.

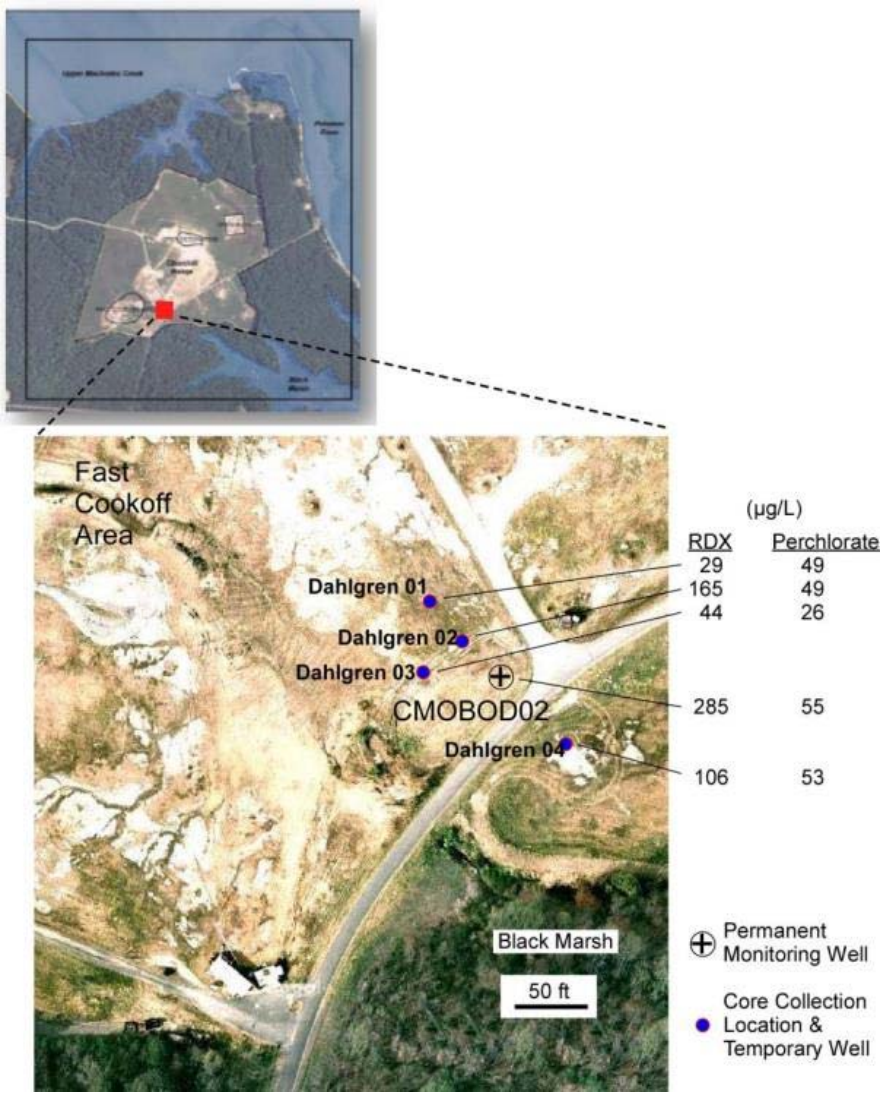

Figure 4.7. Map Showing the Well and Piezometer Locations on the Churchill Range of Dahlgren NSWC (November 2011).

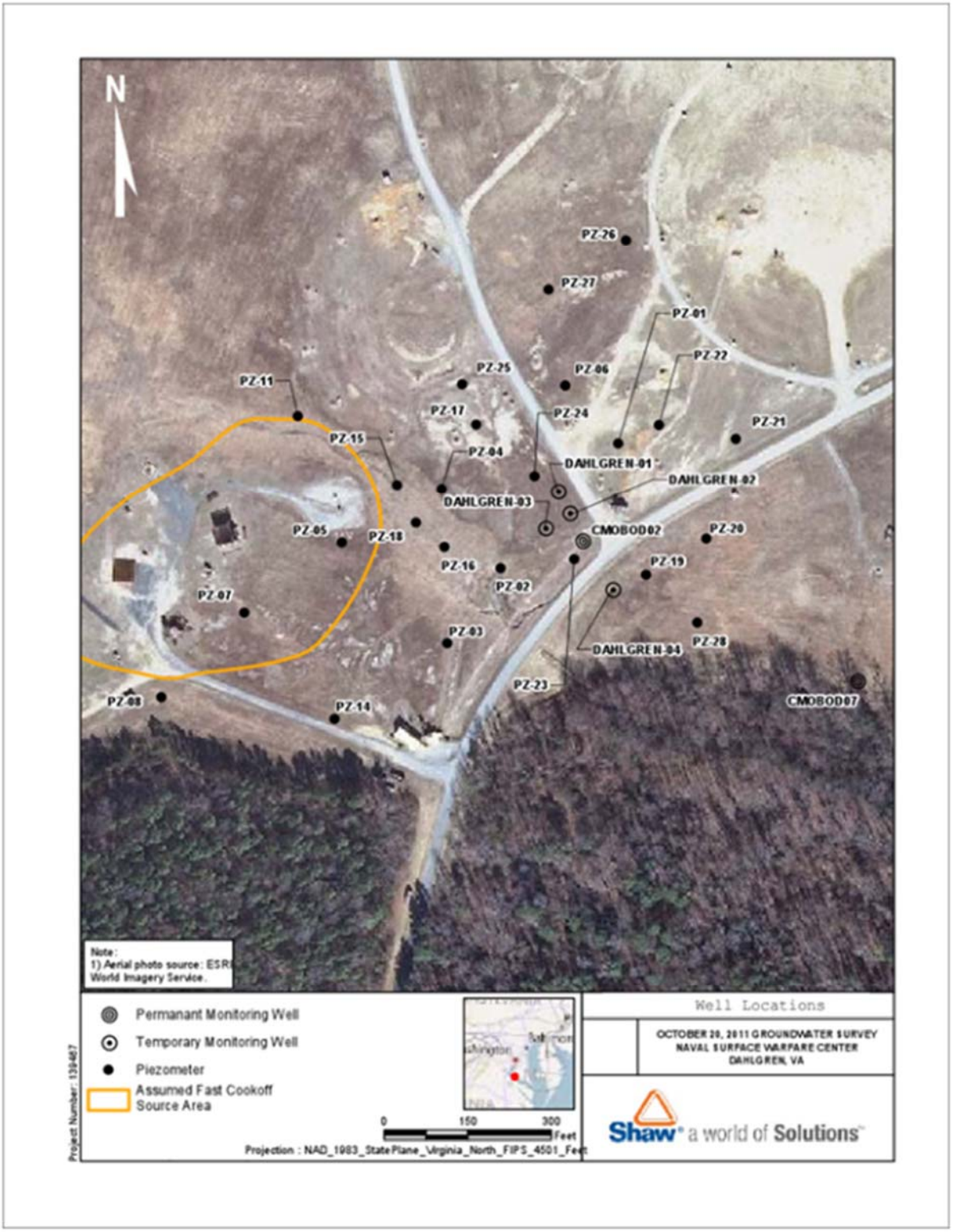

Figure 4.8. Potentiometric Surface Map of the Churchill Range in May 2011.

Figure 4.9. Potentiometric Surface Map of the Churchill Range in October 2011.

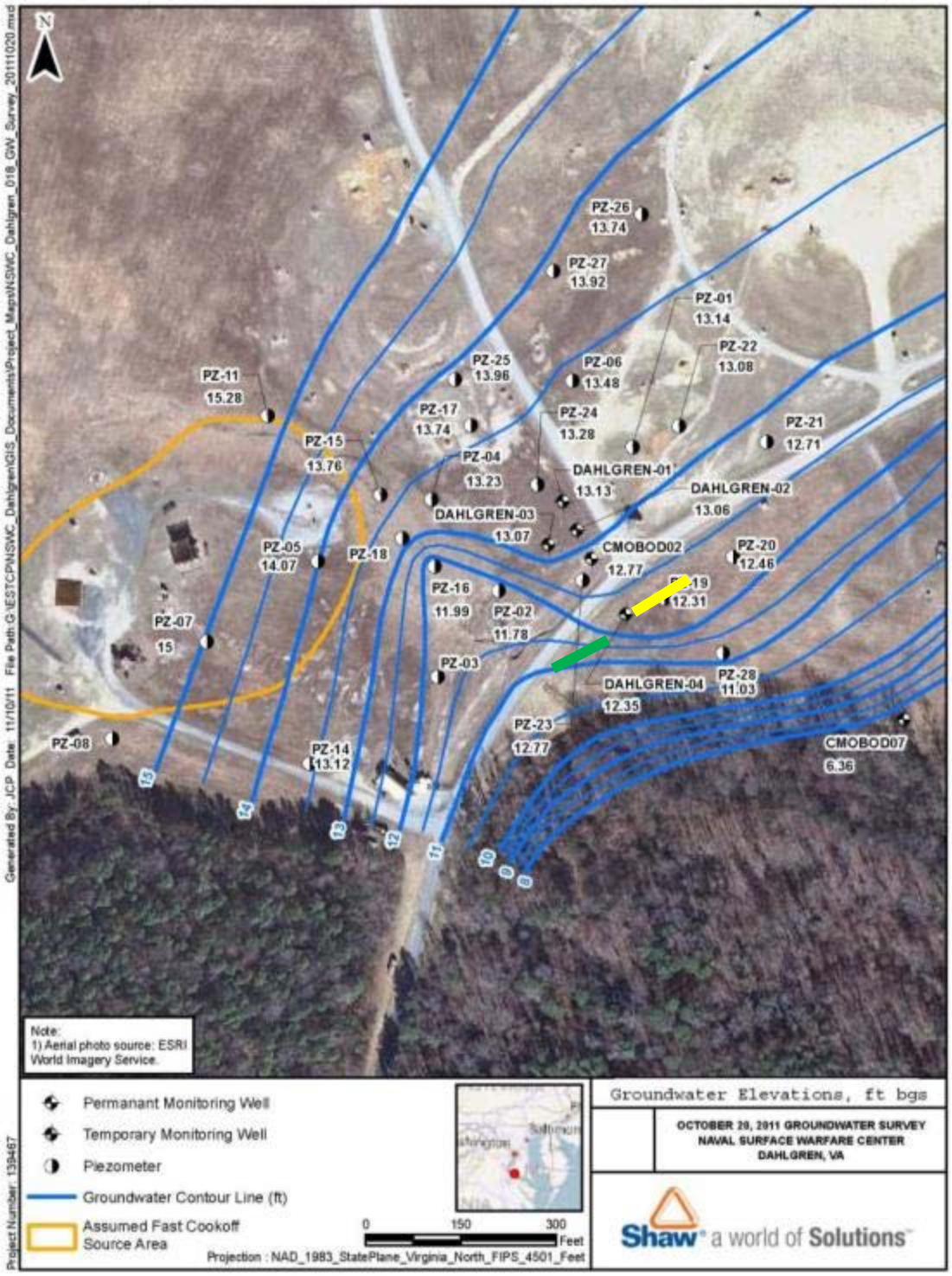

Figure 4.10. Dissolved Oxygen Contours in the Southeast Area of the Churchill Range in October 2011.

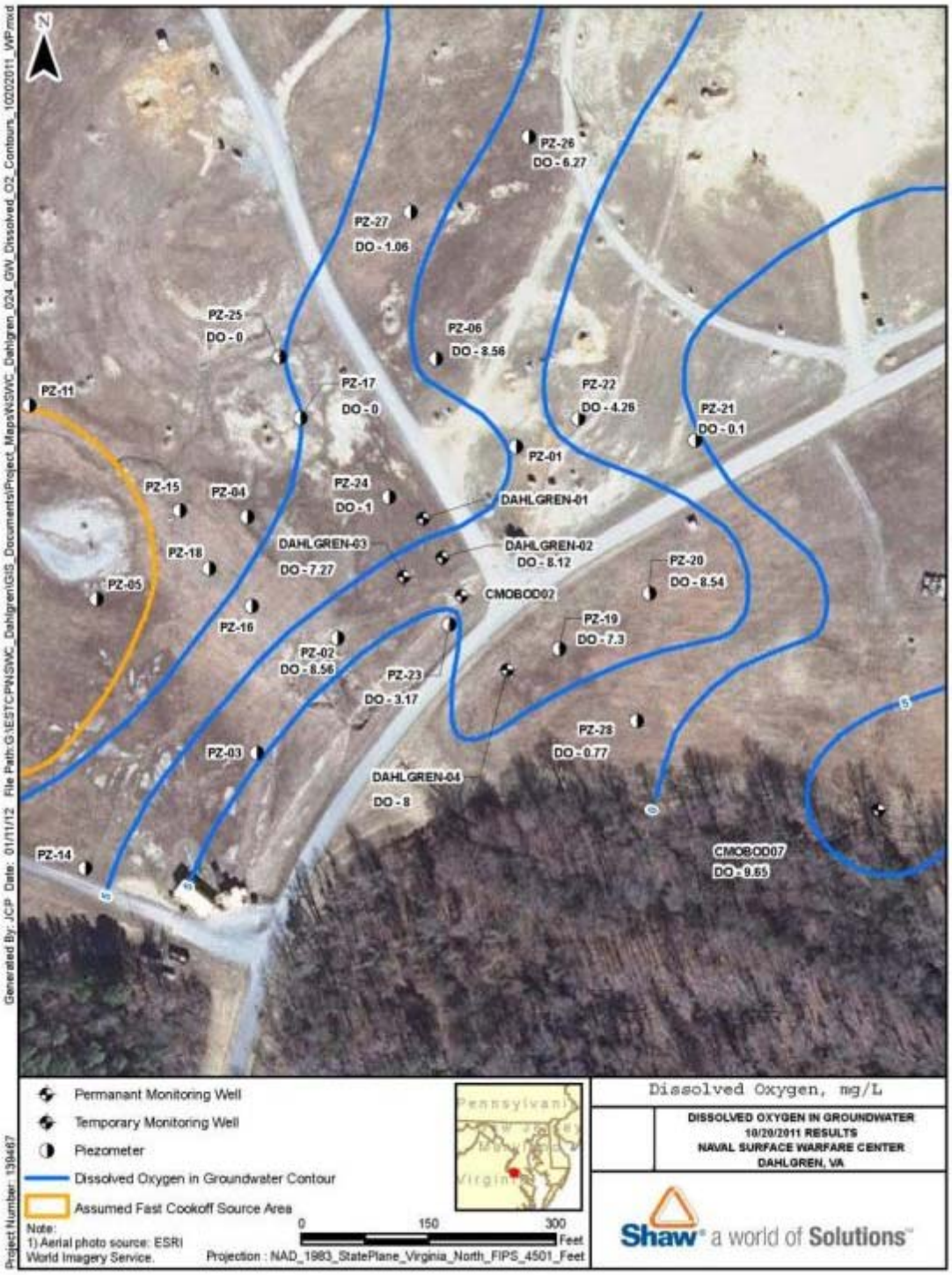

Figure 4.11. pH Contours in the Southeast Area of the Churchill Range in October 2011.

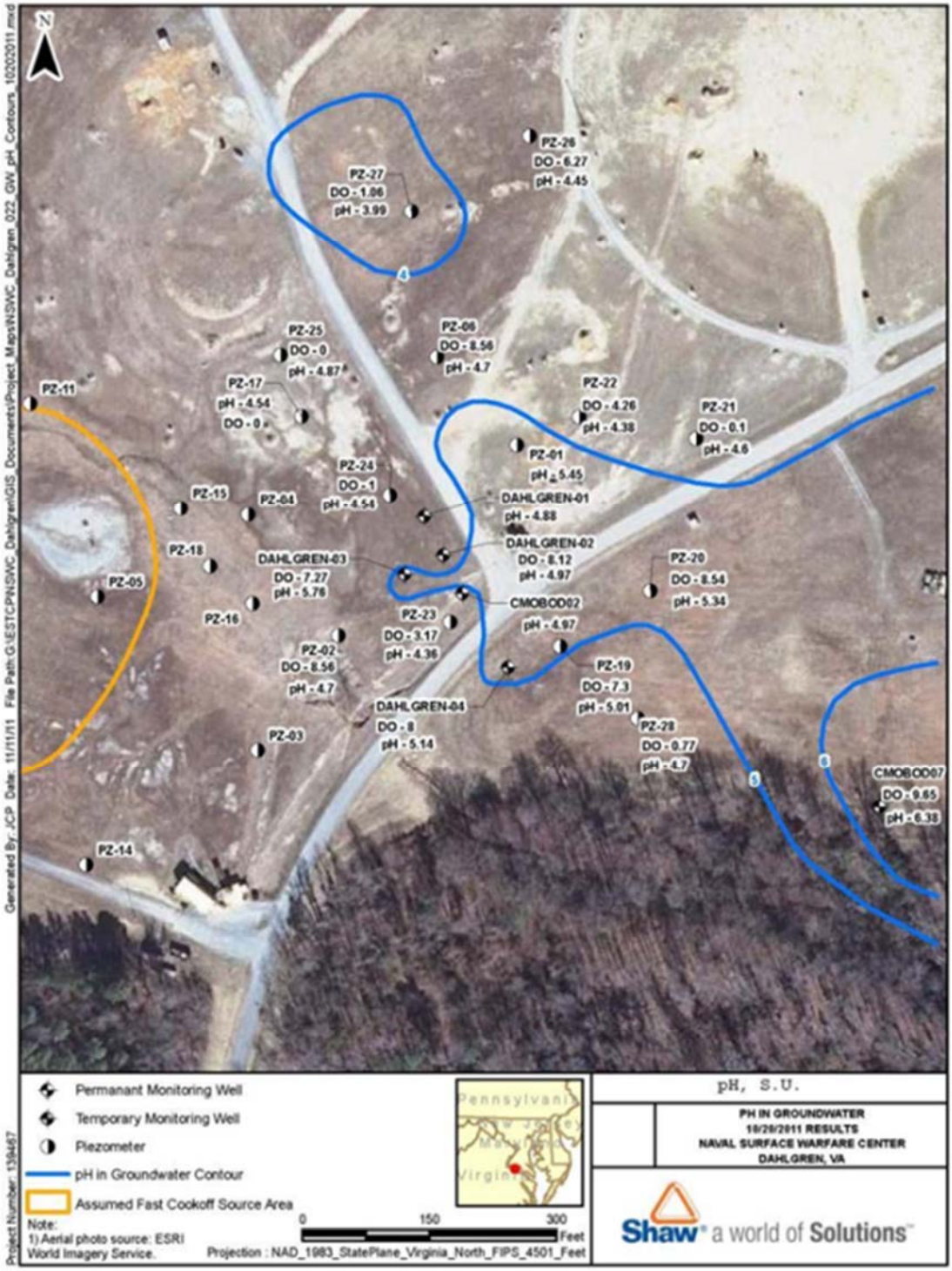

4.1.2.3 Explosives in test site groundwater

Groundwater samples were collected for analysis of explosives by EPA Method 8330 during all three site characterization events. Data from the first sampling event in which wells Dahlgren 01 to Dahlgren 04 were installed are provided in **Figure 4.6**. (Locations L1-L4 in **Figure 4.6** became wells Dahlgren 01-04.). During the second site characterization event in May 2011, piezometers PZ-01 to PZ-07, PZ-11, and PZ-14 to PZ-18 were installed (13 total piezometers) and sampled. The primary focus of this site characterization event was the area to the southeast of the Fast Cookoff region and to the northeast of CMOBOD02, although some piezometers also were installed to the north and south of this region. The data collected for perchlorate, RDX and HMX from this event are provided in **Figure 4.12**. The regions to the north (PZ-11) and directly to the east (PZ-15, PZ-04, PZ-18, PZ-16) of the Fast Cookoff generally had levels of RDX, HMX and perchlorate that were below detection (10 µg/L for HMX and RDX, and 0.5 µg/L for perchlorate). RDX (but no HMX) was detected just south of the Fast Cookoff Area in PZ-07 and a low concentration of HMX (but no RDX or perchlorate) was detected further south in PZ-14. The most significant and consistent concentrations of each target compound in groundwater were found further east (PZ-01, PZ-02, PZ-03, Dahlgren 01-04) and even slightly northeast of the Fast Cookoff Area (PZ-06).

The general absence of explosives directly east of the Fast Cookoff Area was inconsistent with this region being the primary source of these contaminants in the vicinity of well CMOBOD02 as originally hypothesized, particularly considering the general direction of the groundwater gradient in this region to the east-southeast (**Figure 4.8** and **Figure 4.9**). Rather, the data suggest that there are one or more source areas to the north of CMOBOD02, and that contamination may extend further east than originally thought. As a result of the data collected in May 2011, a third site assessment event was conducted in October 2011 to determine contaminant concentrations in groundwater further north, south and east of CMOBOD02. During this event, an additional 10 piezometers were installed (PZ-19 through PZ-28), and groundwater samples were collected from each. A number of the existing piezometers and wells were also sampled during this phase. The piezometers present near the Fast Cookoff area that had low or non-detect concentrations in May 2011 were not sampled during October 2011 due to limited available time on the range.

The data from the October, 2011 sampling event were compiled and contour maps of RDX (**Figure 4.13**) and HMX (**Figure 4.14**) were prepared based on the data. The data indicate that the majority of the contamination in groundwater flowing towards the Black Marsh originates from multiple point sources to the east of the Fast Cookoff Area and to the south and west of the central "arena". The contour maps drawn in the previous figures are our best current interpretation of the data. Based upon all available data, we initially selected two possible locations for the installation of the biobarrier, and subsequently narrowed the location to one based primarily on geological constraints. The region shown in green on **Figures 4.13** and **4.14** was the location of the biobarrier. Injection wells (20) were installed along with a number of new plot monitoring wells in this region. The basic design of the plot is provided in **Figure 4.15**, Further information on the stable isotope sampling that was conducted in this region is provided in Section 5.4.5.

Figure 4.12. RDX, HMX and Perchlorate Data from Piezometers Installed During the May 2011 Site Investigation.

Figure 4.13. Plume Map for RDX in the Southeast Area of the Churchill Range.

Two potential locations for the emulsified oil biobarrier are shown in green and yellow, respectively. The barrier was installed in the green area.

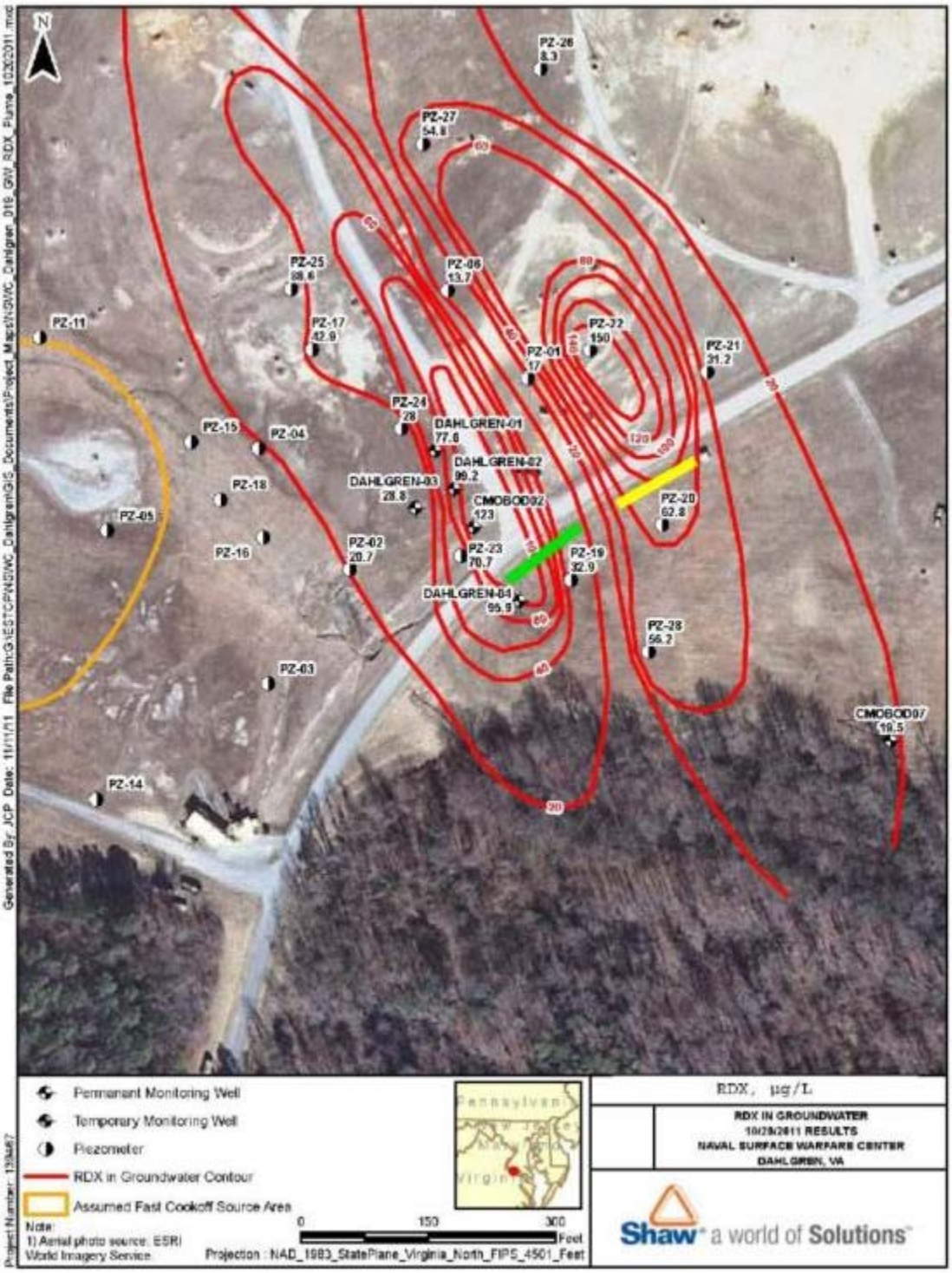

Figure 4.14. Plume Map for HMX in the Southeast Area of the Churchill Range.

Two potential locations for an emulsified oil biobarrier are shown in green and yellow, respectively. The barrier was installed in the green area.

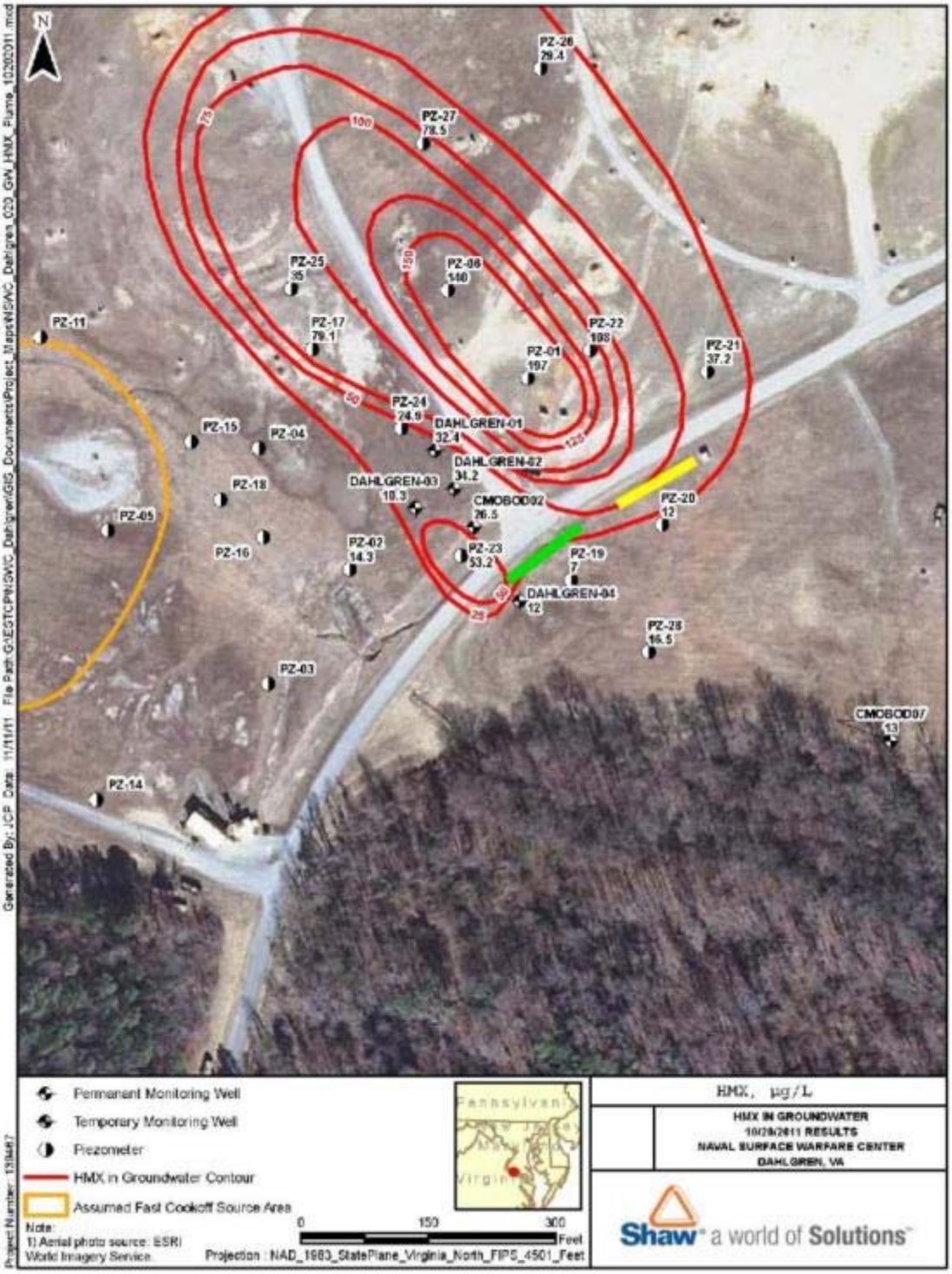

Figure 4.15. Schematic of Biobarrier Demonstration Plot Layout.

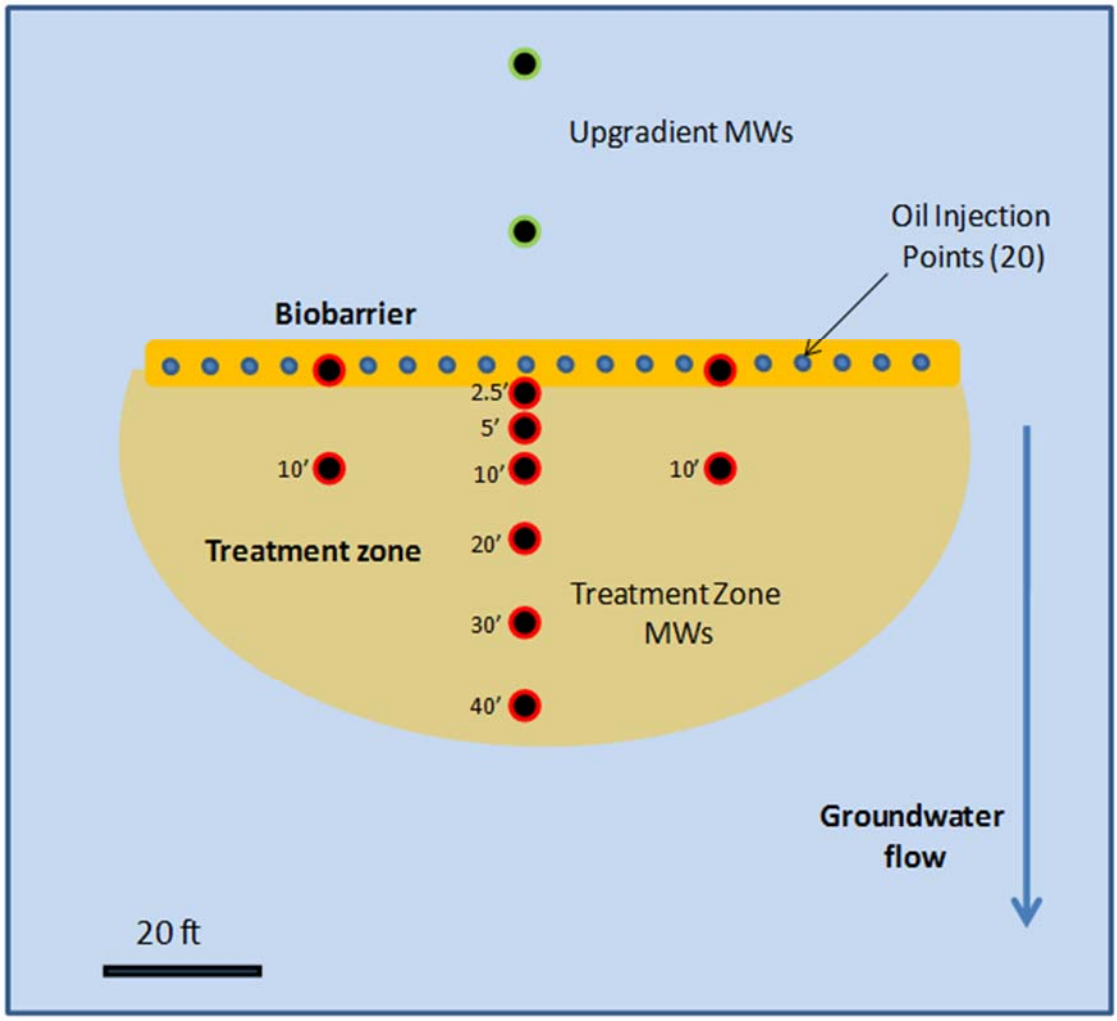

4.2 SITE 2: UMATILLA CHEMICAL DEPOT

The Umatilla Chemical Depot (UMCD) was the second site selected for assessment of C and N stable isotope fractionation of RDX during biodegradation for this project. In this case, the primary objective was to determine isotope fractionation during a field test at the site that involved injection of carbon substrate in one plot to promote anaerobic RDX biodegradation and the injection of aerobic RDX degrading bacteria and carbon source in a second plot to promote aerobic RDX degradation. A preliminary incubation period in the second test plot prior to bioaugmentation was used to assess natural attenuation of RDX under aerobic conditions. This project was funded by ESTCP (ESTCP Project ER-201207 "Bioaugmentation for Aerobic Bioremediation of RDX-Contaminated Groundwater") and led by Dr. Mandy Michalsen at USACE Seattle District. Our laboratory conducted significant treatability study work for this effort in order to evaluate the transport and activity of different aerobic RDX-degrading strains (25) and grew all of the aerobic cultures used for large-scale injection. This presented a unique opportunity to quantify stable isotope fractionation of RDX *in situ* under differing geochemical and microbiological conditions.

4.2.1 UMCD site characteristics

4.2.1.1 UMCD location and history

The Umatilla Chemical Depot (UMCD; formerly called the Umatilla Ordnance Depot) is located on ~ 20,000 acres in northeastern Oregon, approximately 180 miles east of Portland (**Figure 4.16**). The Umatilla Ordnance Depot was constructed in 1941-1942 as an Army ammunition supply depot consisting primarily of 1001 ammunition supply igloos (**Figure 4.17**) and a variety of administration buildings and housing. Areas of the ammunition depot were contaminated with explosives and metals as a result of demilitarization activities, particularly the disposal of ~ 85 million gallons of explosives-containing wastewater from hog-out operations into two unlined lagoons during the 1950s and 1960s (73). A groundwater plume emanates from these lagoons. A groundwater pump-and-treat system installed in 1997 was designed to operate at ~ 150 GPM and to remove explosives through adsorption to granular activated carbon (GAC). Water from the system is re-infiltrated into the ground. Technologies are currently being evaluated to optimize explosives removal and reduce the life of this system.

4.2.1.2 UMCD regional geology

The UMCD is present in the Lower Umatilla Basin, which is a topographic trough between the Blue Mountains of Oregon and the Columbia Hills of Washington (78). The basin is underlain by the Columbia River Basalt Group, above which is up to 250 ft of alluvial sediments and weathered basalt. The alluvial sediments include sands, silts, and gravels deposited largely during the Pleistocene Epoch. The alluvial aquifer is a major source of private water for rural residents and of municipal water for several of the cities in the region, including Hermiston and Boardman. The alluvial aquifer is considered to be very susceptible to contamination from surface activities due to the fact that water readily passes through the unsaturated zone to the alluvium (78). Primary sources of recharge water include irrigation water, and leakage from canals, streams, and reservoirs; rainwater is only a minor source of groundwater recharge. The depth to groundwater under UMCD ranges from 60 to 100 ft below ground surface (bgs), with a saturated thickness of ~ 15 to 35 ft near the explosives washout area (73). The surface gradient is flat with seasonal groundwater flow dependent upon agricultural irrigation in the region.

4.2.1.3 RDX plume in groundwater at UMCD

The washout wastewater described in Section 4.2.1.1 seeped from the two disposal lagoons, ultimately contaminating approximately 350 acres of the alluvial aquifer. The contamination is confined to the shallow alluvium, which is referred to locally as the "Ordnance Gravel Aquifer". This highly conductive aquifer is aerobic throughout the area of the plume and has a neutral pH. A network of 78 groundwater wells was installed to characterize the explosives plume in the 1980's and 1990's. At the time of initial investigation, RDX concentrations ranged from ~ 6,800 µg/L to < 0.6 µg/L at the plume boundary (73). Other explosives, including trinitrotoluene (TNT), 2,4-dinitrotoluene (2,4-DNT), 2,6-dinitrotoluene (2,6-DNT), and HMX also were identified in groundwater, but generally with a smaller footprint than for RDX. A map showing the RDX plume is provided in **Figure 4.18**.

4.2.2 In Situ bioremediation study at UMCD

As previously noted, an *in situ* field demonstration was performed at UMCD to evaluated rates and extents of RDX biodegradation under anaerobic biostimulation and aerobic bioaugmentation. The primary study design and results have been published (21, 55) This study was conducted as a "push-pull" type test in two separate plots, the locations of which are shown on **Figure 4.19**. One plot was amended with a volume of site groundwater containing RDX, growth substrate (e.g., fructose) at a low concentration, a bromide tracer, and an aerobic RDX-degrading culture. Bulk aerobic conditions were maintained by introducing a low concentration of carbon source. The second plot received the same volume of groundwater amended with RDX, bromide tracer, and a higher concentration of an organic substrate to promote anaerobic RDX degradation. After injection ("push" phase) groundwater was pumped slowly from each well ("pull" phase), and sampling was conducted with time to quantify bromide, RDX, RDX metabolites, and the viability and activity of the bioaugmented culture. We collected samples for stable isotope analysis of C and N from both plots. *In situ* RDX degradation rates were determined from dilution-adjusted progress curves for RDX lost and metabolite formation. The fractionation factors for C and N in RDX (i.e., ε values) were compared to the bromide-adjusted rates of RDX loss in the aquifer, which were calculated in two different ways to account for background levels of RDX (Section 5.6.2). This approach was successfully applied to quantify *in situ* fractionation factors for O and Cl in perchlorate and N and O in nitrate at a site in Maryland (37). More details on the testing are provided in Section 5.4.6.

Figure 4.16. Map Showing the Umatilla Ordnance Depot and Boardman Bombing Range in Northeastern OR.

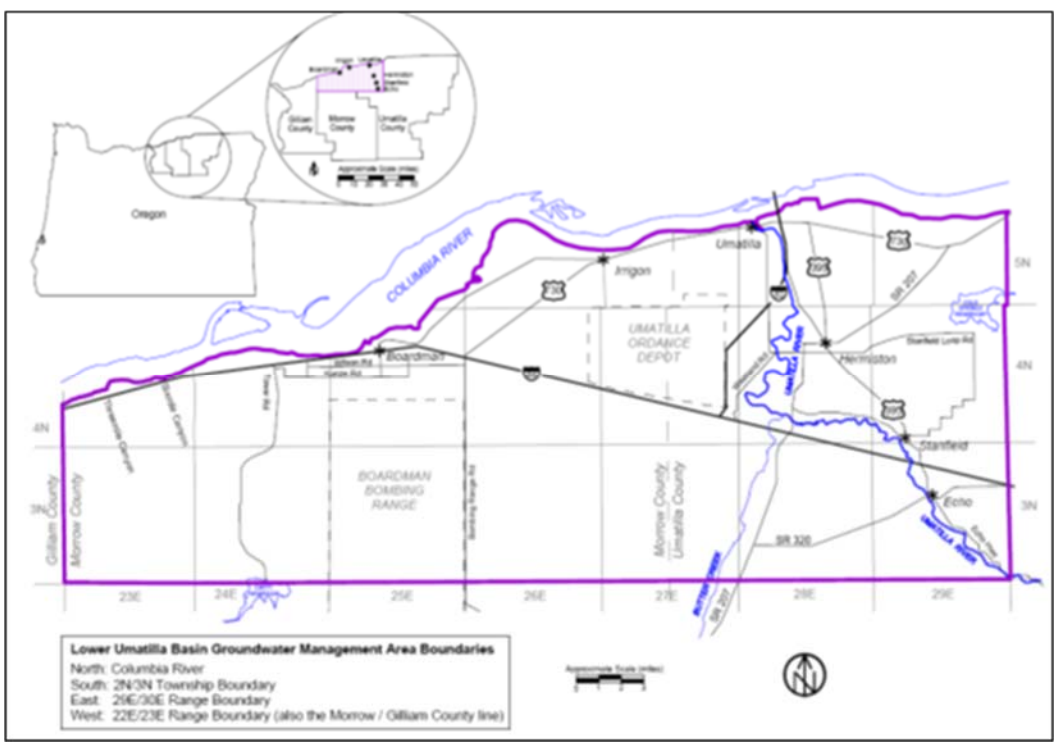

Map from (60)

Figure 4.17. Photo of Ammunition Igloos at UMCD (circa 2006).

Figure 4.18. RDX Plume Map at UMCD as of October 2008 (73).

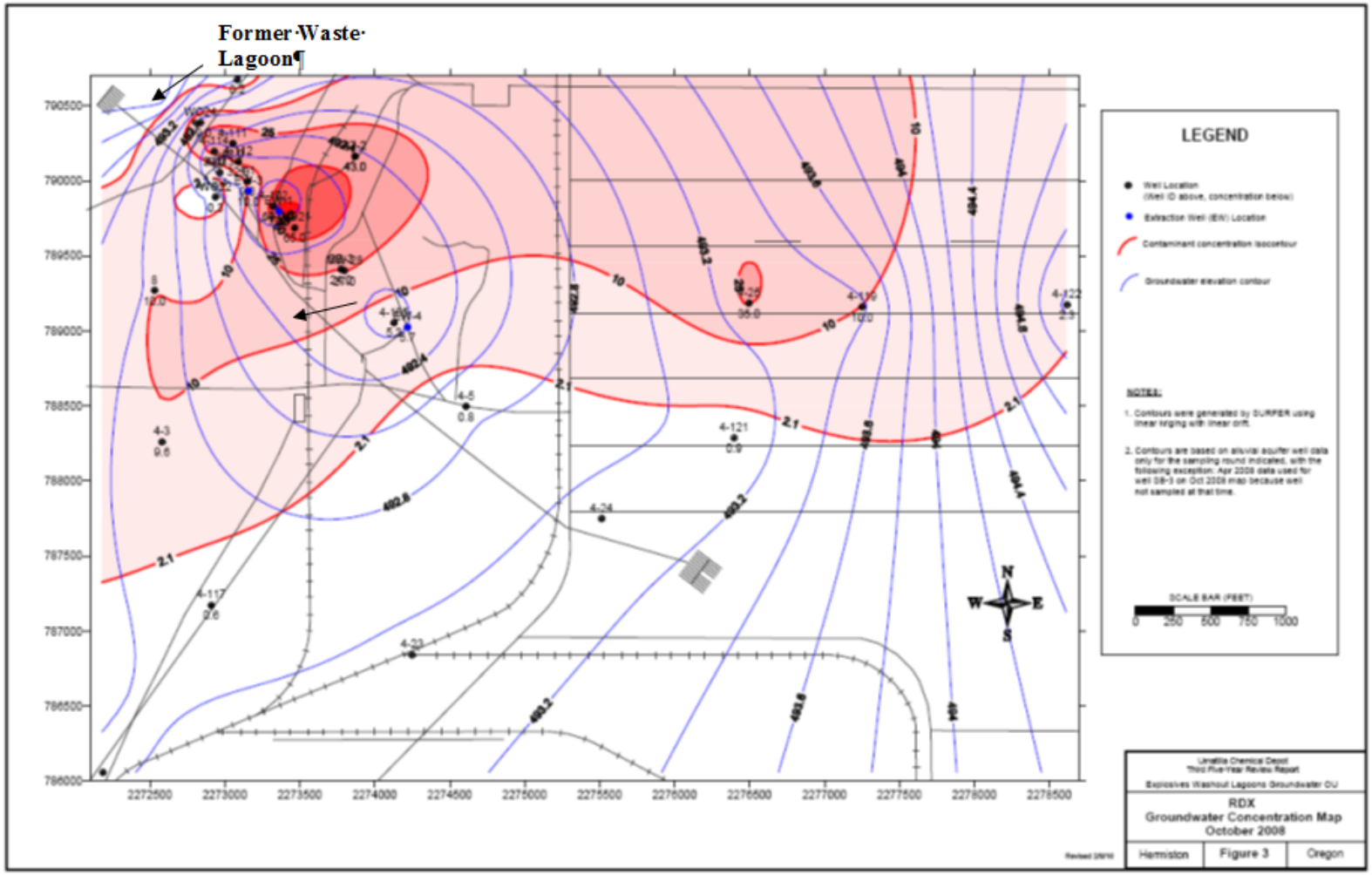

Figure 4.19. Top: Location of the Push-pull Test Plots on UMCD and Inset of test plot configuration. Bottom: A closer view of the wells within the test plot area.

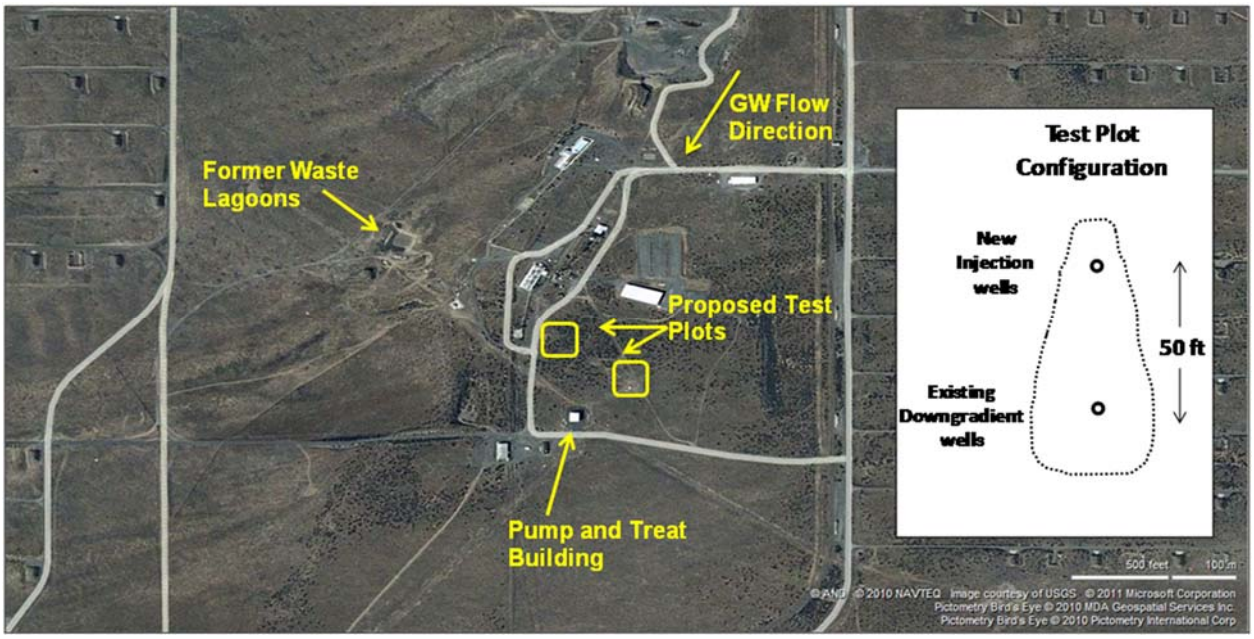

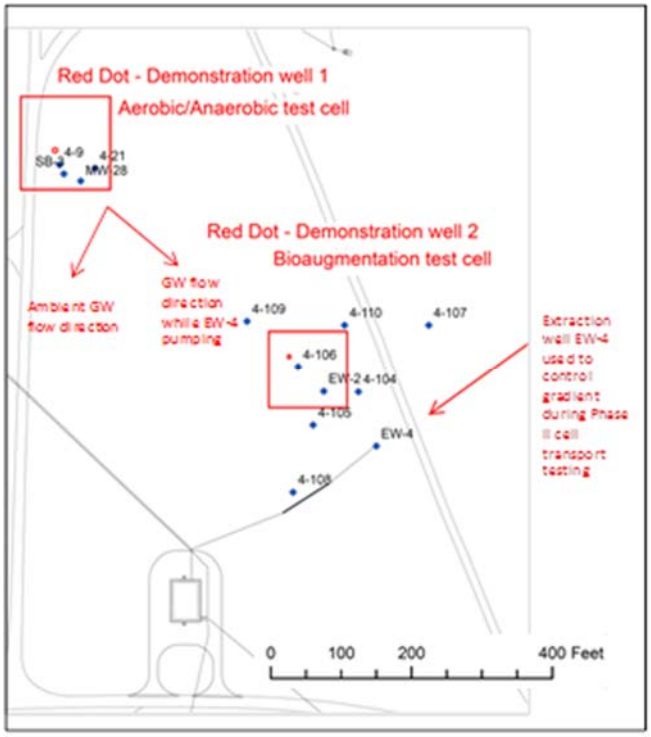

Page Intentionally Left Blank

5.0 TEST DESIGN

5.1 CONCEPTUAL EXPERIMENTAL DESIGN

The isotopic fractionation of RDX was measured at two separate sites (Dahlgren NSWC and UMCD), and in conjunction with two ongoing projects evaluating *in situ* RDX biodegradation under anaerobic and aerobic conditions. The projects at UMCD and Dahlgren were ESTCP ER-201207 "Bioaugmentation for Aerobic Bioremediation of RDX-Contaminated Groundwater" and ESTCP ER-201028 "Passive Biobarrier for Treating Co-Mingled Perchlorate and RDX in Groundwater at an Active Range", respectively. At the UMCD site, separate push-pull tests were conducted to quantify aerobic and anaerobic RDX biodegradation potential. At Dahlgren NSWC (1) an MNA assessment was conducted under bulk aerobic conditions ($\delta^{15}N$ in RDX and $\delta^{15}N$ and $\delta^{18}O$ in NO_3^- were measured) and (2) $\delta^{15}N$ and $\delta^{13}C$ in RDX were measured during anaerobic biodegradation of RDX downgradient of an emulsified oil biobarrier. At the UMCD site, RDX isotope fractionation was evaluated during push-pull testing to assess RDX biodegradation under aerobic bioaugmentation conditions and under anaerobic biostimulation conditions. In addition, in order to support MNA and field assessments, the C and N stable isotope values in a variety of different RDX sources, including some military-produced sources was analyzed, so that the range of initial values is known.

5.2 BASELINE CHARACTERIZATION ACTIVITIES

5.2.1 C and N stable isotope values in RDX from different sources

There are presently few published data on the $\delta^{15}N$ and $\delta^{13}C$ values in RDX samples from different sources. Among the 14 RDX samples analyzed in this project, $\delta^{15}N$ values varied from -15.8 ‰ to +9.1 ‰, with several of the materials tested being analytical standards (for EPA Method 8330) and others derived from custom synthesis **(Table 5.1)**. The average standard deviations of $\delta^{15}N$ for the various samples averaged 0.7 ‰. The $\delta^{13}C$ values of the RDX samples also varied somewhat, ranging from -39.8 ‰ to -29.7 ‰, with an average standard deviation for all of the different samples of 1.1 ‰. Of the RDX samples known or assumed to be derived from material synthesized at Holston Army Ammunition Plant (HAAP, denoted with an asterisk in **Table 5.1**), the average $\delta^{15}N$ and $\delta^{13}C$ values were -0.6 ± 0.8 ‰ and -37.3 ± 2.1 ‰, respectively. In another recent study, Howa et al. (2014) analyzed 100 different RDX samples obtained from 12 different factories (44). They found a range of $\delta^{15}N$ values from -17.4 ‰ to +8.5 ‰ which was similar to our results, and found a somewhat wider range of $\delta^{13}C$ values from -49.5 ‰ to -16.6 ‰.

The variation in $\delta^{15}N$ and $\delta^{13}C$ among the samples tested suggests that some different RDX sources may be distinguishable from one another, and that $\delta^{15}N$ values may be the most diagnostic in determining sources. This would provide additional impetus to further develop an IRMS-based method for forensic source determination of RDX. However, a much larger database of RDX sources (particularly non-US military sources) would be required as many of the samples tested (e.g., standards and custom syntheses) would not be expected to be found in soils or groundwater in the US. The samples presumed to be from HAAP all had a similar stable isotope signature for both N and C isotopes, which may represent the typical expected isotopic values on military sites where this material was utilized. However, it is also possible that these values differed over time, as no historical samples were available for analysis.

Table 5.1. $\delta^{15}N$ and $\delta^{13}C$ Values of Neat RDX from Different Sources.

RDX source	$\delta^{15}N$ (‰ Air)			$\delta^{13}C$ (‰ VPDB)	
	AVG	SD		AVG	SD
Accustandard	-5.8	0.8		-33.6	1.4
Chemservice	0.2	0.7		-32.2	1.0
Restek RDX standard	0.2	0.7		-32.1	0.9
SPEX RDX standard	-6.5	0.6		-33.6	0.9
China Lake (custom synth)	9.1	0.8		-29.7	0.8
China Lake (unlabeled std)	-15.8	1.5		-35.0	1.7
958 (1.6um)*	-0.8	0.4		-37.0	1.5
Class4 ("Swett")*	-0.0	1.5		-37.1	1.2
ClassE*	-1.1	0.2		-38.2	0.9
E-77 Grade A*	-0.3	0.6		-33.3	1.4
HOL99G-021-001*	-0.3	0.5		-35.9	1.0
RDX FC1*	0.2	0.8		-39.4	0.7
RDX FC2*	-2.4	0.2		-37.6	1.0
RDX FC3*	-0.3	0.6		-39.8	1.3

*Assumed HAAP materials

5.2.2 Dahlgren NSWC biobarrier – column study

As previously discussed in Section 4.1, an *in situ* biobarrier study was performed at the Dahlgren NSWC site. The baseline site characterization activities for this project were described in Section 4.1.2. A series of microcosm studies were conducted during Project ER-201028 in order to evaluate the best emulsified oil carbon substrate to use for stimulation RDX and perchlorate biodegradation. A follow-on column study was conducted as a joint effort between this project and ER-201208 in order to assess both the potential to treat RDX, HMX and perchlorate using emulsified oils, and the potential for natural attenuation of these contaminants under site conditions and measurement of biodegradation via CSIA. A summary of the column test results, with a focus on evidence of potential natural attenuation of RDX at Dahlgren NSWC is provided below.

5.2.2.1 Column design and set-up

The columns used for this test are shown in **Figure 5.1**. Three columns were prepared. Each column was made from 7 cm ID aluminum tubing cut to a length of 30 cm. Lexan end plates were prepared and held in place with threaded rods. A 3-way-stopcock was placed on both the influent and effluent end of the column. Side sampling ports were placed at 10 cm and 20 cm to allow collection of effluent with groundwater flow. A Teflon diffuser ring was placed at the bottom of the column to equalize flow through the packed sediment. The total volume of each column was approximately 1200 cm^3. Site sediment collected from the Fast Cookoff plume area was homogenized and packed into the columns, resulting in a bulk density of approximately 1.81 g/cm^3 (dry wt basis) and a pore volume of 240 mL. Groundwater was collected from well CMOBOD02 at the field site in a large steel keg (60 L) and used as the column mobile phase. The groundwater feed was set to approximately 6 to 7 mL/h, equivalent to 0.2 m/d (0.6 ft/d).

Equilibration with site groundwater was performed initially along with a bromide tracer test (data not shown). The dissolved oxygen and pH of the influent groundwater and the effluent of each column were measured. A split of the influent groundwater and the effluent from each column was directed through a solid phase extraction (SPE) column over several days to collect and concentrate the explosive compounds. Explosives were then eluted from the SPE columns and analyzed for explosives (HMX, RDX, and RDX breakdown products) by EPA Method 8330. Additional samples of the effluent were collected and analyzed for perchlorate (EPA Method 314.0), anions (EPA Method 300.0), and TOC (EPA Method 415.1). Periodic samples were collected and preserved with nitric acid for later analysis of dissolved metals (Target Analyte List (TAL) metals).

When the columns were assessed to have equilibrated, they were designated with their respective treatments (**Table 5.2**).

Table 5.2. Treatment Assignments for the Column Experiment.

Column	Treatment	Description
Col 1	EOS-Low Salt	3 pore volumes of 12% (w:v) of EOS 550LS
Col 2	None-Natural Attenuation	No amendments
Col 3	EOS-Low Salt/AquaBupH	3 pore volumes of 12% (w:v) of a 75:25 (v:v) of EOS 550LS:EOS AquaBupH

The amendment addition was performed at a flow rate of 30 mL/h, followed by a 3 pore volume flush of groundwater. The control column had groundwater pumped through at the higher flow rate but no emulsified oil addition. The flow rate was then reduced back to approximately 6 mL/h. Influent and effluent samples were monitored as described above. The aquifer column test continued until concentrations of RDX and perchlorate in the effluent were reduced to <1 µg/L for RDX and <4 µg/L for perchlorate and when the effluent concentrations stabilized such that degradation rates could be extrapolated over a longer flow path (i.e., if the residence time in the columns is not sufficient to achieve the low contaminant concentrations, since residence times in the field are not constrained by column length).

5.2.2.2 Column results

Reducing (anaerobic) conditions were generated in the EOS-amended columns as the added carbon was degraded, as reflected in a rapid decrease in the effluent concentrations of both nitrate and sulfate, indicative of typical biological reduction of both of these anions. Perchlorate also was rapidly biodegraded in the two columns with the emulsified oil formulations, although the rates were somewhat higher in Col 3, which received the buffered EOS mixture (**Figure 5.2**). No significant degradation of perchlorate was observed in the MNA (control) column (Col 2), and only slight losses of sulfate and nitrate were apparent compared to influent concentrations. Steady state degradation rates for the emulsified oil amended columns are shown in **Table 5.3**.

Table 5.3. Apparent Steady State Degradation Rates of Target Compounds.

Column	Treatment	Degradation Rate (µg/L/d)		
		HMX	RDX	Perchlorate
1	EOS-Low Salt	0.6 ± 0.2	3.1 ± 0.5	0.7 ± 0.3
3	EOS-Low Salt/AquaBupH	0.7 ± 0.2	3.1 ± 0.6	0.8 ± 0.1
2	Control (no amendment)	0.6 ± 0.2	2.8 ± 0.6	0

Concentrations of influent and effluent perchlorate, HMX and RDX are shown in **Figure 5.2**, **Figure 5.3** and **Figure 5.4**, respectively. We initially assumed that the equilibration period for HMX and RDX would require less than 30 days of operation due to their physiochemical characteristics (low K_{ow} values in particular). During this time, some adsorption of each of these nitramine explosives to the aquifer solids was expected. Because the columns were prepared from homogenized solids, we anticipated that there could be significant new adsorption sites available for RDX and HMX present in the influent groundwater. For Col 1, the influent and effluent RDX and HMX concentrations reached the same values after ~ 40 days of operation and remained equivalent prior to emulsified oil addition. For Col 2 and Col 3, the effluent RDX and HMX approached but did not reach the influent concentrations after nearly five months of operation with these nitramines in the influent groundwater.

The reasons for the difference among the three columns, which were replicates up to the time that emulsified oil was added (Day 174) are unclear. Based on the data for the common RDX intermediates, MNX, DNX, and TNX (**Figure 5.5**), it appears that some RDX degradation was occurring in Col 2 and Col 3 during the initial 5-month period. It should be noted however, that the combined quantities of these intermediates represents only a small percentage (<15%) of the RDX loss across the two columns. Detectable, but lower, concentrations of these intermediates (particularly DNX and TNX) were observed in the effluent from Col 1, suggesting some level of RDX biodegradation in this column as well. However, interestingly, there was no similar evidence of nitrate, sulfate (**Figure 5.6**) or perchlorate (**Figure 5.2**) degradation in any of the columns. In fact, the effluent concentrations of each of these anions rapidly reached the influent concentration in each of the 3 columns. The loss of RDX and HMX without any similar loss of nitrate or perchlorate (both of which are readily biodegradable under anaerobic conditions), suggests that the apparent loss of RDX and HMX in the columns may reflect either abiotic degradation or aerobic biodegradation in the absence of added substrate.

HMX and RDX decreased rapidly in Col 1 and Col 3 after the emulsified oil was added (**Figure 5.3** and **Figure 5.4**, respectively). However, decreases also were apparent in the control column (Col 2) which only had groundwater pumped in at a higher rate while the others were receiving the oil substrates. Degradation kinetics for RDX were essentially the same for the EOS-amended and unamended columns (**Table 5.3**). The aquifer sediment collected from Dahlgren and used in the columns had a significant fraction of TOC (145 mg/kg of the homogenized aquifer solids), and there was evidence of iron deposits and significant quantities of clays within the aquifer cores (**Figure 5.7**). Although the iron was not quantified and/or speciated, it is feasible that iron minerals were catalyzing the abiotic reduction of RDX and HMX in Col 2 and Col 3, and to a lesser extent in Col 1, as described above.

One significant component of the initial loss of RDX and HMX across the columns may be adsorption to organic matter and/or clays. It is possible that many new binding sites were exposed to the groundwater flow path during homogenization of the aquifer solids. Another possible factor is the abiotic reduction of RDX by iron (Fe), and in particular Fe(II)-surface complexes. Several recent papers suggest that RDX is susceptible to abiotic reduction by a variety of Fe(II)-organic ligands, Fe-oxides (e.g., magnetite) and other Fe(II) mineral complexes (9, 32, 51, 59). The abiotic reduction with many of these Fe minerals/ligands proceeds through MNX, DNX, TNX, similar to biological reduction, so some occurrence of these nitroso-derivatives would be expected. Moreover, perchlorate is unlikely to be abiotically degraded by these minerals, as it is highly stable in solution, even to abiotic reduction by zero-valent Fe (65). This is consistent with the column results, as perchlorate degradation was not observed.

Finally, aerobic biodegradation of RDX and HMX in these columns is a possibility, since the influent DO during the initial equilibration period was approximately 6 mg/L. Aerobic biodegradation of RDX by pure cultures has been widely described as previously discussed, and although much less widely studied, aerobic biodegradation of HMX also has been reported (35, 74).

5.2.2.3 Stable isotope fractionation C and N in RDX in columns

At the conclusion of the column tests, the RDX concentration in the influent to Col 1 and Col 2 was increased to approximately 3 mg/L. The same flow rate was maintained, and samples from the influent, effluent and each of the side ports were collected and analyzed. The RDX was increased to determine if there was any difference in degradation rates of RDX across each of the columns and to provide enough RDX in the influent to be able to evaluate stable isotope fractionation of C and N in RDX from the control column (Col 2) to provide evidence of degradation vs. adsorption of RDX. When the higher concentration of RDX was added, significant loss of the nitramine was still observed across the Col 2, whereas no loss of perchlorate was evident (**Figure 5.8**). The concentration data from this column provide possible evidence of natural attenuation of HMX and RDX at the Dahlgren site, supporting further field evaluation.

Data for $\delta^{13}C$ was not obtained from the column due to the presence of interfering compounds in the effluent, but $\delta^{15}N$ data were obtained. Interestingly, significant fractionation of N was observed over the initial 10 cm of transport in Col 2, but much less fractionation thereafter (**Figure 5.9**). The initial calculated epsilon value ($\varepsilon^{15}N$) over the first 10 cm of transport was - 4.6 ‰ whereas the $\varepsilon^{15}N$ for the last 20 cm was less at - 0.6 ‰. The data suggest that different mechanisms may account for the loss of RDX across the control column, with one mechanism dominating during the first 10 cm of the column and another thereafter (as loss was observed across the length of the column; **Figure 5.8**). The fractionation values suggest that the initial process was destructive, likely biotic or abiotic reduction. The second process, which showed less fractionation, may represent a nondestructive mechanism such as adsorption, or a destructive mechanism that does not fractionate N to the same extent. In either event, the data do provide evidence of natural attenuation, with a destructive process accounting for at least part of the loss of RDX across the column.

Figure 5.1. Column Design for Laboratory Treatability Testing.

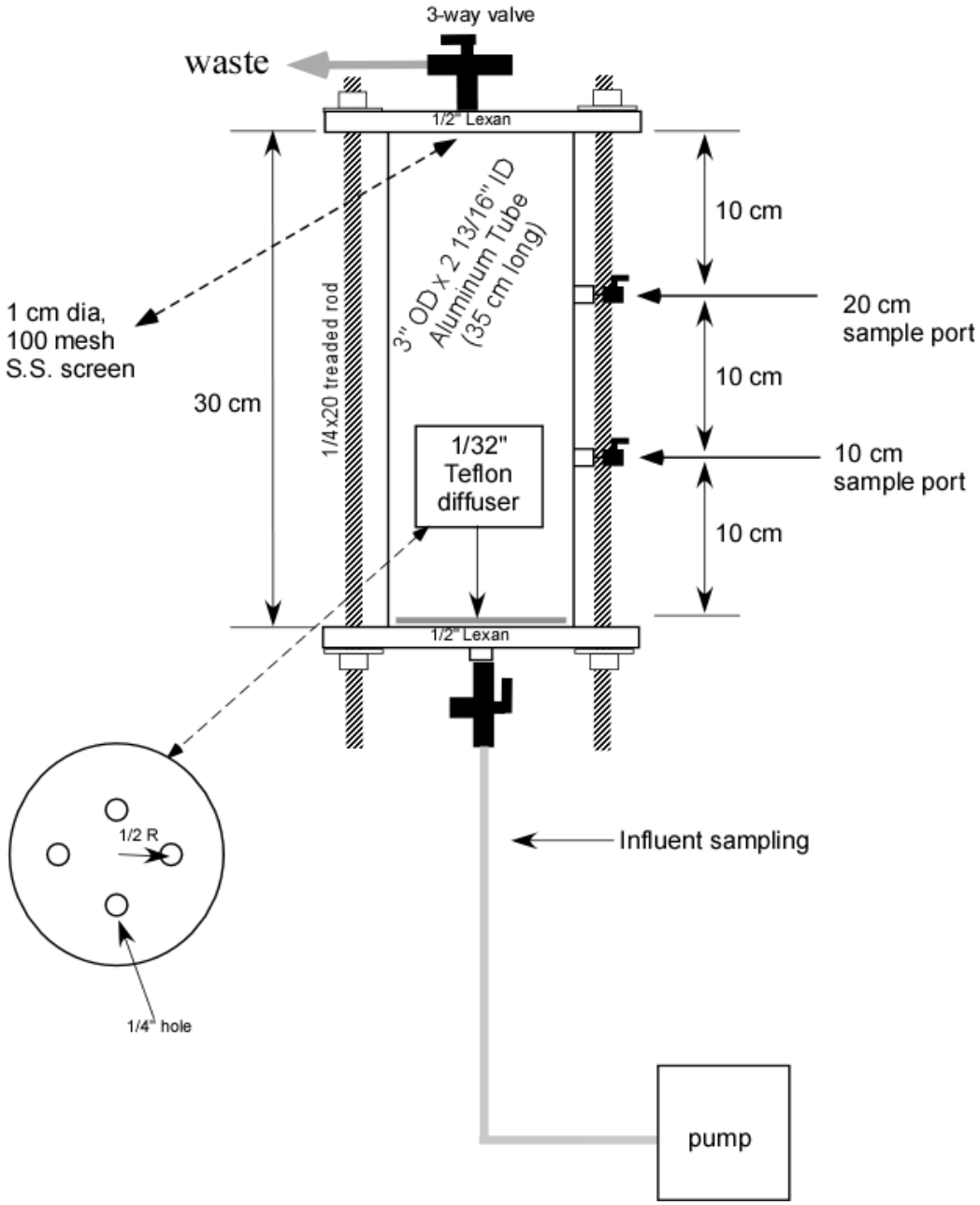

Figure 5.2. Perchlorate in the Influent Groundwater and the Effluent of the Three Flow-through Columns.

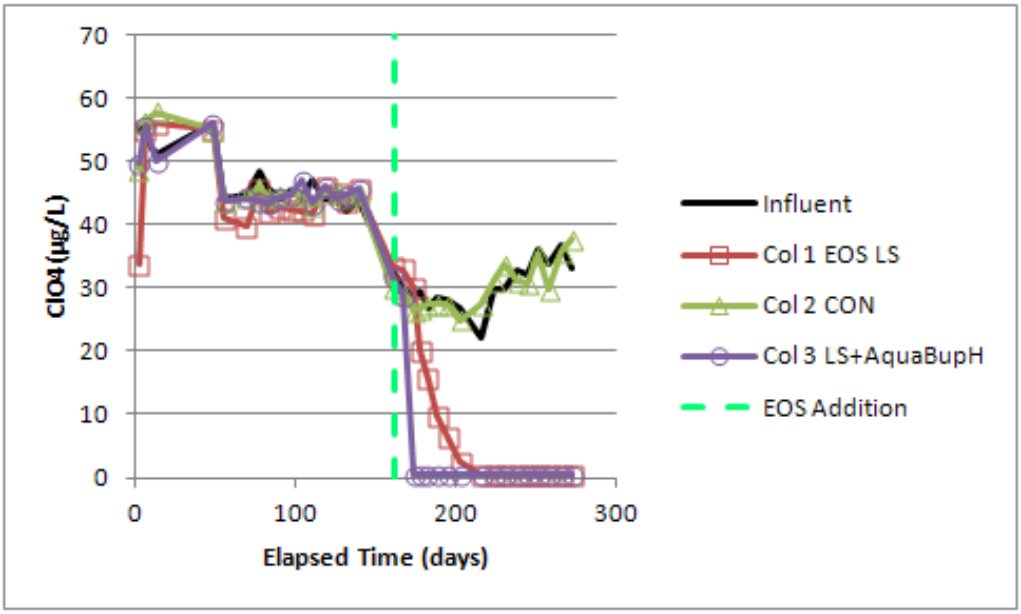

The dashed line indicates the time of emulsified oil addition.

Figure 5.3. HMX in the Influent Groundwater and the Effluent of the Three Flow-through Columns.

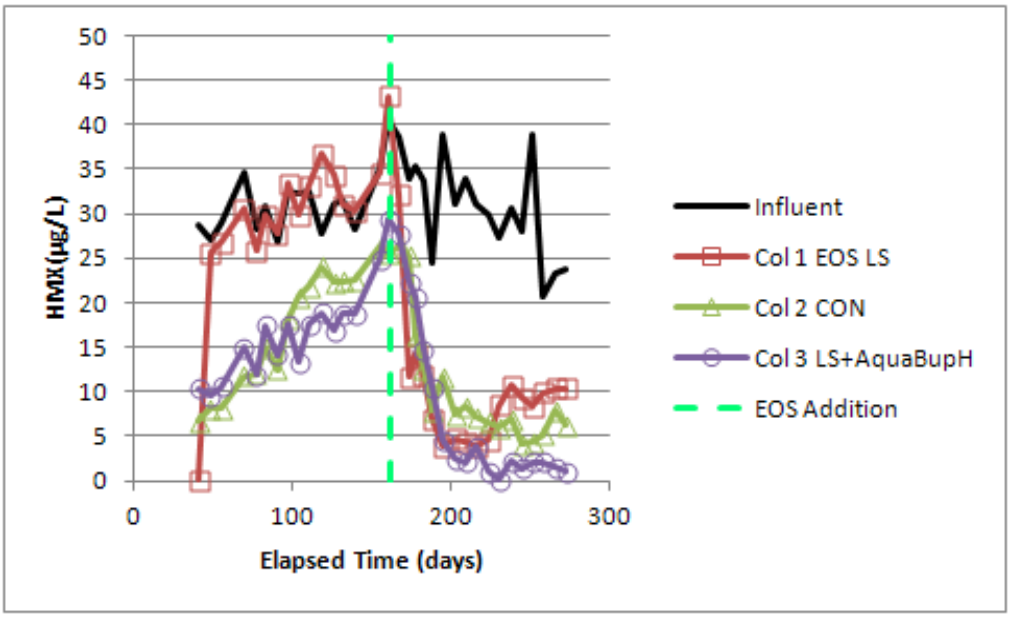

The dashed line indicates the time of emulsified oil addition.

Figure 5.4. RDX in the Influent Groundwater and the Effluent of the Three Flow-through Columns.

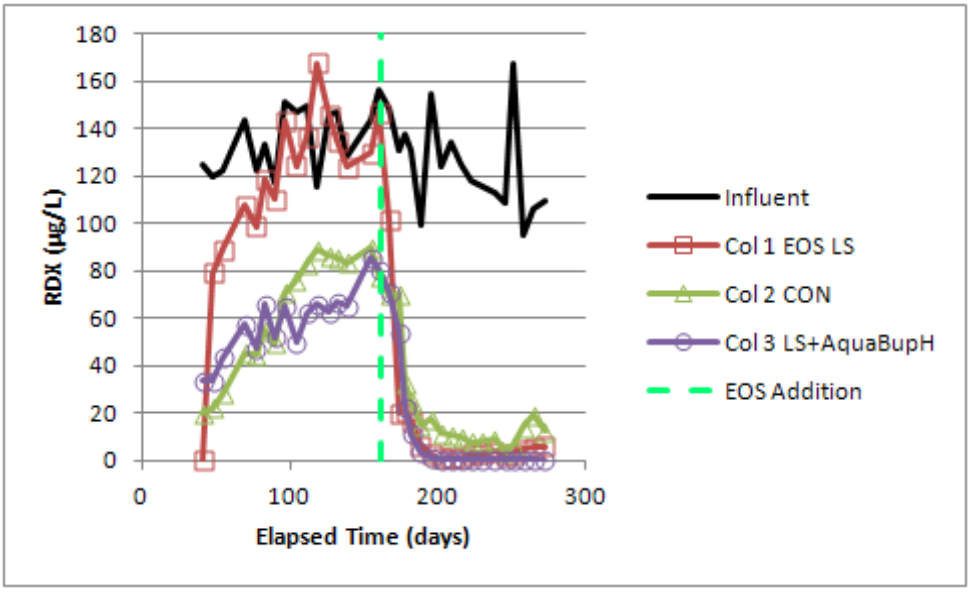

The dashed line indicates the time of emulsified oil addition.

Figure 5.5. MNX, DNX, and TNX in the Influent Groundwater and the Effluent of the Three Flow-through Columns.

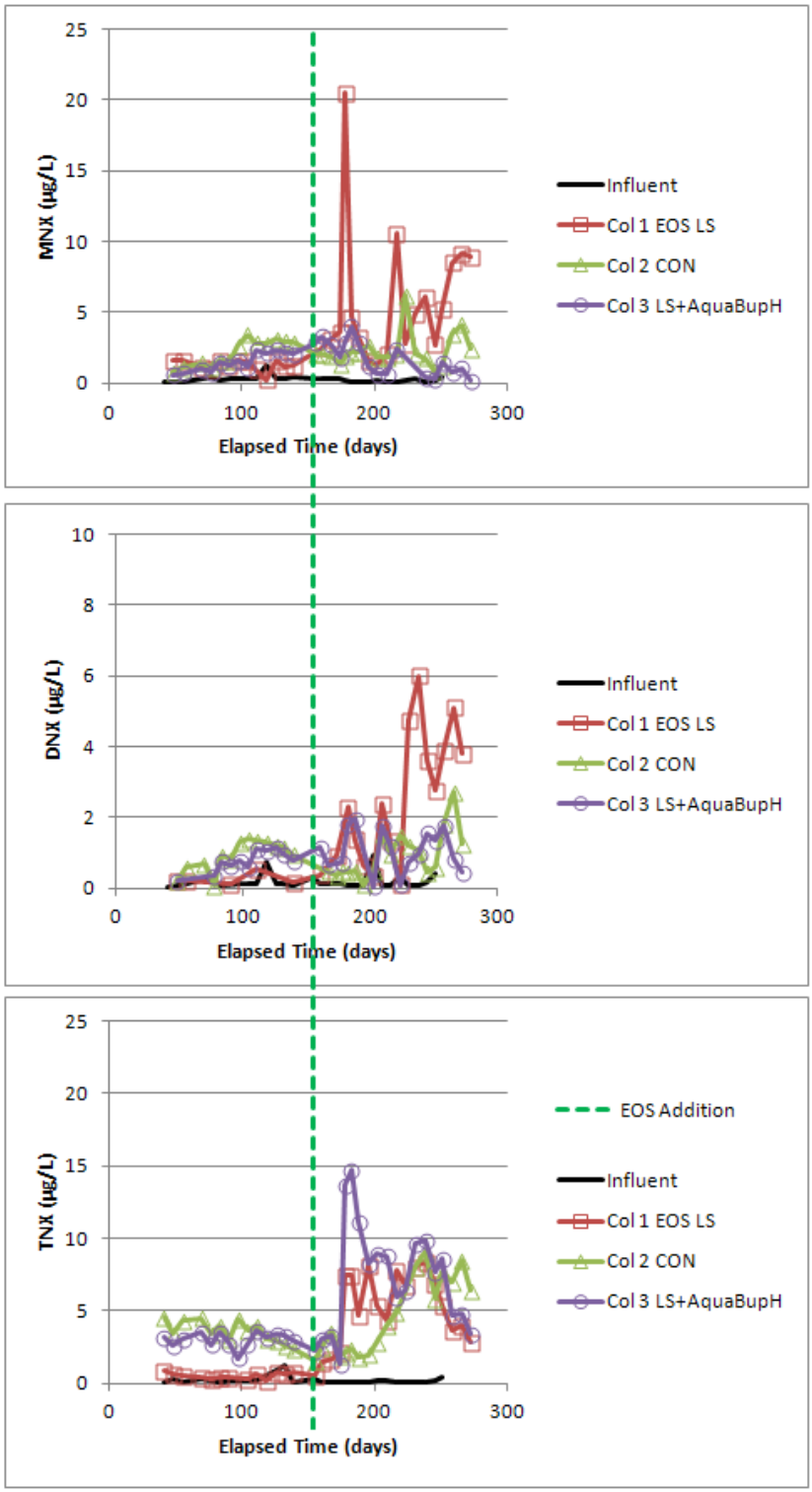

The dashed line indicates the time of emulsified oil addition.

Figure 5.6. Nitrate and Sulfate in the Influent Groundwater and the Effluent of the Three Flow-through Columns.

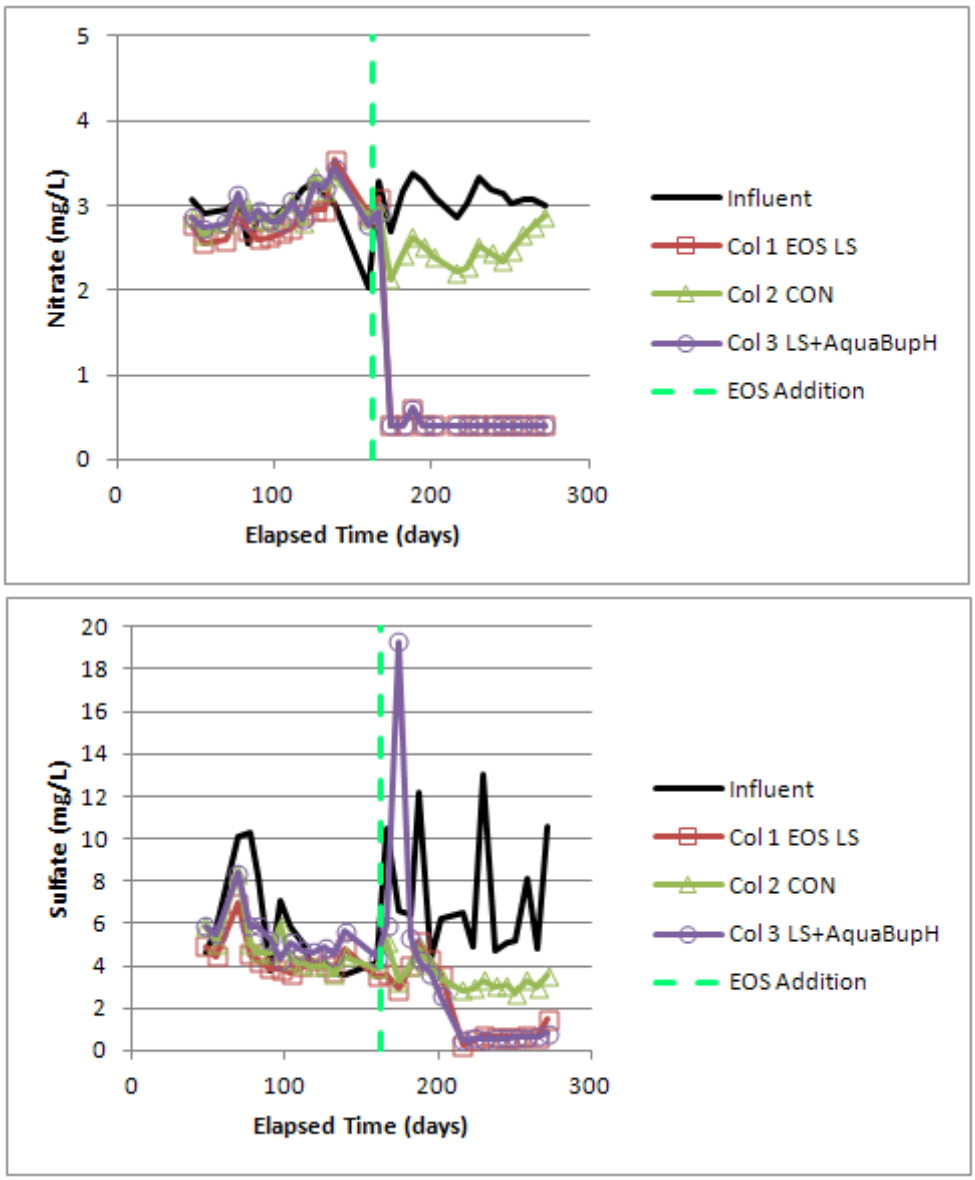

The dashed line indicates the time of emulsified oil addition.

Figure 5.7. Profile of One Geoprobe Core (7.5 to 10 ft, saturated zone) from the Dahlgren Site Showing Significant Amounts of Iron Minerals (orange).

Figure 5.8. Profiles of RDX and Perchlorate as a Function of Distance from the Influent End of the Columns.

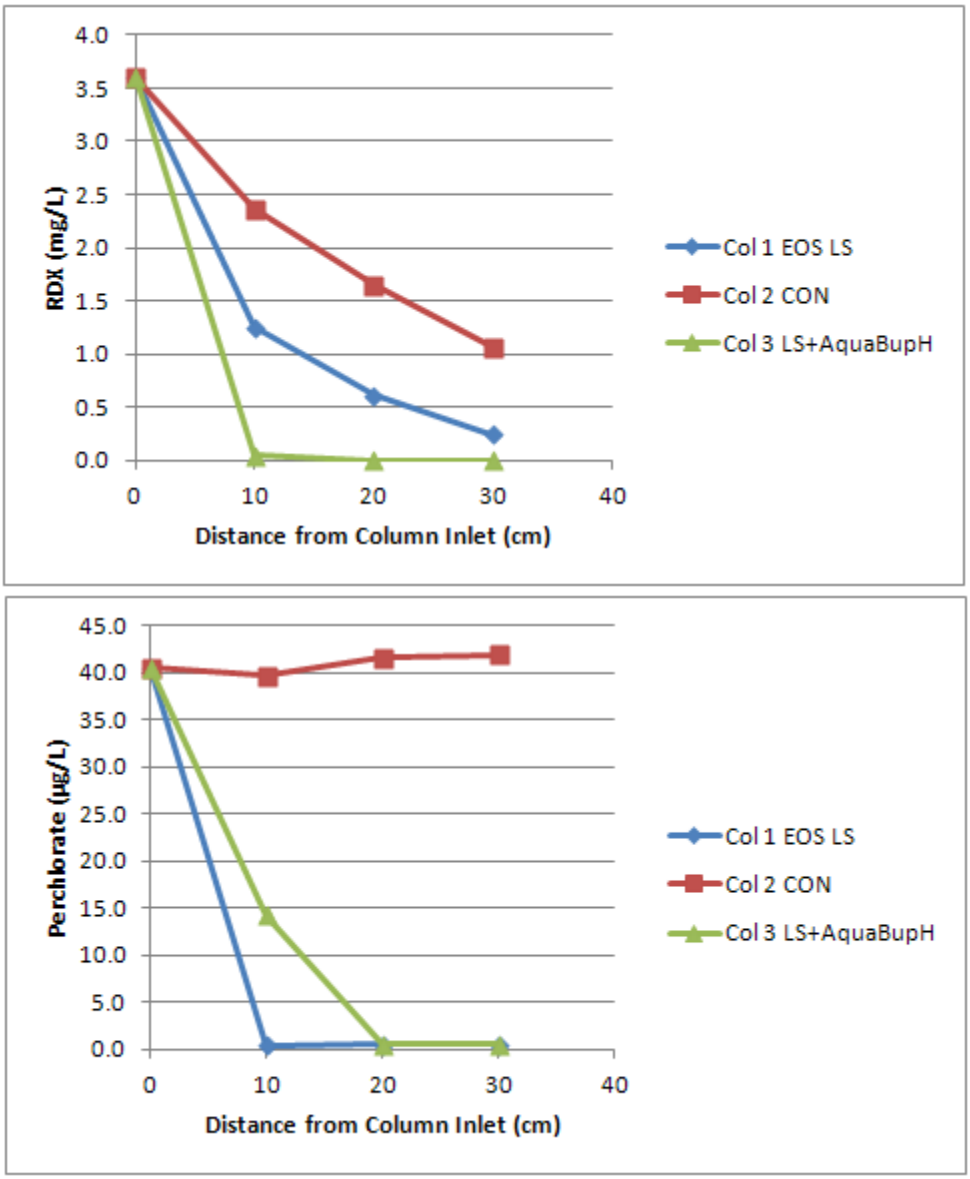

Figure 5.9. Fractionation of N in RDX as a Function of Fraction Remaining (ln f), which Decreases with Distance from Influent End of Column (Col 2).

The ε values provided represent the calculated slopes of the linear fits.

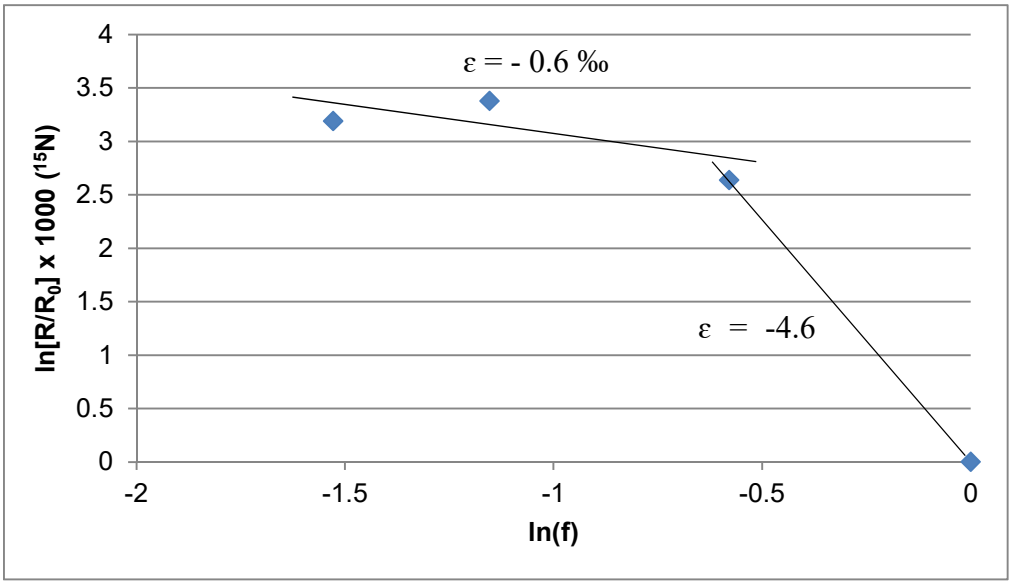

5.2.3 UMCD Field Study

5.2.3.1 Microcosm and column studies

Microcosm and column tests were performed to assess the efficacy of a mixed bioaugmentation culture (microcosms) and of strain KTR9 (column study) to aerobically degrade RDX in the presence of site soil and groundwater. In the microcosms, strains KTR9 Kan^R, RHA1 pGKT2, and *Pseudomonas fluorescens* I-C were inoculated at equal cell densities (1 x 10^6 cells/ml) into slurries of UMCD site soil (2 g) and artificial groundwater (1 ml). Degradation of RDX occurred very quickly in the inoculated microcosms with 98% of the RDX removed to below the 2.1 µg/L site-specific objective in 1 day (**Figure 5.10**). These results provided the necessary information required to proceed with column experiments to evaluate cell transport and RDX degradation under dynamic flow conditions in actual UMCD sediments.

Figure 5.10. RDX Concentrations in UMCD Microcosms in Both Uninoculated (control) and Inoculated with Strains KTR9 Kan^R, RHA1 pGKT2, and *P. fluorescens* I-C.

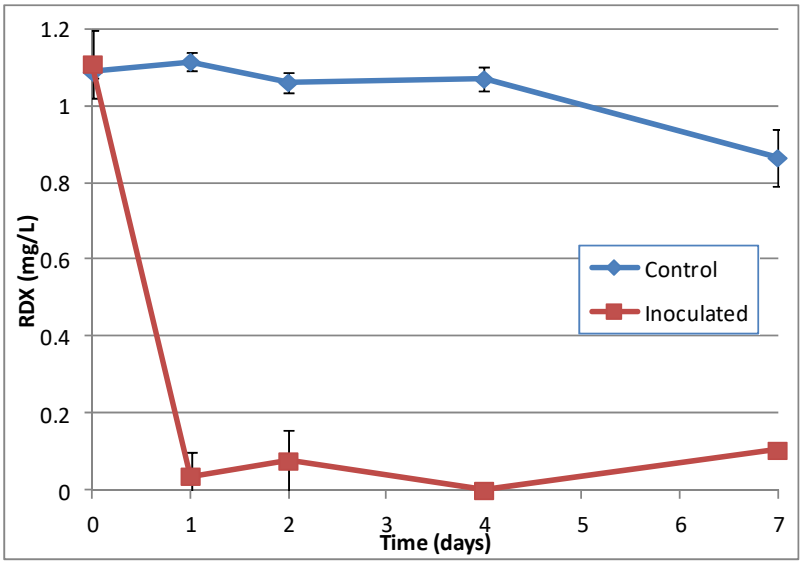

Flow-through aquifer studies were performed in order to evaluate the transport and biodegradative activity of strain KTR9 under simulated field conditions. Strain KTR9 was subsequently chosen as the strain bioaugmented into the aquifer at UMCD during the aerobic push-pull test. UMCD site soil was initially packed into laboratory columns. Artificial site groundwater (AGW) containing RDX was pumped through the column at seepage velocities representative of field values. The column was inoculated with a cell concentration of $1x10^9$ cells/mL KTR9 Kan^R, followed by monitoring effluent cell counts, as well as RDX, nitrate/nitrite, and other standard chemistry components. A distinctive breakthrough curve of KTR9 Kan^R cells was observed, confirming this strain was transportable in UMCD site soil (**Figure 5.11**). After cell injection, the

system was allowed to stabilize for 30 pore volumes (PV) until influent RDX equaled effluent RDX. When 0.1 mM fructose was then injected into the column, a rapid decrease in RDX effluent concentrations was observed, followed by a gradual increase in RDX concentrations as the fructose was utilized or flushed out of the column. This result showed that the injected strain maintained RDX-degrading activity post inoculation in the soil column. Subsequent fructose additions each resulted in rapid RDX degradation. Results of Phase I laboratory tests confirmed (a) KTR9 could be successfully transported through UMCD soil over laboratory column relevant scales, and (b) KTR9 retained RDX degrading activity in site soil during long periods without fructose addition. Further details concerning this study are available (27).

5.2.3.2 Isotopic fractionation of C and N during aerobic biodegradation in pure culture and column experiments.

Isotopic fractionation of N and C by *Gordonia* sp. KTR9 under aerobic conditions was quantified in liquid culture (27). The *Gordonia* strain was grown in basal salts medium (BSM) with RDX at 20 mg/L and sodium succinate was added initially at 1 g/L. Studies were conducted in 950-ml amber glass bottles with stirring (400 rpm), and the headspace in the bottles was continuously purged with sterile humidified air to maintain aerobic conditions.

Small aqueous samples (10 ml) were periodically removed, filtered through glass microfiber filters (GMF; 13 mm x 0.45 µm pore size), and analyzed for residual RDX concentrations using HPLC (EPA Method 8330). For CSIA, larger samples (40 ml to 250 ml) were removed over the course of the incubation, representing fractional RDX degradation in the range of approximately 0.05 to 0.95. These samples were filtered through GMF filters (25 mm x 0.45 µm pore size) to remove cells and then passed over a pre-conditioned Supelclean™ ENVI-Chrom P solid phase extraction column (250 mg packing; Sigma-Aldrich, St. Louis, MO, USA). The analytes on the SPE column were eluted with acetonitrile according to the manufacturer's instructions, and the extract was dried to a volume of 1 ml. These samples were they analyzed for C and N stable isotopes according to the methods described in Section 5.5.3.

The mean $\varepsilon^{15}N$ value for strain KTR9 in pure culture was of -2.3 ± 0.5 ‰ and the corresponding $\varepsilon^{13}C$ value was -0.9 ± 0.6 ‰ (**Table 2.1**, **Figure 5.12A**; average of slopes for each isotope). These results are consistent with other strains tested in our laboratory (see Sections 2.1.3 and 2.1.4 and ref 27). Based on these data, it was determined that C fractionation in the field would not be measurable during the UMCD work, but that N fractionation might be detectable under the controlled conditions of the push-pull test. Moreover, the $\varepsilon^{15}N$ data could be compared to those from the anaerobic plot, where much higher N isotope fractionation would be anticipated based on laboratory data.

At the end of the column experiment described above the influent RDX concentration was increased to 20 mg/L from 0.5 mg/L. Upon fructose addition, samples were collected from side ports (located 3.25, 7.50, and 15 cm from the column influent), as well as from the column influent and effluent, processed to concentrate the RDX, and subjected to isotopic analysis as described in section 5.5.3. Sampling for isotopic fractionation of C and N in RDX was performed on two separate occasions. As shown in **Figure 5.12B**, moderate fractionation of N was observed ($\varepsilon^{15}N$ value of -4.1 ‰, n = 2), whereas C showed no significant fractionation ($\varepsilon^{13}C$ value of -0.3 ‰, n = 2). The slightly higher $\varepsilon^{15}N$ observed in second column experiment could indicate the contribution of RDX degradation pathways other than the aerobic pathway used by KTR9 since no effort was made to keep other bacteria from growing in the column. Anaerobic RDX pathways have been shown to fractionate nitrogen more than the aerobic pathway (27). Repeated addition of fructose to the column may have allowed these other bacteria to increase in number, as well as promote the formation of anaerobic microsites within the column.

Figure 5.11. Breakthrough Curves for Bromide, Cells, and RDX for Column Experiment with UMCD Site Samples.

The initial breakthrough results and the results of the entire experiment are shown, where C is the measured solute or cell concentration in the column effluent; Co is the influent tracer or cell concentration.

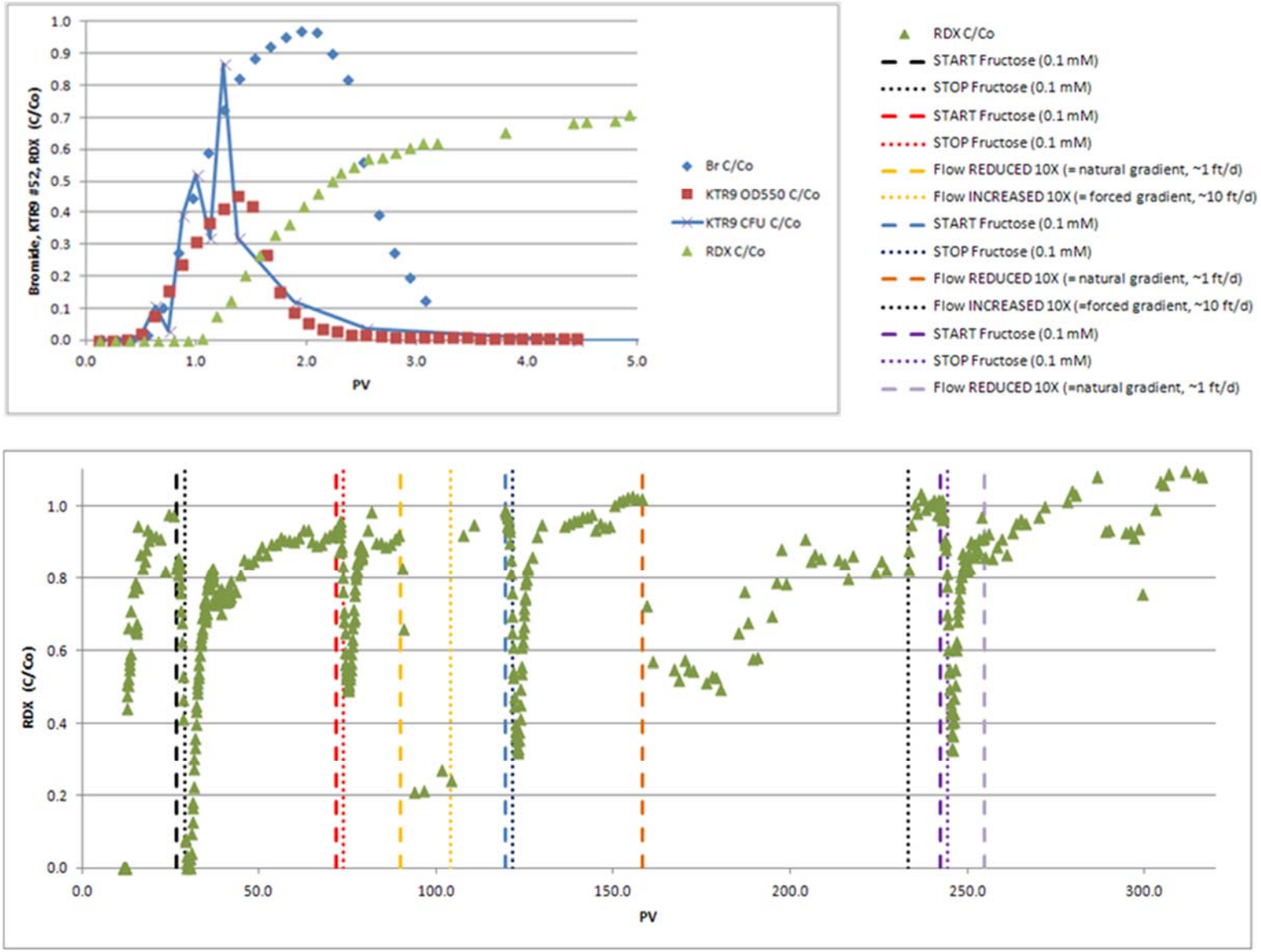

Figure 5.12. Fractionation of C (left panel) and N (right panel) isotopes by *Gordonia* sp. KTR9 in A) liquid culture and B) column experiments.

A) Pure culture experiments

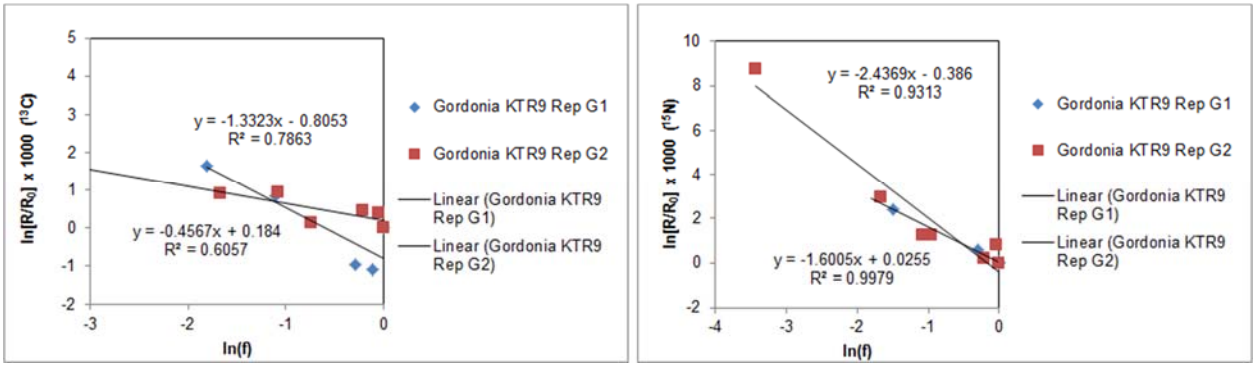

B) Column experiments

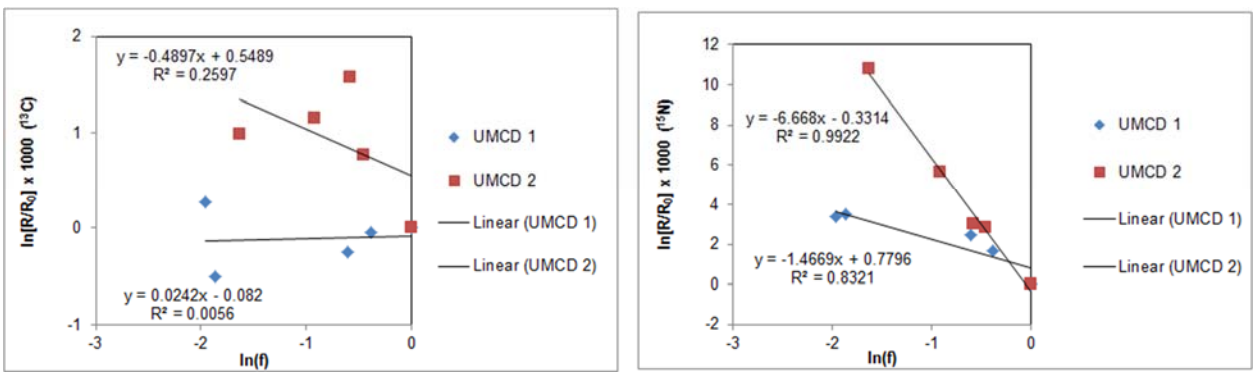

5.3 DESIGN AND LAYOUT OF TECHNOLOGY COMPONENTS

This project was designed primarily to document stable isotope fractionation of C and N in RDX during aerobic and anaerobic biodegradation. The project was conducted in conjunction with two other ESTCP demonstrations designed to assess RDX degradation under these conditions (ER-201207 and ER-201028). Thus, the primary technology components were those of the other two demonstrations, which are described in detail in the relevant project reports.

5.4 FIELD TESTING

The field testing for the stable isotope method was conducted at the two sites, as detailed in the previous sections. A column sampling technique was developed and validated during the initial testing for this project. The column technique allows for field processing of large volumes of water (e.g., 10 L) rather than shipping to a laboratory for processing. The column results are described below in Sections 5.4.1 to 5.4.3.

5.4.1 Sample collection in the field using SPE columns

A series of laboratory experiments were conducted to develop a solid phase extraction (SPE) technique to collect samples in the field for stable isotope analysis of RDX. The variables examined during this testing included sample flow rate, solid phase type and mass, elution volume, aqueous matrix characteristics, and stable isotope effects of in-field vs. in laboratory SPE processing. The criteria used for evaluating the field SPE vs. laboratory technique were % recovery, mass recovered, and stable isotope effects.

In an initial study, the capacity of two different potential adsorbents of RDX (ENVI-Chrom P and ENVI-CARB) were evaluated. The first sorbent is typically used to concentrate RDX for EPA 8330 analysis and the second is reported to have a much higher capacity for RDX adsorption. The sorbents were packed in 0.5 g quantities into plastic SPE columns, and 10L of artificial groundwater was passed through each column (triplicates) at a flow rate of 100 ml/min. The total percent of RDX captured was determined using 8330 analysis of the influent and effluent water, and the recovery of the captured RDX was determined after extraction from the resin using acetonitrile. The total recovery of RDX was low for both resin types at the flow rate selected (**Table 5.4**). The RDX was not easily extracted from the ENVI-CARB resin, so further studies with this resin were discontinued.

Table 5.4. Adsorption and Recovery of RDX Using Two Different SPE Media.

Sorbent	RDX Captured (%)	Recovery of Captured RDX (%)	Total %
ENVI-Chrom P	38	65	27
ENVI-CARB	22	25	6

The flow rate through the SPE column was varied in a second study from 10 ml/min to 100 ml/min to determine the effect of flow on RDX capture by the ENVI-Chrom P media. The initial RDX concentration was ~ 5 µg/L, but all other conditions were the same as described in the previous experiment. The total recovery of RDX by the process (passing 10L of AGW through each column) was ~ 30 %, with lower percent capture at the higher flow rate, but greater recovery of captured RDX (**Table 5.5**). In the next study, the effect of adsorbent quantity on RDX capture was evaluated. In this case small columns were packed with either 2 g or 0.5 g of the ENVI-Chrom P adsorbent, and the columns received 10 L of AGW with 5 µg/L RDX at a flow rate of 100 ml/min. The percentage of RDX capture was dramatically improved by using the larger quantity of adsorbent, reaching 97% on average for the 2 g cartridges compared to 33 % for the 0.5 g cartridges (**Table 5.6**). The percent extraction of the adsorbed RDX from the 2 g cartridges was marginally lower than for the 0.5 g cartridges, but the total % recovered at the end of the study was 83 % for the 2 g cartridges compared to only 32 % for the 0.5 g cartridges.

Table 5.5. Influence of Flow Rate on the Adsorption and Recovery of RDX Using ENVI-Chrom P Media.

Flow Rate (ml/min)	RDX Captured (%)	Recovery of Captured RDX (%)	Total %
10	41	76	31
25	40	77	31
100	33	98	32

The previous experiments indicated that a 2 g cartridge containing ENVI-Chrom P resin could be used to adsorb RDX at low µg/L concentrations from up to 10 L of water at a flow rate of 100 ml/min. This flow rate and volume was deemed to be suitable for many field applications. A final adsorption study was completed to compare extraction efficiency of the selected column using distilled water compared to a site groundwater from New Jersey. The study was conducted in triplicate using 2 g cartridges, at a 100 ml/min flow rate with ~ 5 µg/L of dissolved RDX. A total of 10 L of volume was passed through each column. The amount of RDX captured was equivalent between distilled water and groundwater (**Table 5.7**). Moreover, although the extraction efficiency of RDX was slightly higher from the distilled water than the groundwater, the total mass recovered was statistically indistinguishable, and similar to that previously observed for AGW (**Table 5.6**).

Table 5.6. Influence of Sorbent Mass on the Adsorption and Recovery of RDX Using ENVI-Chrom P Media.

Sorbent Mass (g)	RDX Captured (%)	Recovery of Captured RDX (%)	Total %
0.5	33	98	32
2	97	86	83

Table 5.7. Comparison of Adsorption and Recovery of RDX from Distilled Water and Groundwater.

Sorbent Mass (g)	RDX Captured (%)	Recovery of Captured RDX (%)	Total %
Distilled water	97 ± 0.3	85 ± 1.2	82 ± 2
Groundwater	97 ± 1.0	79 ± 3.5	77 ± 4

5.4.2 Comparison of stable isotope values between field and laboratory SPE samples

One of the critical issues that had to be examined in developing a field collection method for RDX stable isotope analysis is whether isotope fractionation occurs during sample collection and elution. This is particularly true in that not 100 % of the RDX in the groundwater is collected during the field process; rather ~ 80 % is retained and analyzed for stable isotope ratios. In order to assess potential fractionation, the samples processed in **Table 5.7** were analyzed for $\delta^{15}N$ in RDX, and compared with the original RDX source material. The data from this analysis suggested that N isotopes were not fractionated during column collection and processing (**Table 5.8**). The $\delta^{15}N$ values of the RDX standard were statistically indistinguishable from those in the aqueous samples from which RDX was removed by SPE, then re-extracted and analyzed.

Table 5.8. Comparison of $\delta^{15}N$ in RDX from a Standard, with that Extracted from Distilled Water or Groundwater via SPE.

Sample ID	$\delta^{15}N$ of RDX		
	Mean	St. Dev.	(n)
Solid RDX standard	9.82	1.43	15
SPE with distilled H_2O	9.75	0.56	3*
SPE with groundwater	10.47	0.49	3*

* triplicate isotope analysis of triplicate columns
* no significant difference at 95% CI between standard and water samples via t-test

5.4.3 Development and testing of an SPE column for field application

Based on the laboratory results in Sections 5.4.1 and 5.4.2, a field-ready sampling cartridge was designed and built using a Schedule 80 PVC cap and adaptor to hold the SPE column in place. The components of this cartridge and a photograph are provided in **Figure 5.13**. This cartridge was subsequently tested at the Dahlgren NSWC site to evaluate the collection efficiency under field conditions compared to collecting and shipping groundwater to the laboratory for processing. The results from this analysis are described in Section 5.4.4.

Figure 5.13. Design and Photograph of Field Sampling Column for RDX Isotopes.

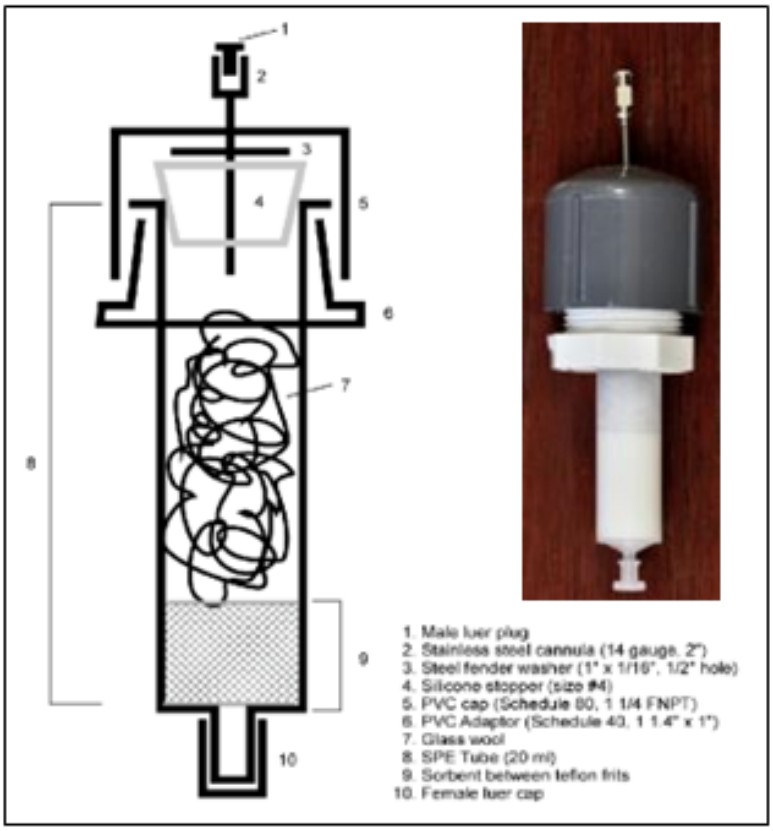

5.4.4 Dahlgren NSWC – Natural attenuation testing

Stable isotope sampling was conducted at selected piezometers at the Dahlgren site in order to: (1) evaluate the field application of SPE sampling columns developed for the project (Section 5.4.1-5.4.3), and (2) to provide information on whether there was isotopic fractionation of N in RDX occurring at the site indicative of natural attenuation, and in what location(s) those processes are evident.

The piezometers that were selected for sampling are indicated on **Figure 5.14**. The piezometers were selected based on the concentration of RDX and predicted plume/groundwater flow paths, local geochemistry, and the capacity of the piezometers to provide water (as some of the piezometers at the site do not produce significant water). An attempt was made to sample along

the length of both of the RDX plumes in the location, and to sample piezometers located to the southwest of the two plumes (PZ-17, PZ-02) where groundwater becomes increasingly anaerobic due to the presence of a swale area. Little RDX was present in this region.

RDX in groundwater was collected in bottles for processing in the laboratory and also was trapped on specially-designed SPE columns from several wells, so that results of (1) collection efficiency and (2) possible isotope fractionation due to sample collection on the columns could be evaluated in the laboratory. A photograph of field collection using the specialized SPE cartridge is provided in **Figure 5.15**.

In addition to RDX, samples were collected from the piezometers for stable isotope evaluation of $\delta^{15}N$ and $\delta^{18}O$ in NO_3^-. Based on our recent studies with pure cultures, and a few recent papers where NO_3^- stable isotopes were analyzed from range sites, NO_3^- from the aerobic degradation of explosives (nitramines and/or nitroaromatics), which is derived from released NO_2^- via oxidation, can differ isotopically from that from other sources such as atmospheric production and nitrification (10, 22) (see **Figures 2.5 and 2.6)**. Nitrate samples were collected from the same piezometers from which RDX was collected for isotopic analysis, and the stable isotope composition of N and O in NO_3^- was measured using established methods (14, 67) by Dr. J.K. Böhlke and colleagues at USGS. One of the difficulties with NO_3^- is that the compound is readily "recycled" in the environment, being formed (e.g., nitrification and atmospheric production) and lost (via denitrification, plant assimilation, etc.), so results may be difficult to interpret. However, the stable isotope data collected from Dahlgren were evaluated against those of Bordeleau et al (2008) (10) and our experimental data (27) to see if similar stable isotope characteristics could be documented on two different bombing ranges.

These data, combined with the local geochemical data, were used to assess the most likely natural attenuation degradative process(es) occurring in the groundwater at Dahlgren NSWC.

Figure 5.14. Plume Map for RDX in the Southeast Area of the Churchill Range with Locations Demarcated (yellow well markers) for the First Round of Stable Isotope Sampling.

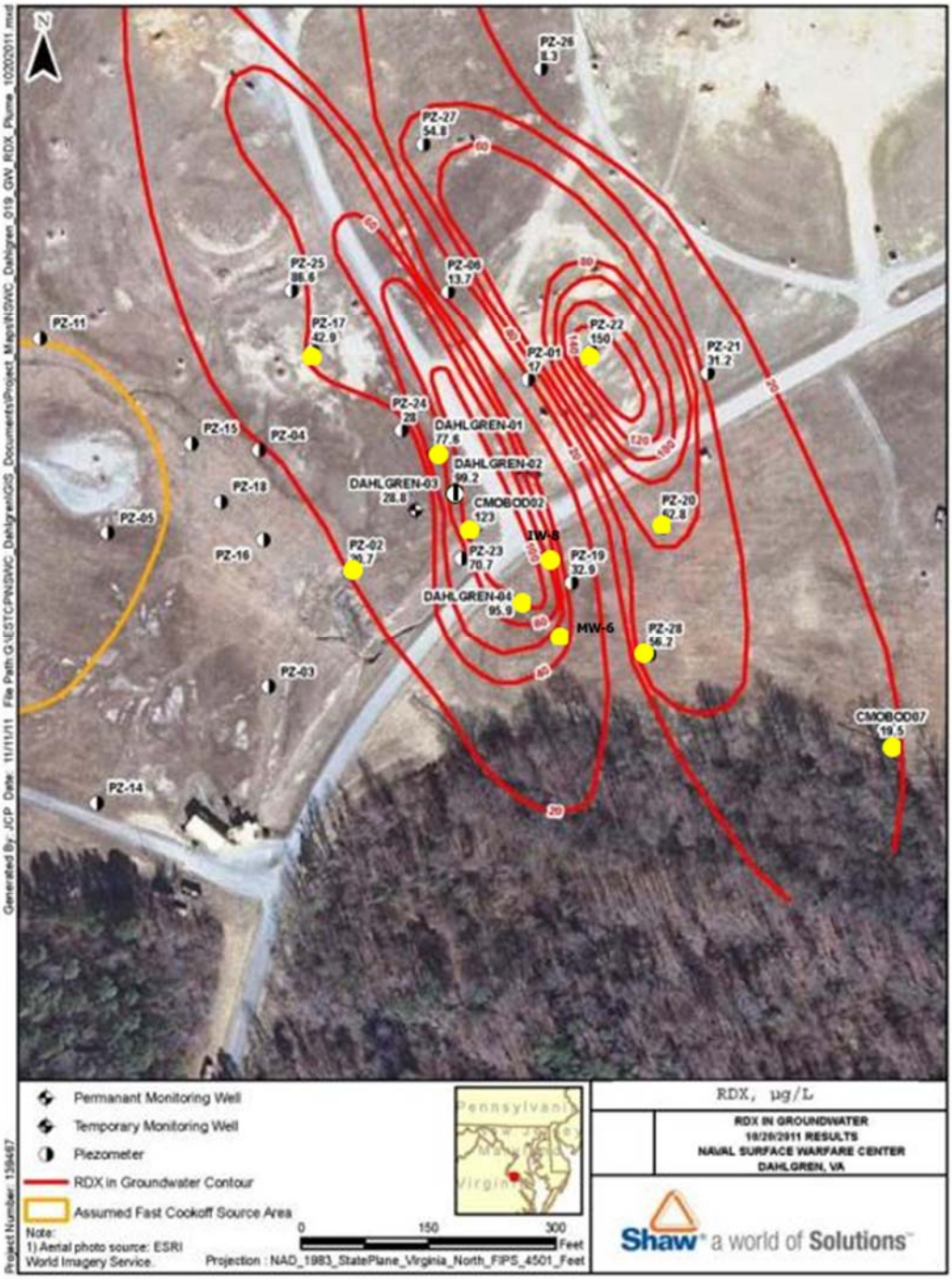

An attempt was made to sample along the flow path of each RDX plume (general groundwater flow to the southeast), and to sample to the southwest of the plumes near the swale area where the aquifer is more anaerobic and RDX declines appreciably.

Figure 5.15. Collection of RDX for Stable Isotope Analysis on a Small SPE Column at the Dahlgren Site.

5.4.5 Dahlgren NSWC – Isotopic fractionation during anaerobic RDX biodegradation

As detailed previously in Section 4.1, an *in situ* biobarrier consisting of emulsified oil and buffer was previously installed at Churchill Range at Dahlgren NSWC under ESTCP Project ER-201028. During this project, we collected samples from a subset of wells upgradient and downgradient of the biobarrier in order to measure stable isotope fractionation in C and N in RDX as biodegradation occurs. The details of the testing are provided below.

A schematic of the Dahlgren NSWC biobarrier is provided in **Figure 5.16**. Refer to **Figure 4.13** for a larger view of the site including plume maps. The biobarrier was installed in February 2013, with upgradient and downgradient monitoring wells (shown on the inset in **Figure 5.16**) used to evaluate the performance of the biobarrier. A subset of the wells in the demonstration plot were selected for isotopic sampling in addition to standard sampling parameters (See Section 5.5.1), which included one upgradient well and a series of downgradient wells along the centerline of the plume. The timing of sample collection was dependent, in part, on the observed reaction progress for RDX during the biobarrier demonstration.

The RDX results along the centerline of the plot (from MW-10 to MW-6) during the initial phase of the project are provided in **Figure 5.17**. RDX biodegradation occurred rapidly along this transect to a distance of ~ 40 ft from the biobarrier after emulsified oil injection.

Samples for RDX stable isotope analysis were collected during the October 2012 (baseline) and June 2013 (4 months after barrier installation) sampling events. Additional rounds of sampling were scheduled, but the RDX concentrations had decreased below the level that would allow collection of enough RDX mass for isotopic analyses.

Figure 5.16. Map (top) and Layout (bottom) of the Dahlgren NSWC Passive *in situ* Emulsified Oil Biobarrier.

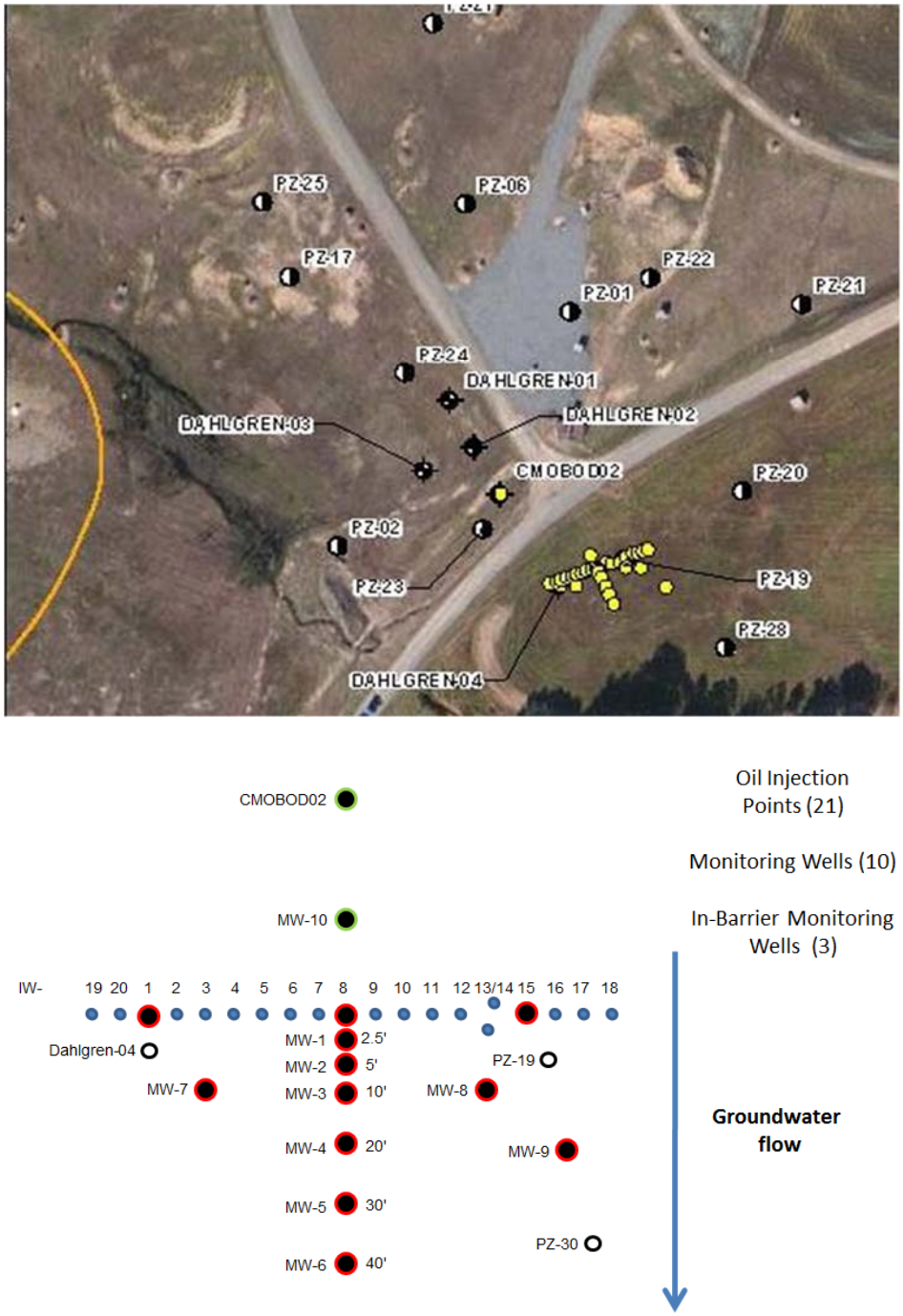

Figure 5.17. RDX Concentrations Along the Centerline of the Biobarrier Monitoring Well Network.

Samples for stable isotope analysis were collected in October 2012 and June 2013.

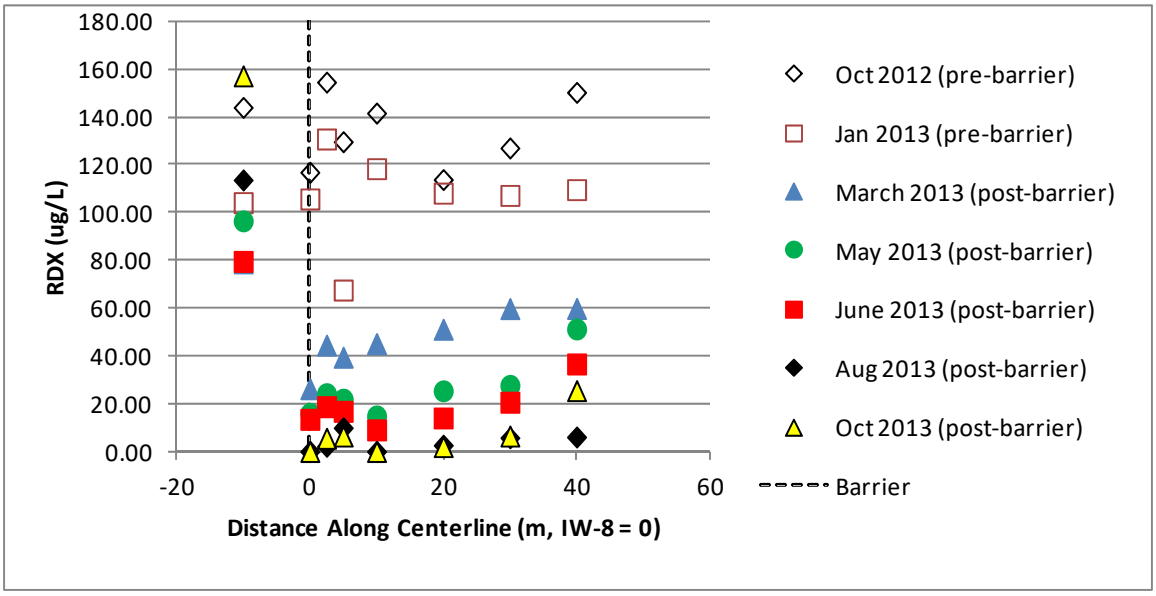

5.4.6 UMCD push pull tests

The field demonstration at UCMD was conducted in two field plots, one for aerobic bioaugmentation only and the other for sequential evaluation of aerobic and anaerobic biostimulation (**Figures 5.18 and 5.19**). RDX degradation rates and RDX stable isotope sampling was conducted in both the biostimulation and bioaugmentation test plots under natural gradient conditions (extraction well EW-4 not pumping). In the biostimulation plot, low concentration fructose additions to wells DW-1 and EW-2 were first used to create conditions that favored aerobic RDX degradation. Higher concentration fructose additions to the same wells were then used to stimulate anaerobic RDX degradation. In the bioaugmentation plot, *Gordonia* sp. KTR9 (produced by APTIM'S's Fermentation facility in Lawrenceville, NJ) was injected into wells DW-2, 4-106, and EW-2 under natural gradient conditions (extraction well EW-4 not pumping). The initial RDX degradation rates in all three plots/conditions were assessed via push-pull testing. Additional push-pull tests were conducted in each well to evaluate degradative activity over time under each set of conditions. Biweekly substrate injections were performed between push-pull tests, and groundwater samples were collected to monitor redox indicators including dissolved oxygen, oxidation-reduction potential, and dissolved ferrous iron.

The push-pull tests consisted of injecting site groundwater amended with NaCl and/or KBr (100 mg/L) and dissolved RDX (~1 mg/L) into a single well and then monitoring the changing composition of the injected test solution/groundwater mixture by sampling the same well over time. For each test, 4,000 L of site groundwater was injected into the well using a high-speed transfer pump at a rate of ~ 140 gpm. Then samples were collected from the same well using a submersible pump. RDX degradation was measured by plotting diluted adjusted RDX concentrations vs. time as in previous push-pull tests conducted at the UMCD site (56).

Stable isotope fractionation during RDX biodegradation in the UMCD field demonstration was determined by quantifying the extent of fractionation as a function of residual RDX concentration, as described in Hatzinger et al., (2009) (37) for perchlorate and nitrate. Two different mixing models were evaluated to account for the presence of background RDX as described further in Section 5.6.2. Triplicate push-pull tests were performed to allow statistical comparison of RDX degradation rates for the different treatments.

Figure 5.18. Well layout for UMCD push-pull tests.

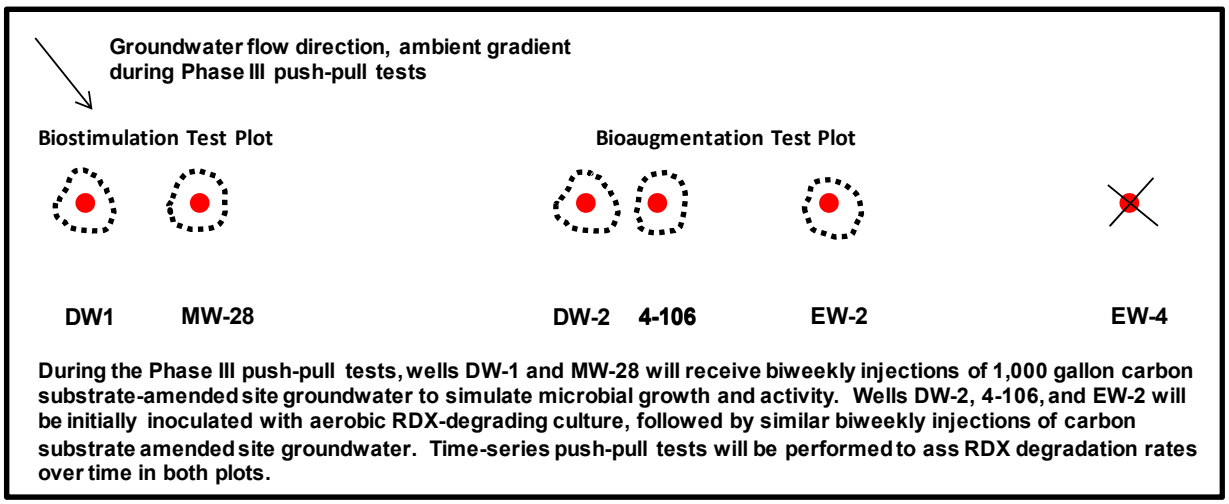

Figure 5.19. Overview of Field Push-pull Test in Bioaugmentation and Biostimulation Test Plots

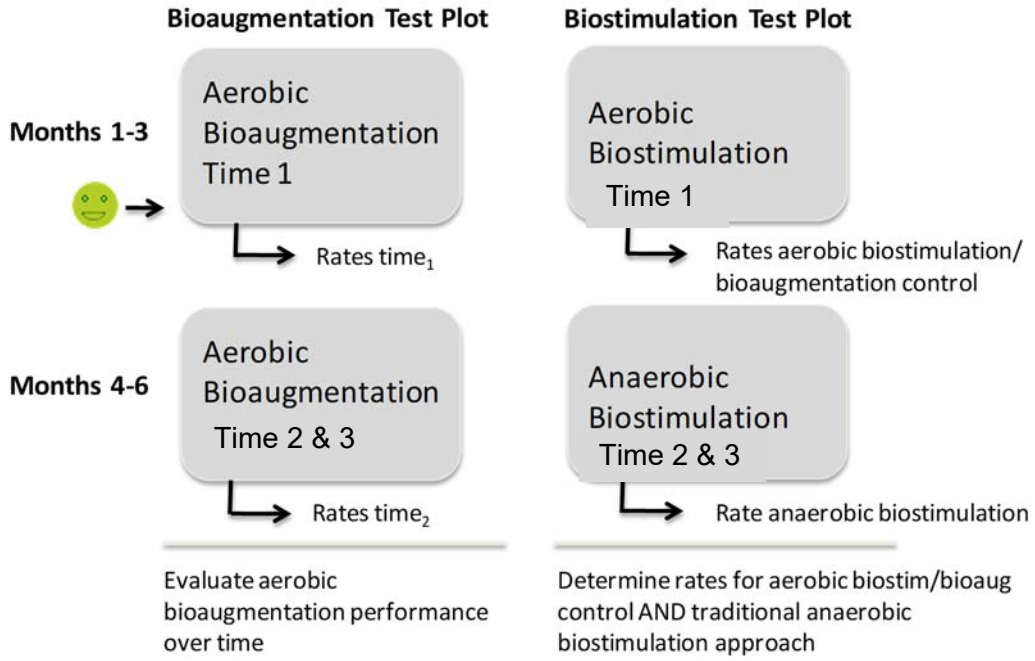

5.5 SAMPLING PLAN

5.5.1 Dahlgren NSWC sampling plan

5.5.1.1 Groundwater sampling

Groundwater samples were collected at Dahlgren NSWC to look for RDX isotope fractionation under natural attenuation conditions and active biostimulation conditions resulting from the installation of an emulsified oil biobarrier.

Sampling was performed utilizing low-flow purging in general accordance with EPA Low-Flow Ground-Water Sampling Procedures (62). Prior to each sampling event, the well ID was checked and recorded on a field sheet, then groundwater elevation measurements were collected using an electronic water level probe (ORS Model #1068013 or equivalent) prior to collecting groundwater samples. Measurements were obtained from the top-of-casing and recorded to the nearest 0.01-ft. The tubing used to sample all wells was dedicated and therefore did not require decontamination prior to sampling. Tubing was set at mid-screen depth within the wells.

A peristaltic pump was used to withdraw water from the wells at a flow rate of 0.1 to 0.5 L/min, and the water level in the well was monitored. It was desirable that the groundwater pumping resulted in <0.3 ft of drawdown in the well, so the pumping rate was adjusted accordingly (i.e., if drawdown was too great, the pumping rate was reduced). For some of the Dahlgren NSWC wells, drawdown was greater than 0.3 ft even at 0.1 L/min due to low groundwater yield. The extent of drawdown in each well was recorded during stabilization.

The extracted groundwater was directed through a flow cell connected to an in-line multi-parameter groundwater meter (e.g., Horiba Model U-22 or equivalent). All field meters were calibrated once at the beginning of the day and checked periodically throughout the day to determine if re-calibration is required.

Parameters, including temperature, conductivity, dissolved oxygen, oxidation-reduction potential (ORP), turbidity, and pH were measured as a function of pumping time, and the values recorded on the field sampling log sheet every 5 to 10 min. An example field sheet is shown in **Figure 5.20.** Water was purged from the well until all parameters were stable for three consecutive readings. Stability was defined as variation of <1% for pH, <3% for temperature and specific conductivity, and <10% for dissolved oxygen, ORP, and turbidity. When parameters were stable according to the above guidelines, sampling time was recorded and all samples were collected. The final data collected on each field sheet was recorded in the project database as the measured readings in each well.

5.5.1.2 Analytical

Groundwater samples from the biobarrier were collected and analyzed for basic field parameters and analytes listed in **Table 5.9**. A more limited list of sampling parameters was evaluated for the natural attenuation testing, including basic field parameters. Sample collection entailed filling appropriate bottles and using the preservative methods listed in **Table 5.10.**

Figure 5.20. Example Groundwater Parameter Stabilization Form for Low Flow Sampling.

Project Name _____
ESTCP Project # _____
CB&I Project # _____
Location _____

WELL ID: _____ Sampling Date: _____
Well Depth [ft-btoc]: _____ Sampler(s): _____
Depth to Water Prior to Purging [ft-btoc]: _____ Sampling Device: _____
_____ Probe S/N _____
Well Casing Diameter [in]: _____ Weather Conditions: _____
Start Time (purging): _____ _____

FIELD PARAMETERS

Time [hh:mm]	pH [std]	Temperature [°C]	Dissolved Oxygen [mg/l]	Redox Potential [mV]	Specific Conductance [µS/cm]	Turbidity [ntu]	Depth To Water [ft-btoc]	Volume Purged [liters]	Approximate Purge Rate [ml/min]
Stabilization Criteria	+/- 1%	+/-3%	+/-10%	+/-10mV	+/-3%	+/-10%	not to exceed 0.3 feet drawdown		100 to 500 mL/min

Sample Time: _____

Comments: _____

Table 5.9. Analytical Methods and Total Samples Collected During Field Sampling at Dahlgren NSWC.

Analyte	Method/ Laboratory	Preservative	Bottle	Total Number Collected
Explosives (RDX, HMX, nitroso intermediates)	EPA 8330 APTIM (modified)	4°C	950 mL amber glass screw-cap (x2)	13 x 16 wells for biobarrier 11x1 for natural attenuation
RDX Stable Isotopes	GC-IRMS at UIC	4°C[a]	950 mL amber glass screw-cap or SPE field column[b]	5 x 9 wells for biobarrier 11x1 for natural attenuation
Perchlorate	EPA 314.0 APTIM	4°C	50 mL sterile polyethylene screw-cap tube (x2)	13 x 16 wells for biobarrier None for natural attenuation
Anions	EPA 300.0 APTIM	4°C	100 mL polyethylene screw-cap (x1)	13 x 16 wells for biobarrier 11x1 for natural attenuation
Total Organic Carbon (TOC)	SM5310B,C,D APTIM	4°C with H_3PO_4	100 mL polyethylene screw-cap (x1)	13 x 16 wells for biobarrier None for natural attenuation
Methane	EPA 3810, RSK175 APTIM	4°C with HCl	40 mL VOA vial (x2) No headspace	13 x 16 wells for biobarrier None for natural attenuation
Volatile Fatty Acids	EPA 300m APTIM	4°C	40 mL VOA vial (x2) No headspace	13 x 16 wells for biobarrier None for natural attenuation
Metals (Fe, Mn, As)	EPA 200.7 External	Capsule filter, 4°C with HNO_3	100 mL polyethylene screw-cap (x1)	13 x 16 wells for biobarrier None for natural attenuation
ORP Dissolved Oxygen pH Conductivity Temperature	Field Meter	--	--	13 x 16 wells for biobarrier 11x1 for natural attenuation

[a]Samples are stored at 4°C and generally processed within 48hrs via SPE with acetonitrile. Preservation is not specified in EPA 8330.

[b]Volume to be collected or filtered based on best estimate of current RDX concentrations and volume required to collected at least 100 µg of RDX for isotopic analysis.

5.5.2 UMCD sampling plan

Three separate push-pull tests were conducted in the aerobic bioaugmentation plot, and three separate push-pull tests were conducted in the anaerobic biostimulation plot (including one test under aerobic conditions prior to addition of large quantities of fructose as a substrate). Sampling was also conducted before each of the tests to characterize baseline conditions, and from the cell/tracer solution to determine total RDX, RDX isotope values, and tracer concentration. Sample preservation and analyses conducted are provided in **Table 5.10** and the total number of samples collected in the background sampling and during the push-pull tests is provided in **Table 5.11.** Additional details on sampling at UMCD are available in the Final Report for ESTCP Project ER-201207 "Bioaugmentation for Aerobic Bioremediation of RDX-Contaminated Groundwater" led by Dr. Mandy Michalsen at USACE, Seattle District and in Michalsen et al. (2016).

Table 5.10. UMCD Phase III Push-pull Testing Sampling Preservation.

Phase III Groundwater Sample Type	Analyte	Method/Laboratory	Container	Preservative	Hold Time
Microbial Community Samples	*xplA* gene copy numbers	qPCR w/ gene-specific primers/USACE-ERDC	1 L PP Bottle	4°C	7 d
KTR-9 cells	Colony Forming Units (CFUs)	Plating on selective and non-selective media/USACE-ERDC	0.5 L PP bottle	4°C	7 d
Anion Samples	Br^-, Cl^-, NO_3^-, NO_2^-, SO_4^{2-}	Ion Chromatography /APTIM	15 mL plastic tube	4°C	14 d
Explosives and Metabolite Samples	Nitramines (e.g. RDX)	HPLC/EPA 8330/ APTIM	0.5 L amber glass bottle w/sea salt[1]	HCl, 4°C	7 d
RDX Stable Isotopes	$\delta^{15}N$ and $\delta^{13}C$ in RDX	GC-IRMS/ UD	1 L HDPE bottle	HCl, 4°C	NA

(1) From ref 59.

Table 5.11. Phase III Push-pull Testing Sampling Plan.

Phase III Push-Pull Testing	Microbial Community Samples, 4°C	Explosives Analysis, 250 mL amber, pH <2 HCl and 4°C	RDX Isotopes (1 L HDPE) 4°C (both tests)		Microbial Samples, 4°C	Explosives Analysis, 250 mL amber, pH<2 HCl and 4°C	RDX Isotopes (1 L amber glass) 4°C (both tests)
	BIOAUGMENTATION TEST Wells DW-2, 4-106, EW-2 PRE INJECTION SAMPLING - 3 wells total – before 3 push-pull tests				**BIOSTIMULATION TEST Wells DW-1, MW-28- 2 wells total – before 2 push-pull tests PRE INJECTION SAMPLING**		
Pre-injection	30	3	30		10	2	22
	BIOAUGMENTATION TEST Wells DW-2, 4-106, EW-2 POST INJECTION SAMPLING FREQUENCY				**BIOSTIMULATION TEST Wells DW-1, MW-28 POST INJECTION SAMPLING FREQUENCY**		
Total Samples Per Test	15	45	45		2	30	30
Total tests	3	3	3		2	2	2
Total samples	45	135	135		4	60	60
	75	138	165		14	62	82

5.5.3 Compound specific isotope analysis of RDX

The methods for analysis of $\delta^{15}N$ and $\delta^{13}C$ in RDX including sample preparation, GC-IRMS analysis, and relevant isotopic standards for quantification are provided in this section. This technique was used for all samples collected at Dahlgren NSWC and UMCD. The method is also summarized elsewhere (27).

5.5.3.1 Explosive compound analysis

Groundwater samples with RDX were initially analyzed to determine RDX concentrations prior to further processing for stable isotope analysis as described below.

Solid phase extraction and concentration. Water samples were concentrated using pre-conditioned Supelclean™ ENVI-Chrom P solid phase extraction (SPE) columns (250 mg packing; Sigma-Aldrich, St. Louis, MO, USA). Internal recovery standards 1,2-dinitrotoluene (1,2-DNT) and 2,4-dinitroanisole (DNAN) were added prior to passage through the SPE column. The SPE column was then rinsed with ultrapure water, and dried under a vacuum. Concentrated analytes were eluted with acetonitrile, the extract was reduced to a volume of 1 ml under nitrogen, then diluted 1:1 (v:v) with ultrapure water.

Explosive concentration determination. The concentrations of the RDX, RDX breakdown products (MNX, DNX, TNX), and any other explosives were determined using HPLC using a modified EPA Method 8330 using an Agilent 1100 HPLC with an Acclaim Explosives E1 column (4.6 x 250 mm, 5µm particle diameter). The photodiode array detector collected peak spectral data and UV adsorption data at both 230 and 254 nm. The mobile phase started out at 20:80 methanol:water at a flow of 0.85 ml/min for 3 minutes, stepped to 38:62 methanol:water from 3 min to 9 min at 0.9 ml/min, then stepped to 43:57 methanol:water over 5 min at 1.05 ml/min and held for 24 min. The column was then washed with 80 % methanol for 6 min to remove any residual compounds before being re-equilibrated to a 20:80 methanol mix for the next run. The column temperature was set at 34 °C. The method detection limit was approximately 20 µg/L for RDX and 50 µg/L for the RDX breakdown products.

Extraction of RDX for isotopic analysis. After the RDX concentrations were determined, the RDX in the remaining water sample was concentrated using SPE as described above. The volume of sample concentrated was varied with sample, but was at least enough to obtain a minimum of 100 µg of RDX in the final extract. The internal recovery standards were not used to avoid interference with isotopic analysis, and the final extract was kept in 100 % acetonitrile without dilution with ultrapure water.

The concentrations of the RDX in the final acetonitrile extract were determined via HPLC using a Dionex 3000 Ultimate HPLC with a Agilent Zorbax Bonus-RP column (4.6 x 75 mm, 3.5 µm particle diameter), variable wavelength detector (254 nm), and a photodiode array detector collecting peak spectral data. The mobile phase was 50:50 methanol:0.2 % (v:v) trifluoroacetic acid in water, at a flow rate of 1 ml/min. The column temperature was set at 33 °C. The method detection limit was approximately 10 µg/L for RDX. After determination of the RDX concentrations, the samples were shipped to the Environmental Isotope Geochemistry Laboratory at the University of Delaware (formerly at the University of Illinois at Chicago) for determination of $\delta^{15}N$ and $\delta^{13}C$ in RDX.

5.5.3.2 Determination of $\delta^{15}N$ and $\delta^{13}C$ in RDX

GC-IRMS techniques were developed for analysis of $\delta^{15}N$ and $\delta^{13}C$ in RDX. For analysis of $\delta^{13}C$ in RDX, carbon was converted to CO_2 gas after chromatographic separation. Isotopic measurements were typically done with 5 µg aliquots of RDX, which is at the low end of the feasible range for isotopic analysis of RDX according to Gelman et al. (2011) (31) who used 50 µg to obtain 0.3 to 0.4 ‰ precision on pure RDX. However, injecting smaller amounts of RDX yielded improved GC resolution for C isotopic analysis and provided a good balance between better chromatographic separation and slightly lower analytical precision. Gas chromatographic interferences near RDX, as observed in C isotopic analyses, were much less common in N isotopic analyses. If the RDX peak could not be fully resolved for a given sample, isotopic data for that sample were rejected.

An RTX-5MS GC column (15 m length x 0.53 mm inner diameter x 0.5 µm film thickness; Restek, Inc.), with a 20 mL/min flow of He was used. The inlet temperature was 190 °C, which did not result in thermal decomposition of the injected RDX. The following GC program was used for C separation: 75 °C x 1.5 min, ramp at 10 °C/min to 200 °C, then ramp 20 °C /min to 300 °C, which was maintained for 5 min. From the GC column the sample passed through a pre-oxidized Ni/Cu/Pt combustion furnace at 940 °C, and the combustion products were then reduced in a separate furnace of Cu at 600 °C. The resulting CO_2 was introduced to the mass spectrometer (Thermo Finnigan Delta Plus XP) by an open split interface (Thermo Finnigan GCCIII) for quantification of C isotope amounts.

The N in RDX was converted to N_2 gas prior to IRMS analysis. The method for N isotopic analysis of RDX was similar to that described for $\delta^{13}C$ with modifications as follows: 1) The GC oven temperature program started at 75 °C x 1.5 min, ramped at 10°C/min to 220 °C, then ramp at 20 °C/min to 300 °C, which was maintained for 5 min. 2) From the GC column the sample passed through a Ni/Cu/Pt combustion furnace which was not pre-oxidized (unlike that for CO_2) in order to minimize formation of NO, then passed through a Cu reduction furnace at 600 °C. CO_2 was trapped from the continuous flow He stream using liquid N_2 before the analyte N_2 was introduced to the mass spectrometer as described for C. 3) Following each N_2 isotopic measurement, the open-split interface was isolated and the trapped CO_2 was flushed away by removing the liquid nitrogen trap from the He stream prior to the next analysis. Each data point generated was the mean of replicate GC-IRMS injections (two to seven per sample).

The C isotope ratio in RDX was reported as $\delta^{13}C$:

$$\delta^{13}C_{sample} = (^{13}C/^{12}C_{sample}) / (^{13}C/^{12}C_{VPDB}) - 1 \qquad (1)$$

where VPDB is Vienna Pee Dee Belemnite. The $\delta^{13}C$ data are reported in parts per thousand (‰), and were calibrated by analyzing a RDX standard reference material from ChemService (West Chester, PA; 1000 µg/mL in acetonitrile) for which a $\delta^{13}C$ value of -32.2 ‰ was determined independently by comparison with international L-glutamic acid isotopic reference materials USGS40 and USGS41 (63). The average reproducibility of normalized RDX $\delta^{13}C$ values (one standard deviation) was ± 1.0 ‰, based on 300 replicate analyses of aliquots (ranging from 2 to 10 micrograms) of ChemService RDX. The reproducibility of $\delta^{13}C$ values for sample replicate injections ranged from ± 0.01 to ± 2.87 ‰.

The N isotope ratio in RDX was reported as $\delta^{15}N$:

$$\delta^{15}N_{sample} = (^{15}N/^{14}N_{sample}) / (^{15}N/^{14}N_{AIR}) - 1 \quad (2)$$

where AIR is N_2 in air. The $\delta^{15}N$ data are reported in parts per thousand (‰) and were calibrated by analyzing the ChemService RDX standard listed above, for which a $\delta^{15}N$ value of 0.22 ‰ was determined independently by comparison with international L-glutamic acid isotopic reference materials USGS40 and USGS41 (63). The average reproducibility of normalized RDX $\delta^{15}N$ values (one standard deviation) was ± 0.7 ‰, based on 400 replicate analyses of aliquots (ranging from 2 to 10 µg) of ChemService RDX. The reproducibility of $\delta^{15}N$ values for replicate sample injections ranged from ± 0.12 to ± 2.13 ‰.

5.5.4 Compound specific isotope analysis of NO3-

The isotopic composition ($\delta^{15}N$ and $\delta^{18}O$) of NO_3^- collected from the Dahlgren NSWC site groundwater was evaluated using a bacterial reduction method, in which NO_3^- is converted to N_2O for IRMS (14, 20, 67). The data were calibrated by analyzing NO_3^- isotope reference materials using calibration data (7). For USGS34, $\delta^{15}N$ = -1.8 ‰ and $\delta^{18}O$ = -27.9 ‰; for USGS32, $\delta^{15}N$ = 180.0 ‰; for USGS35, $\delta^{18}O$ = +57.5. NO_2^- was not detected by ion chromatography (EPA Method 300).

5.6 DATA ANALYSIS AND SAMPLING RESULTS

5.6.1 Determination and analysis of isotope fractionation factors

An isotopic fractionation factor (expressed as the ε value = see text below) was determined for the studies conducted at both UMCD and Dahlgren NSWC. The factor directly compares the isotopic enrichment in a given element in a chemical of interest with the amount of the chemical remaining (*f*) during biodegradation. For push-pull or other *in situ* reaction testing, the *f* value and isotopic fractionation values were adjusted for dilution with background based upon recovered tracer concentrations in the "pull" phase of the test as described below in Section 5.6.2. Once corrected, these values were used in the equations below to calculate ε.

The isotopic fractionation factor, α, is defined as

$$\alpha = R_A/R_B \quad (3)$$

where R is an isotope-amount ratio ($n(^iE)/n(^jE)$), and A and B are two substances (in the present case, RDX after varying degrees of bioreduction). For C and N compounds, R represents the isotope ratios $^{13}C/^{12}C$ and $^{15}N/^{14}N$, respectively. Values of α were obtained from the experimental results by assuming the exponential Rayleigh-type function

$$R/R_0 = f^{\alpha-1} \quad (4)$$

where R and R_0 are the C or N isotope ratios of the residual reactant (RDX) and the initial (unreacted) RDX, respectively, and f is the fraction of reactant remaining (C/C_0). In terms of the δ values, Equation 4 can be rewritten as:

$$(\delta + 1)/(\delta_0 + 1) = f^{\alpha-1} \quad (5)$$

where δ represents the isotopic composition of the reactant at any value of f, and δ_0 represents the isotopic composition at $f = 1$. The value of α was obtained by linear regression of data using a logarithmic form of Eq 5:

$$\alpha\text{-}1 = \ln [(\delta + 1)/(\delta_0 + 1)]/\ln (C/C_0) \quad \text{or alternatively} \quad (6)$$

$$\alpha\text{-}1 = \ln [R/R_0)]/\ln f \quad (7)$$

Isotopic fractionation effects also are commonly expressed in terms of ε, where

$$\varepsilon = \alpha - 1. \quad (8)$$

The ε values for C and N in RDX that were determined from the stable isotope fractionation data were compared with the laboratory-derived ε values for reactions that may occur under the relevant geochemical conditions (see **Table 2.1, Figure 2.1** and **Figure 2.2**). These comparisons provided data concerning the expected extent of fractionation of C and N *in situ* during anaerobic (UMCD and Dahlgren NSWC) and aerobic (UMCD) biodegradation. For anaerobic biodegradation, where detectable fractionation of both C and N is anticipated, the isotope fractionation factor ratio ($\varepsilon^{13}C/\varepsilon^{15}N$) was calculated. This ratio was reasonably expected to be similar between laboratory and field studies if RDX was degrading by the same mechanism/pathway, and allows confirmation of a specific route of degradation.

For the natural attenuation study conducted at Dahlgren, samples were collected along the flow paths of RDX in the groundwater. If biodegradation was occurring along those flow paths, both a decline in contaminant concentrations and isotopic enrichment of ^{15}N (and ^{13}C for anaerobic degradation) would be anticipated. In this case, stable isotope values in the downgradient and upgradient wells was used essentially to substitute for R and R_0, respectively (Eq.4).

5.6.2 Corrections to RDX and isotope data based on mixing with background RDX

RDX was concentrated from selected samples from push pull tests for analysis of the C and N stable isotopes as described above. Background contributions to measured RDX concentration data and stable isotope values were accounted for using two simple mixing models hypothesized to bracket the true in situ behavior: 1) mixing of injected and background waters occurred only during injection, and 2) mixing of distinct injection and background waters occurred only during sampling.

The conservative tracer cannot distinguish between either model, only describing the fractions of injected and background waters:

$$X_{inj}(t) = \frac{CT_{smp}(t) - CT_{bk}}{CT_{inj} - CT_{bk}} \quad (9)$$

Where X_{inj} is the estimated mixing fraction of water derived from the injected water, and CT_{smp}, CT_{bk}, and CT_{inj} are the concentrations of the conservative tracer in sampled water, in background water, and in the injected water, respectively. The fractions of injected and background waters were assumed to sum to 1 (i.e., injected and background water account for all water).

The degradation and isotope fractionation of reactive tracers (e.g., the contaminant of interest) in the subsurface is evaluated differently in the two models as described below.

5.6.2.1 Model 1: Mixing during injection

In this model, the reactive tracer is assumed to mix with the same estimated fractions as the conservative tracer during injection:

$$RT_0(t) = X_{inj}(t) \times RT_{inj} + \left(1 - X_{inj}(t)\right) \times RT_{bk} \tag{10}$$

Where RT_0 is the initial concentration of reactive tracer in the subsurface corresponding to the estimated mixing fractions sampled at time t, and RT_{inj} and RT_{bk} are the reactive tracer concentrations in the injected and background water, respectively. Loss/degradation reactions are then assumed to impact both injected and background reactive tracers with time and sampling is assumed not to further mix waters, such that the fraction of reactive tracer remaining after degradation, F, is described as:

$$F(t) = \frac{RT_t(t)}{RT_0(t)} = \frac{RT_{smp}(t)}{RT_0(t)} = \frac{RT_{smp}(t)}{X_{inj}(t) \times RT_{inj} + \left(1 - X_{inj}(t)\right) \times RT_{bk}} \tag{11}$$

Where RT_t and RT_{smp} correspond to the reactive tracer concentrations in the subsurface and in samples collected at times t.

The assumed mixing of injected and background reactive tracer also affects the estimated initial isotope composition as follows:

$$\delta RT_0(t) = \frac{X_{inj}(t) \times RT_{inj} \times \delta RT_{inj} + \left(1 - X_{inj}(t)\right) \times RT_{bk} \times \delta RT_{bk}}{X_{inj}(t) \times RT_{inj} + \left(1 - X_{inj}(t)\right) \times RT_{bk}} \tag{12}$$

Where δRT_0 describes the initial isotope composition of the reactive tracer in the subsurface corresponding to the estimated mixing fractions sampled at time t, and δRT_{inj} and δRT_{bk} describe the isotope composition of the injected and background reactive tracers, and the other terms are as defined earlier.

The extent of isotope fractionation occurring during the in situ reaction can then be estimated as:

$$\delta RT_{reac}(t) = \left(\delta RT_t(t) - \delta RT_0(t)\right) = \left(\delta RT_{smp}(t) - \delta RT_0(t)\right) \tag{13}$$

Where δRT_{reac}describes the extent of isotope fractionation due to the reaction, and δRT_t and δRT_{smp} describe the isotope composition of the reactive tracer in situ and in samples, respectively.

5.6.2.2 Model 2: Mixing during sampling

In this model, the reactive tracer remains distinct from background water and only mixes at the time of sampling with the same estimated fractions as the conservative tracer during injection:

$$RT_{smp}(t) = X_{inj}(t) \times RT_t(t) + \left(1 - X_{inj}(t)\right) \times RT_{bk} \quad (14)$$

Where all the terms are defined as before. Loss/degradation reactions are assumed to impact only injected reactive tracers with time, such that F in situ is described as:

$$F(t) = \frac{RT_t(t)}{RT_0(0)} = \frac{RT_t(t)}{RT_{inj}} = \frac{RT_{smp}(t) - \left(1 - X_{inj}(t)\right) \times RT_{bk}}{X_{inj}(t) \times RT_{inj}} \quad (15)$$

Note that RT_0 is constant and estimated to equal RT_{inj} because the injected reactive tracer is assumed to remain distinct from background.

The assumed mixing of injected and background reactive tracer during sampling also affects the estimated isotope composition as follows:

$$\delta RT_t(t) = \frac{RT_{smp}(t) \times \delta RT_{smp}(t) - \left(1 - X_{inj}(t)\right) \times RT_{bk} \times \delta RT_{bk}}{RT_{smp}(t) - \left(1 - X_{inj}(t)\right) \times RT_{bk}} \quad (16)$$

As before, the extent of isotope fractionation occurring during the in situ reaction can be estimated as:

$$\delta RT_{reac}(t) = \left(\delta RT_t(t) - \delta RT_0(0)\right) = \left(\delta RT_t(t) - \delta RT_{inj}\right) \quad (17)$$

The above mixing models were translated into appropriate Microsoft Excel formulas, with the measured RDX and conservative tracer (chloride or bromide) serving as inputs, and the corrected, dilution-adjusted RDX concentration, ^{15}N, and/or ^{13}C isotope values as outputs. The corrected values were then used to calculate fractionation factors (ε) as described in section 5.6.1 above.

5.6.3 Dahlgren NSWC - Natural attenuation sampling

5.6.3.1 RDX extraction from groundwater - laboratory vs. field SPE

A comparison of the total RDX collected using the field SPE columns compared to sample processing in the laboratory for several wells was performed (**Table 5.11**). For the wells for which both field and laboratory collection of RDX was conducted and volumes of groundwater extracted were the same, the following observations were made. In 4 out of 5 wells for which these conditions were met, the percentage of RDX captured in the field was within 20 % of that collected in the laboratory. In 1 well (PZ-17), significantly more (~ 2.5x) RDX was collected in the field than was collected in the laboratory for the same volume of groundwater processed. The reason for this discrepancy is unclear, although the most likely explanation is that more groundwater was passed through the column in the field than recorded on the field sheet. A direct comparison could not be performed for several of the wells because the volume processed in the field and in the laboratory were different.

For many of the wells, the amount of RDX present after SPE was similar irrespective of whether the technique was conducted in the field or in the lab (**Table 5.11**). However, there were a few discrepancies where the RDX in the final extract from field samples was appreciably lower than in the lab extracted samples (wells MW6 and CMOBOD02 in **Table 5.11**).

However, the $\delta^{15}N$ data in RDX from these samples were comparable (see Section 5.6.3.2), and more than 40 µg of RDX was extracted from the groundwater from each piezometer, which was sufficient for the current stable isotope analysis methods. Thus, the data suggest that the field SPE column is a viable approach to obtain RDX samples for stable isotope analysis from low concentration wells.

5.6.3.2 RDX isotope fractionation during RDX extraction - laboratory vs. field SPE

A comparison of $\delta^{15}N$ data from RDX derived from the field SPE columns vs the laboratory SPE columns indicated that there was no significant difference between the two methods (**Table 5.12** and **Figure 5.21**), given the variability in stable isotope data. When relevant samples were compared for the entire dataset, the $\delta^{15}N$ for RDX from the laboratory processed samples was 1.1 ± 1.2 ‰ (n = 8), while that for the field-processed samples was 1.1 ± 1.7 ‰ (n = 11). If the same 8 wells are taken into account for the field samples, the mean $\delta^{15}N$ was 1.4 ± 1.8 ‰. Interestingly, the variability in the $\delta^{15}N$ analyses on a well by well basis (i.e., replicate $\delta^{15}N$ measurements on the same sample) was somewhat higher in the field-processed samples than in the laboratory processed samples. With one exception, the laboratory samples had a standard deviation < 0.5 ‰, while the field samples were typically > 1 ‰. Further investigation would be required to determine the reason for this discrepancy, and potential solutions.

5.6.3.3 RDX isotope fractionation under natural attenuation conditions

Results of the ^{15}N isotope analysis of RDX collected across the Churchill Range at Dahlgren NSWC are shown in **Figure 5.22**. No apparent trends in the $\delta^{15}N$ of RDX versus RDX concentration were evident. Additionally, no trends along assumed transects through the RDX plume were detected. Taken together, these results do not indicate that natural attenuation of RDX is occurring in RDX plumes that were sampled. Because of the bulk aerobic conditions at the site and the lack of ^{15}N fractionation, $\delta^{13}C$ analysis was not conducted. These data are inconsistent with the laboratory column results that appeared to show loss of RDX in some of the site samples (2/3 columns) (Section 5.2.1) by either an abiotic or biotic mechanism, or they may indicate that the loss was due to RDX adsorption to the soil matrix. It should also be noted that a previous investigation by our group at this site revealed no detectable NDAB (an aerobic degradation product of RDX) or MNX, DNX, or TNX (common anaerobic degradation products) in groundwater from the Churchill Range. Taken together with the general low pH of the groundwater at this site (~ 4.5), the data may indicate a general lack of biological attenuation of the RDX plumes at this location via degradation.

5.6.3.4 NO_3^- isotope fractionation under natural attenuation conditions

The $\delta^{15}N$ and $\delta^{18}O$ values of NO_3^- collected across the Churchill Range at Dahlgren NSWC are shown in **Figure 5.23**. Along with the Dahlgren data, $\delta^{15}N$ and $\delta^{18}O$ values for NO_3^- generated by various other natural processes, as well as NO_2^- generated by pure cultures degrading RDX by various pathways, are also presented. With the exception of one sample, the combined $\delta^{15}N$ and $\delta^{18}O$ data from Dahlgren NSWC samples fall within the range of "biogenic NO_3^-" on the dual isotope plot in **Figure 5.23**. This is typically NO_3^- produced via nitrification in soils. The $\delta^{18}O$ values for most of the Dahlgren NSWC samples were in the general range of those of NO_2^- produced during aerobic degradation of RDX, but the $\delta^{15}N$ values were appreciably higher.

The one sample that did not fall within this range from PZ-2 had a very high value of $\delta^{15}N$ (> + 30 ‰) and a somewhat elevated value of $\delta^{18}O$ (nearly + 20 ‰), which could be consistent with N isotope fraction during biological degradation of biogenic NO_3^-, as revealed in the trend lines on **Figure 5.23**. It is interesting to note on **Figure 5.23** how distinctive the $\delta^{15}N$ is for NO_2^- generated by anaerobic degradation processes, with values ranging from 20 ‰ to nearly 40 ‰ lower than the lowest range for biogenic NO_3^-. Although natural attenuation of RDX was not detected in this case via either RDX or NO_2^-/NO_3^- stable isotope analysis, the data suggest that these combined analyses may be used to confirm natural degradation processes, particularly under anaerobic conditions.

Table 5.12. Natural Attenuation Sampling Data Obtained Using Field and Laboratory Collection of RDX from Groundwater.

	RDX mass collected (µg)		LAB / FIELD	RDX Captured (%)[a]		$\delta^{15}N$ (‰)	
Well ID	**LAB**	**FIELD**	**(%)**	**LAB**	**FIELD**	**LAB**	**FIELD**
Dahlgren-01	264	253	104	82	78	1.5 ± 0.3	2.5 ± 1.0
Dahlgren-04	185	159	116	112	92	1.5 ± 0.4	1.3 ± 1.3
IW-8	225	246	91	101	105	2.1 ± 0.1	3.1 ± 1.7
PZ-17	167	436	38	102	264	-0.8 ± 1.4	2.6 ± 3.8
PZ-22	164	152	108	94	88	0.0 ± 0.2	-1.0 ± 2.5
PZ-2	44	110	NA[b]	72	60	1.5 ± 0.3	1.0 ± 1.9
MW-6	364	106	NA[b]	85	18	0.1 ± 0.5	-1.0 ± 0.7
CMOBOD02	262	74	NA[b]	77	12	2.8	2.8 ± 1.6
CMOBOD07	-	108	NA[b]	-	96	-	0.2 ± 0.6
PZ-20	-	156	NA[b]	-	65	-	-1.5 ± 6.3
PZ-28	-	517	NA[b]	-	119	-	2.0 ± 0.7
			Average	**91**	**91**	**1.1**	**1.1**
			Standard Deviation	**14**	**67**	**1.2**	**1.7**

[a] Mass RDX captured divided by mass RDX present based on RDX concentration.

[b] Different groudwater volumes processed preclude direct comparison of lab vs. field for these samples.

-, No sample collected.

Figure 5.21. $\delta^{15}N$ isotope Data from RDX Extracted from Dahlgren NSWC Groundwater in the Laboratory and the Field.

SD, standard deviation of ^{15}N isotope data.

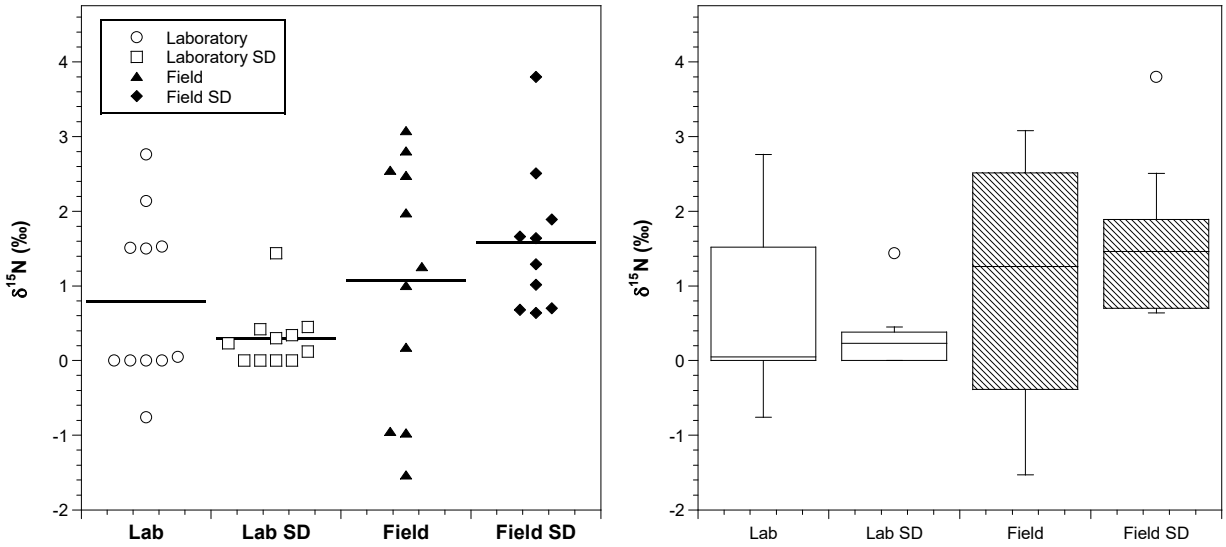

Figure 5.22. Plot of $\delta^{15}N$ (RDX) vs RDX Concentration Across the Churchill Range at Dahlgren NSWC.

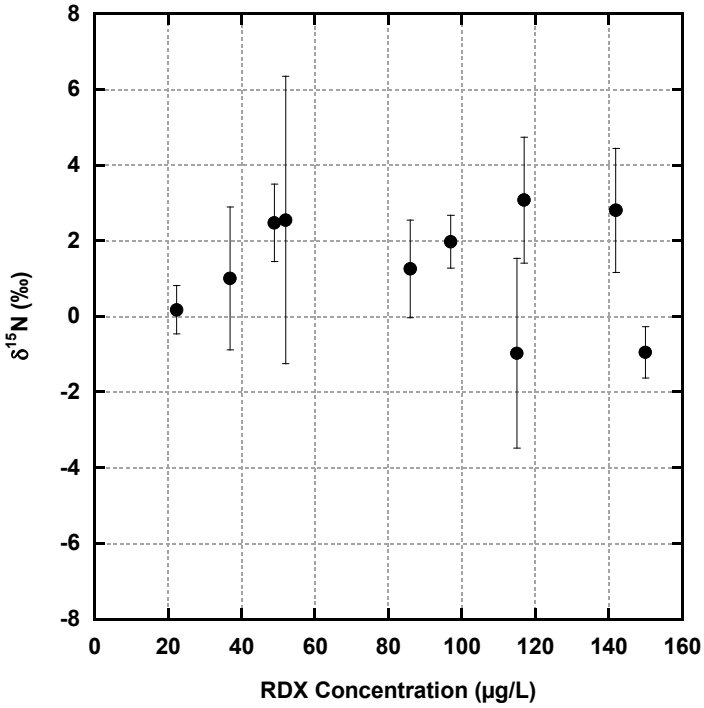

Figure 5.23. Plot of $\delta^{18}O$ vs $\delta^{15}N$ in NO_3^- Across the Churchill Range at Dahlgren NSWC Compared to Common Sources and NO_2^- Generated by Aerobic and Anaerobic RDX Biodegradation.

Dahlgren NSWC groundwater data are shown as solid black circles (data provided in Appendix B; Table B-2). Values from NO_2^- generated via aerobic RDX degradation by pure bacterial strains are represented with solid red circles, while those from anaerobic degradation are represented by solid blue circles (Pathways C and B, respectively, ***Figure 2.1****) (Table B-1) (27). Colored fields for common sources of NO_3^- in mid-latitude non-arid settings are modified from (48, 50, 57), and references therein.*

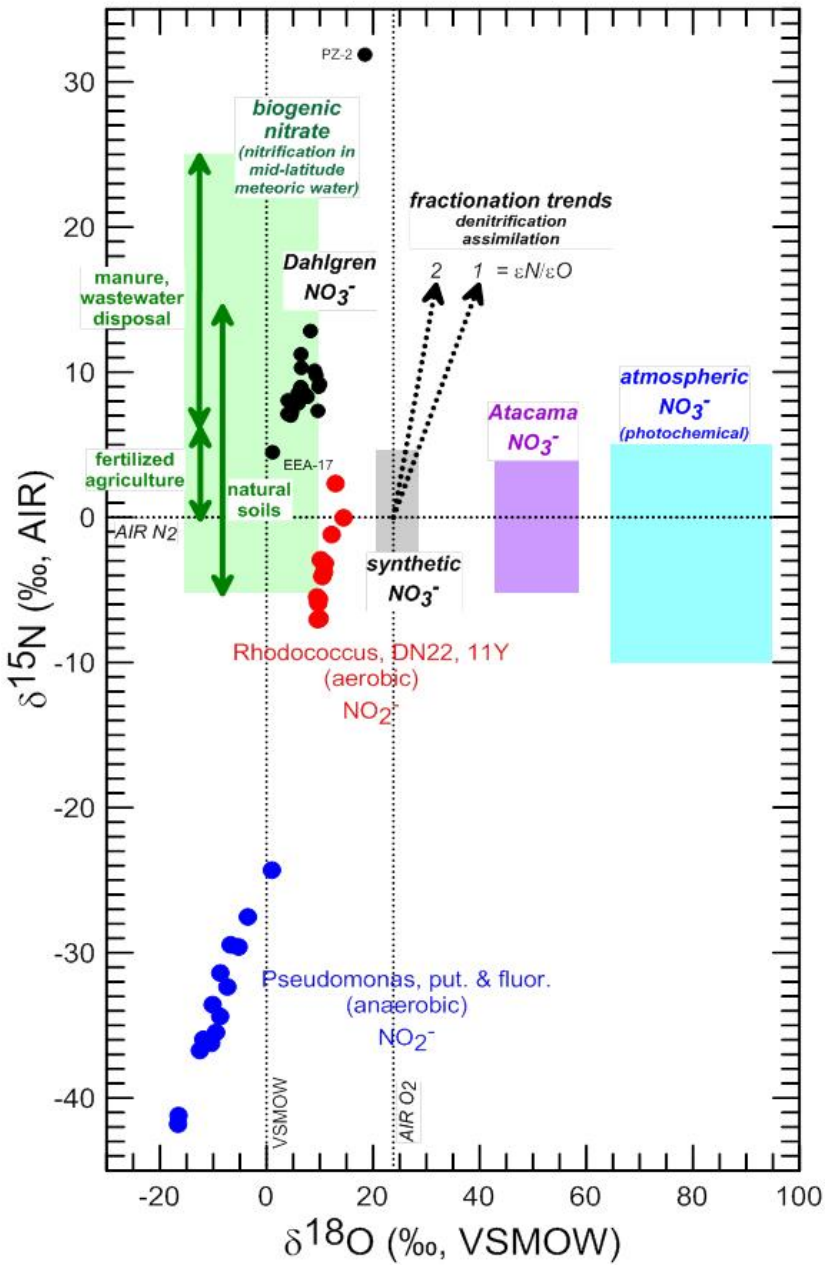

5.6.4 Dahlgren NSWC - Biobarrier sampling

5.6.4.1 RDX isotope fractionation

Samples for C and N isotopic analysis were collected from several different wells in the field test plot upgradient and downgradient from the emulsified oil biobarrier. RDX concentrations along the centerline of wells before (October 2012) and after (June 2013) the biobarrier was installed are shown in **Figure 5.24** as a function of distance upgradient and downgradient of the biobarrier. The complete dataset of all wells sampled is provided in **Table 5.13**. Specific well locations are shown in **Figure 5.16**, and the full details and results from ESTCP project ER-201028 entitled "Passive Biobarrier for Treating Co-Mingled Perchlorate and RDX in Groundwater at an Active Range" (40). The $\delta^{13}C$ and $\delta^{15}N$ values of RDX along the centerline of wells at the two timepoints are presented in **Figure 5.25**. Enrichment of both ^{13}C and ^{15}N are apparent in many of the downgradient test plot samples in June 2013 (post-biobarrier) compared to October 2012 (pre-biobarrier), with the highest fractionation occurring over the initial 20 ft downgradient of the plot. This is consistent with the zone of influence of the initial injection and the estimated groundwater flow in the range of up to 20 ft/yr. However, the geology at this shallow aquifer was extremely complex and consisted of small sand seams interspersed within thick clay layers, so an actual groundwater flow rate through the plot was difficult to calculate as some of the sand seams appeared to be terminal, possibly leading to very slow transport of groundwater within the plot.

The ^{13}C and ^{15}N fractionation factors (ε) are shown graphically in **Figure 5.26**, and the best fit linear regressions are presented in **Table 5.14,** along with regressed values for anaerobic RDX degradation using pure cultures (27) and RDX degradation under various electron acceptor conditions in enrichments derived from Dahlgren NSWC sediments. Because groundwater flow through the plot could not be readily calculated (as previously noted), and likely was exceedingly slow, the calculation of R/R_0 from the plot was based on a "batch" system, with values for R and R_0 compared from individual wells assuming the parcel of water in the plot was largely static.

Using the batch calculation, calculated values of $\varepsilon^{13}C$ and $\varepsilon^{15}N$ in the plot were -2.2 ‰ and -6.8 ‰, respectively. The slight depression in the $\varepsilon^{13}C$ and $\varepsilon^{15}N$ values in the field compared to laboratory studies has been observed during the degradation of other compounds (37, 58, 75), and is attributed abiotic effects (e.g., dispersion, dilution, incomplete mixing) occurring in the aquifer matrix compared to a well-mixed system (47, 75). The isotope fractionation factor ratio ($\varepsilon^{15}N$ /$\varepsilon^{13}C$) for the samples was ~ 3.1 which falls well within the relatively wide range determined from anaerobic pure cultures (1.5-5.5), and most closely matches that determined for *Clostridium acetobutylicum* ATCC 824, at ~ 2.9. The relatively broad range of this parameter most likely reflects the differing or mixed anaerobic pathways of RDX degradation. More studies are required to determine if fractionation factor ratios could be linked to specific mechanisms of anaerobic degradation because many of the cultures tested appeared to degrade RDX via multiple mechanisms (27). However, this study clearly documents anaerobic RDX biodegradation in an aquifer using C and N stable isotope analysis.

Figure 5.24. RDX Concentrations Along the Centerline of the Biobarrier before (October 2012) and After (June 2013) Oil Injection.

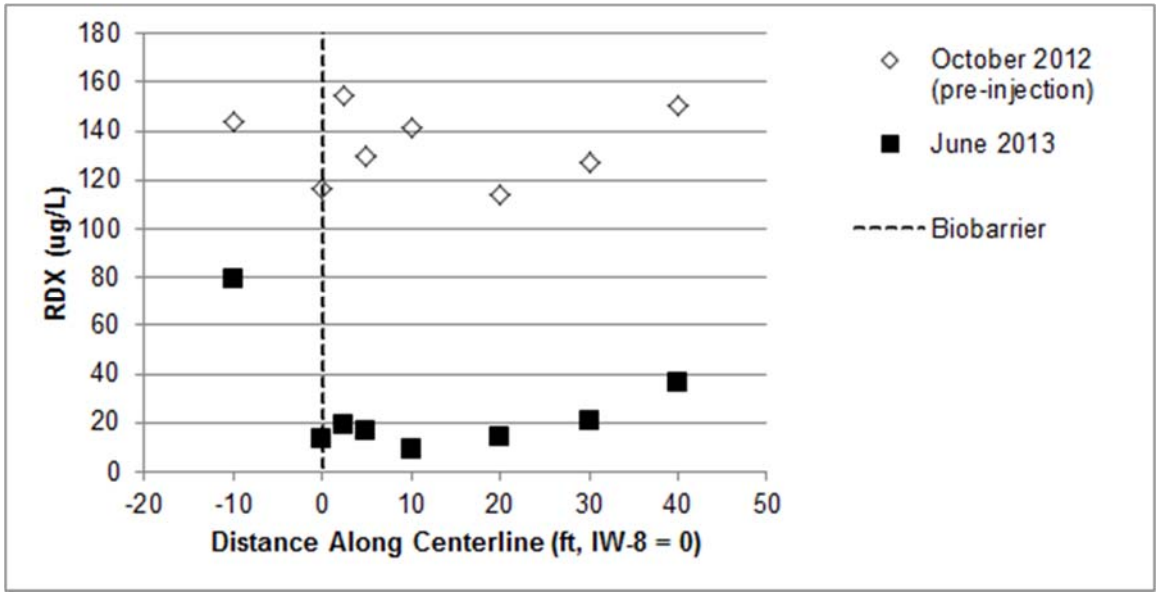

Table 5.13. $\delta^{13}C$ and $\delta^{15}N$ from RDX in Biobarrier Wells at Dahlgren NSWC.

Samples were collected prior to barrier installation (October, 2012), and approximately 130 days after installation (June, 2013).

	October, 2012 (pre injection)			June, 2013 (post injection)		
Well ID	**$\delta^{13}C$**	**$\delta^{15}N$**	**µg/L**	**$\delta^{13}C$**	**$\delta^{15}N$**	**µg/L**
CMOBOD02	-35.66	3.32	102.85	-34.89	2.19	120.39
MW-1	-35.36	2.80	130.70	-29.88	13.16	18.71
MW-2	-35.91	3.50	67.52	NA	NA	16.77
MW-3	-35.59	2.30	118.29	-28.01	18.32	9.01
MW-4	-35.52	2.50	108.07	-31.28	12.68	14.00
MW-5	-35.91	2.95	107.11	NA	NA	20.60
MW-6	-35.74	1.91	109.53	-34.58	3.26	36.60
MW-8	NA	NA	97.23	-35.04	2.34	60.07
MW-9	-34.94	1.40	64.34	-34.67	5.15	30.76
MW-10	-35.50	NA	104.08	-35.95	1.84	79.51
PZ-19	-35.08	2.80	57.37	NA	NA	20.98
IW-1	-36.22	2.68	125.18	NA	NA	16.19
IW-8	-35.50	2.63	105.62	NA	NA	13.44
PZ-30	NA	NA	72.57	-34.89	2.04	84.35

NA - data not available

Figure 5.25. $\delta^{13}C$ and $\delta^{15}N$ of RDX Collected from Sampled Along the Centerline of the Biobarrier before (October 2012) and after (June 2013) Oil Injection.

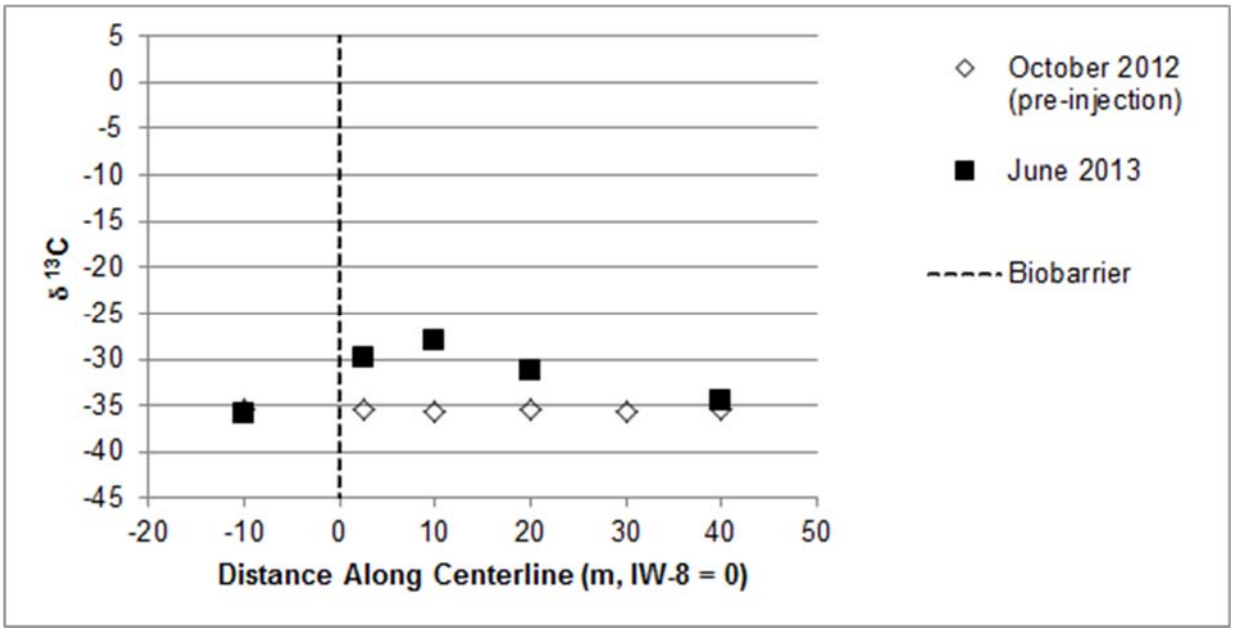

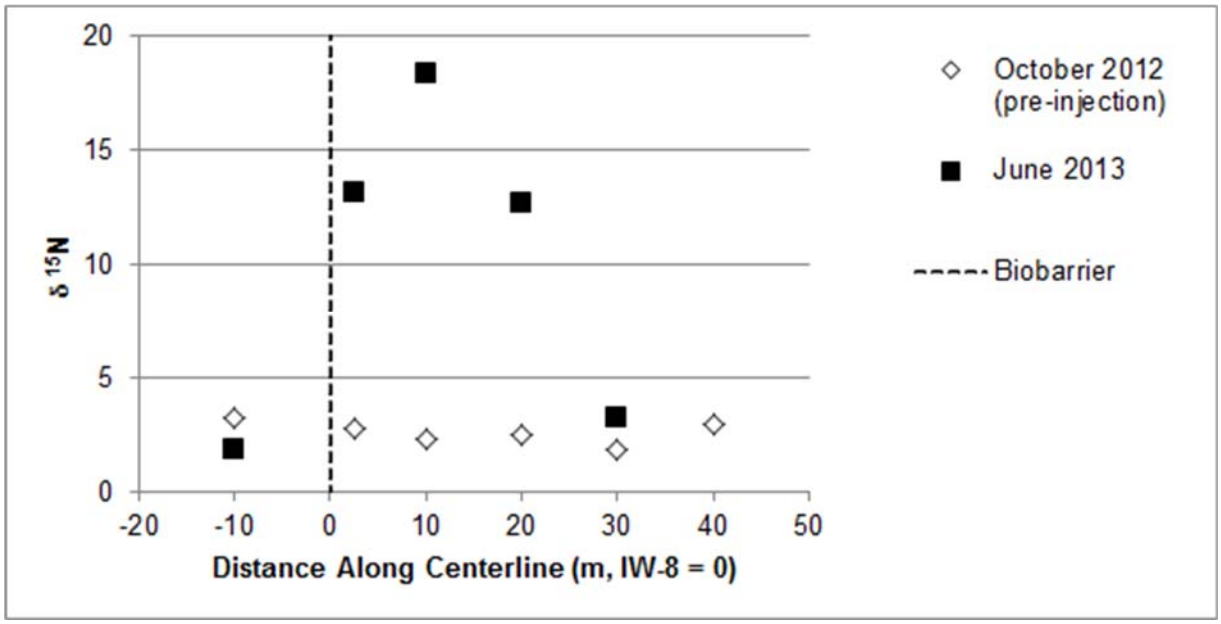

Figure 5.26. Plot of $\delta^{15}N$ and $\delta^{13}C$ and versus RDX Concentration Expressed as ln (f) for Samples Collected Along the Centerline of the Dahlgren Biobarrier in June 2013.

Fractionation factors (□) are shown based on the slopes of the fitted lines.

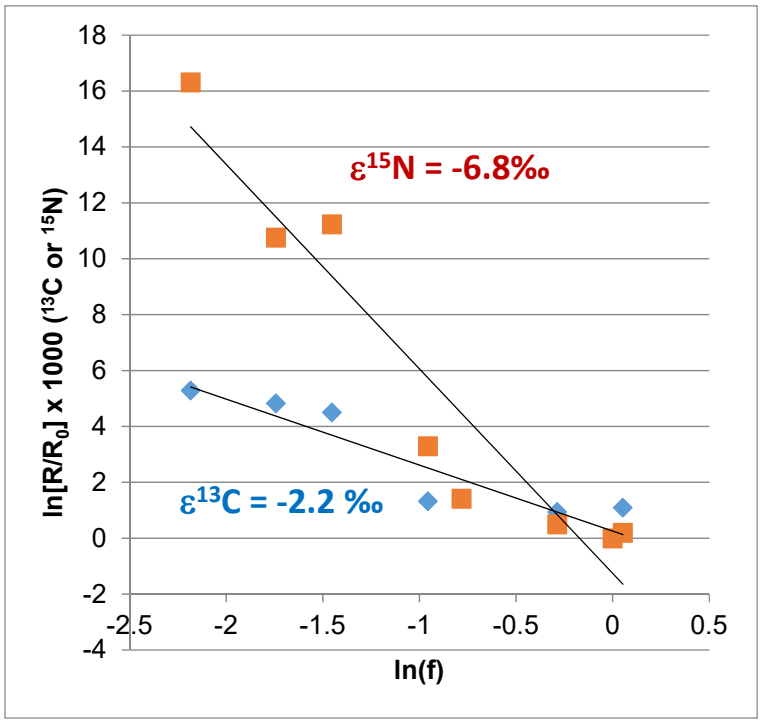

Table 5.14. Compiled ^{13}C and ^{15}N RDX Fractionation Factors from Dahlgren NSWC Biobarrier Sampling.

	ε ^{13}C			ε ^{15}N		
	‰	±	P-value	‰	±	P-value
Dahlgren NSWC Anaerobic Biobarrier[a]	-2.2	1.1	4.7E-03	-6.8	3.1	3.7E-03
Anaerobic Pure Cultures						
Shewanella oneidensis MR-1	-6.0	2.6	2.0E-04	-9.6	1.3	5.6E-12
Klebsiella pneumoniae SCZ-1	-4.1	1.6	4.7E-05	-5.8	2.6	6.3E-04
Desulfovibrio sp.	-2.0	0.5	2.8E-06	-10.9	1.2	5.2E-10
Clostridium acetobutylicum ATCC 824	-2.8	1.6	2.7E-03	-8.0	5.5	1.9E-02
Composited Anaerobic Pathway[a]	**-4.7**	**1.1**	**1.8E-11**	**-9.9**	**0.7**	**1.8E-32**
Dahlgren NSWC Anaerobic Enrichment Cultures						
Mn Reducing	4.0	0.0	9.1E-01	-4.0	0.0	4.0E-07
Fe Reducing	8.9	7.7	3.4E-02	-5.8	3.3	1.2E-02
Sulfate Reducing	-0.4	0.7	1.6E-01	-6.4	0.7	2.5E-06
Methanogenic	-1.2	4.4	5.0E-01	-4.2	2.7	1.2E-02

[a] Values represent the slope of the linear regression of the field data ± the 95% confidence interval of the slope. P-values represent the probability that the observed slope is different from zero.

5.6.5 UMCD - Push-pull test sampling

RDX was concentrated from selected samples from push pull tests for quantification of $\delta^{13}C$ and $\delta^{15}N$ as described above. Hundreds of samples were collected from the various push-pull tests. A subset of these samples was selected and analyzed via CSIA based upon the obsesrved extents of RDX degradation. Corrections of the measured RDX concentration data and stable isotope values using the conservative tracer (Br^- or Cl^-) to account for mixing of the injected water and dilution with the background groundwater (and background RDX) were compared under two scenarios expected to bound the potential mixing: 1) mixing during injection, and 2) mixing during sampling.

RDX degradation during four aerobic and two anaerobic push-pull tests at UMCD, corrected for mixing during injection and mixing during sampling are presented in **Figure 5.27** and **Figure 5.28**, respectively. ^{15}N isotope data ($\ln(f)$ vs. $\ln[R/R_0] \times 1000$) from each of the individual push-pull tests are shown in **Figure 5.29** (mixing during injection) and **Figure 5.30** (mixing during sampling). Compiled linear regressions are presented in **Table 5.15** and **Figure 5.31** (mixing during injection) and **Table 5.16** and **Figure 5.32** (mixing during sampling). When data was aggregated from the two anaerobic biostimulation push-pull tests, the resulting fractionation factors (-5.6 and -7.9 ‰ depending on the modeled mixing scenario) compared well to those observed during anaerobic RDX degradation by pure cultures (**Figure 5.31** and **Figure 5.32**) (27) and during the Dahlgren NSWC test. The anaerobic push-pull test ^{15}N fractionation was also comparable to what was observed in enrichment cultures derived from Dahlgren NSWC sediments degrading RDX under iron-reducing, manganese reducing, sulfate reducing, and methanogenic conditions (**Table 5.15** and **Table 5.16**). As noted for the Dahlgren data, there is slight depression in the ε ^{15}N values in the field compared to laboratory studies, likely due to aquifer heterogeneity as previously described.

Due to unknown compounds in the samples that interfered with the GC-IRMS analysis, no data regarding ^{13}C fractionation were obtained. The analytical laboratory at UD is evaluating potential interfering compounds for ^{13}C analysis.

The fractionation of ^{15}N during one of the push-pull tests (EW2-PPT1) provided a consistent indication of aerobic RDX biodegradation with an $\varepsilon^{15}N$ values of -1.5 and -1.6 ‰ under the two different mixing scenarios. Results from the other three tests, however, were less conclusive and varied significantly with the mixing model employed. The relatively low ε value for N fractionation during aerobic RDX biodegradation (~ 2.4 ‰ based on pure culture studies), makes it challenging to clearly document aerobic RDX degradation in the field unless the extent of RDX loss is high, variability in $\delta^{15}N$ measurements in the environmental samples is low, and a large number of samples across a range of fractionation values are available. Further discussion is provided in Section 8.

Figure 5.27. RDX Degradation during Aerobic Bioaugmentation (top) and Anaerobic Biostimulation (bottom) Push Pull Testing at UMCD Under the Mixing During Injection Scenario.

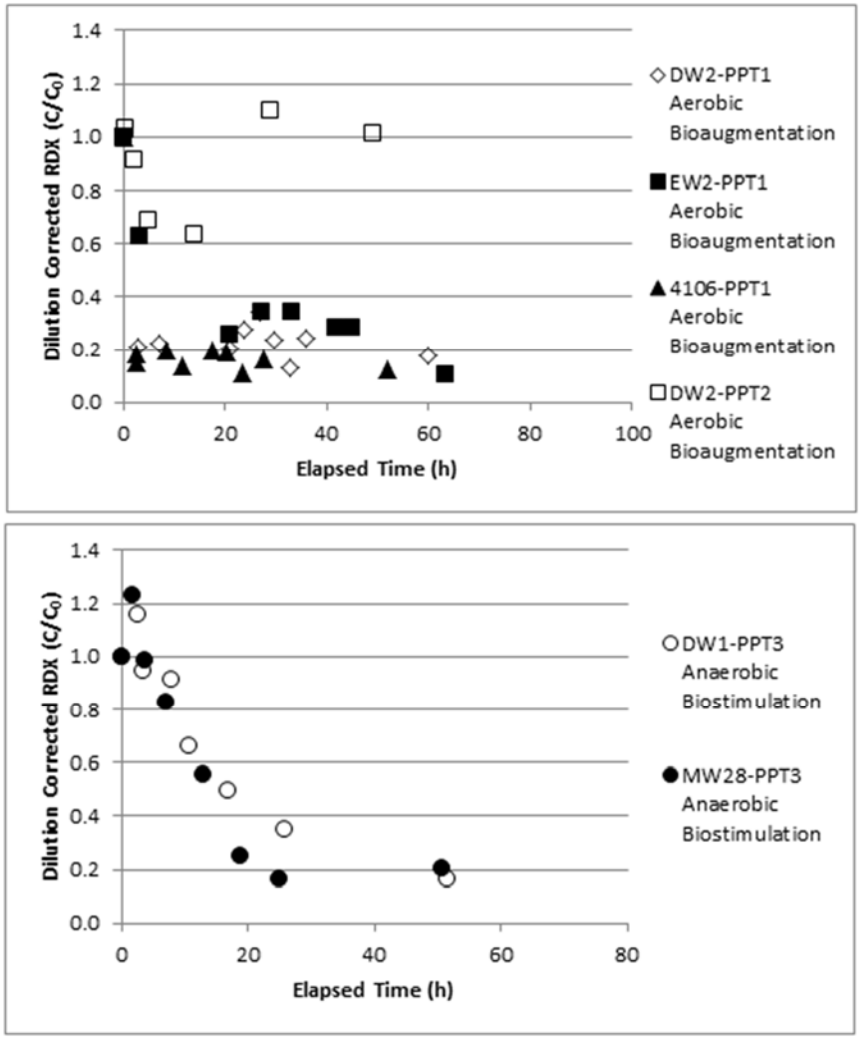

Figure 5.28. RDX Degradation During Aerobic Bioaugmentation (top) and Anaerobic Biostimulation (bottom) Push Pull Testing at UMCD Under the Mixing during Sampling Scenario.

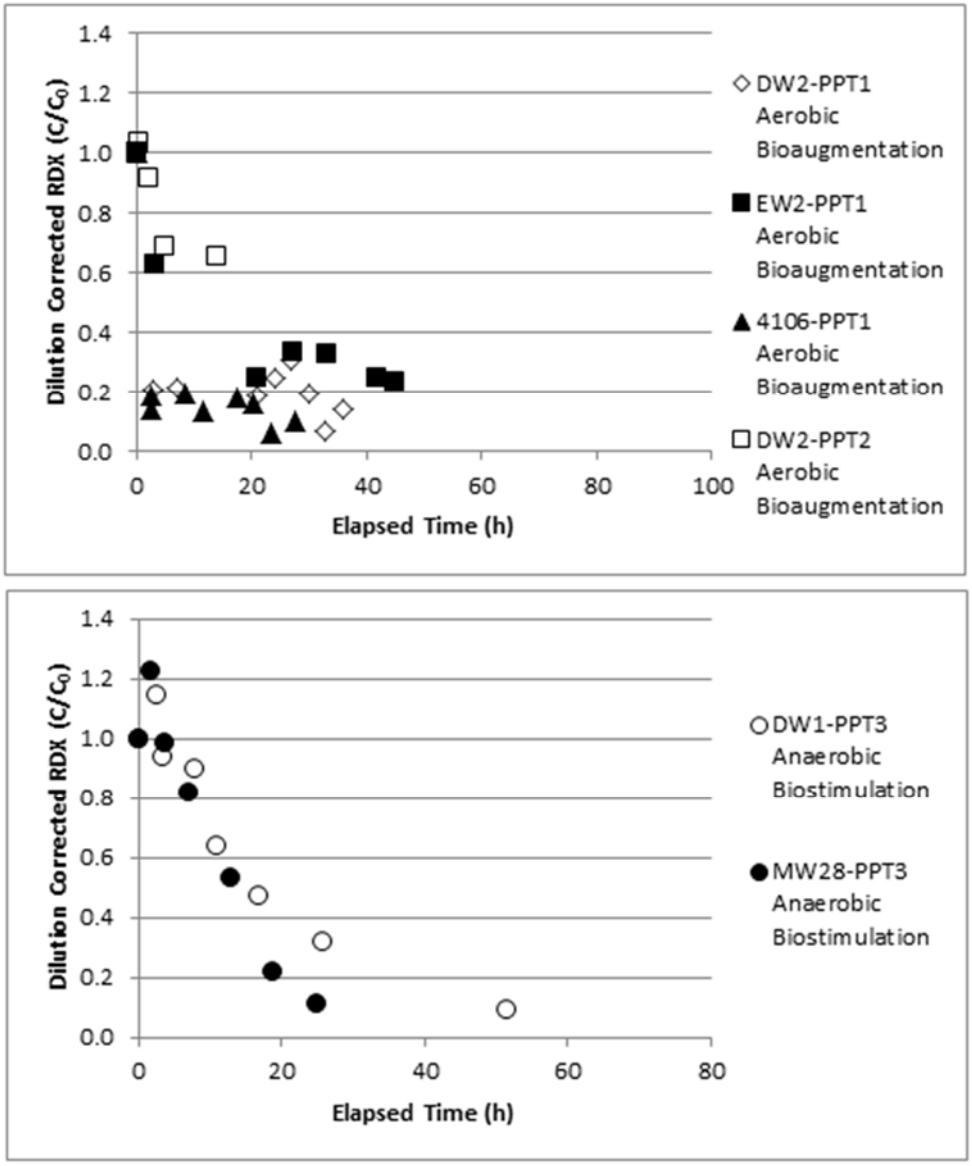

Figure 5.29. Fractionation of ^{15}N During RDX Degradation During Aerobic Bioaugmentation (left) and Anaerobic Biostimulation (right) Push Pull Testing at UMCD Under the Mixing During Injection Scenario.

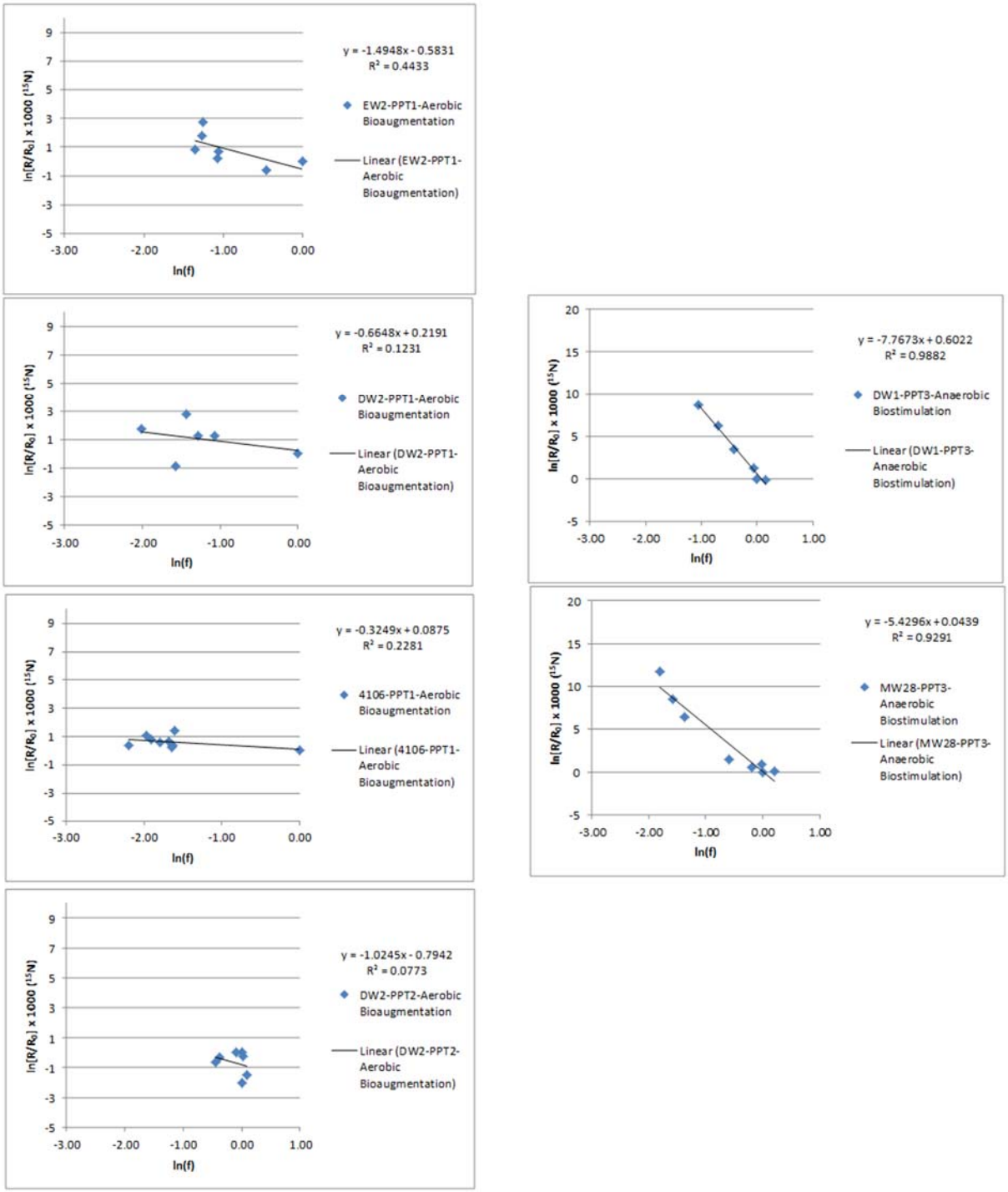

Figure 5.30. Fractionation of ^{15}N During RDX Degradation During Aerobic Bioaugmentation (left) and Anaerobic biostimulation (right) Push Pull Testing at UMCD under the Mixing During Sampling Scenario.

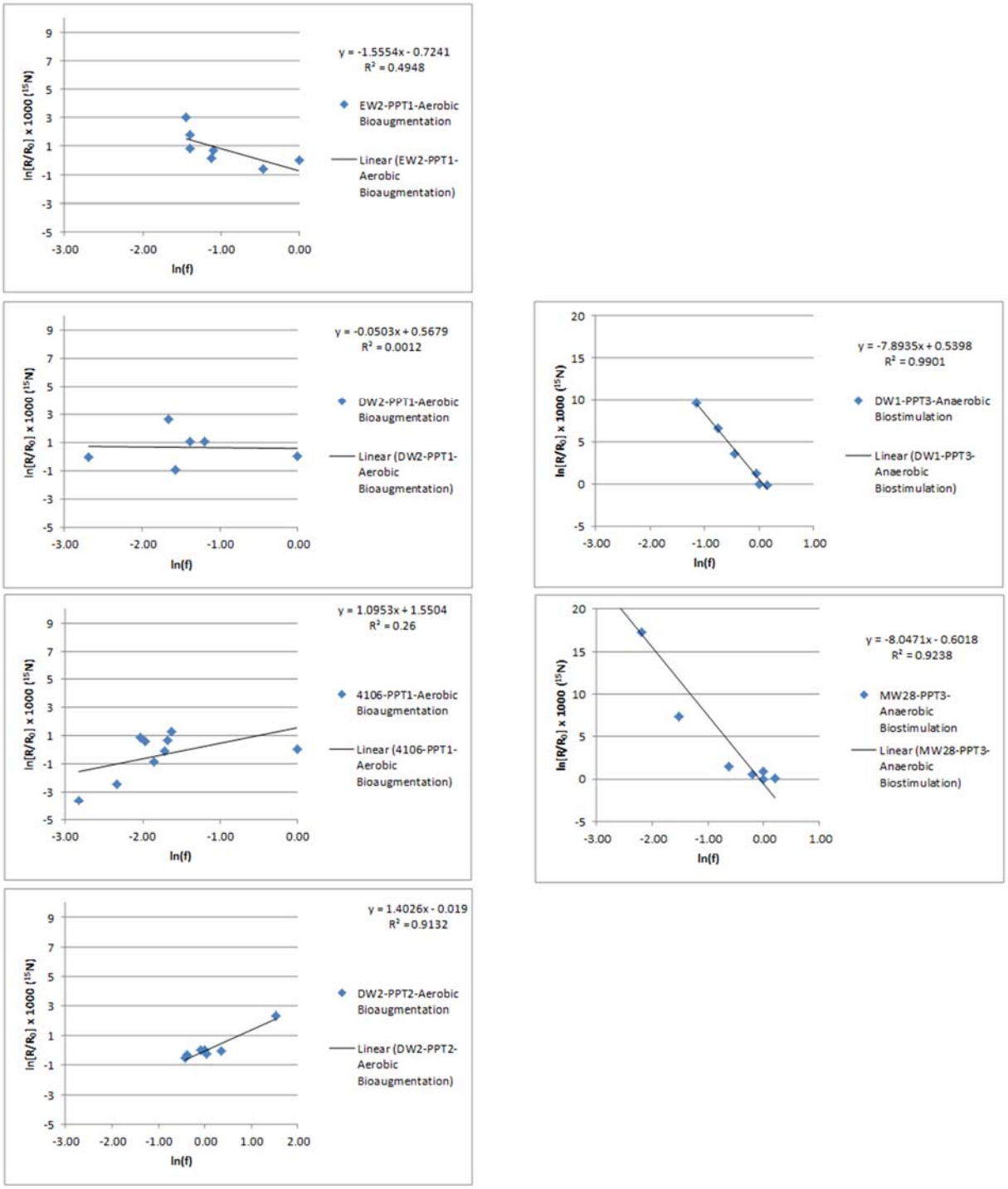

Figure 5.31. Fractionation of ^{15}N in RDX Degradation During Aerobic Bioaugmentation (top panel) and Anaerobic Biostimulation (bottom panel) Push Pull Testing at UMCD Compared with Pure Culture Data (Mixing during Injection Scenario).

Solid lines represent best-fit linear regression of the data, and dashed lines represent 95 % confidence intervals around the best-fit line. Pure culture data are from (27).

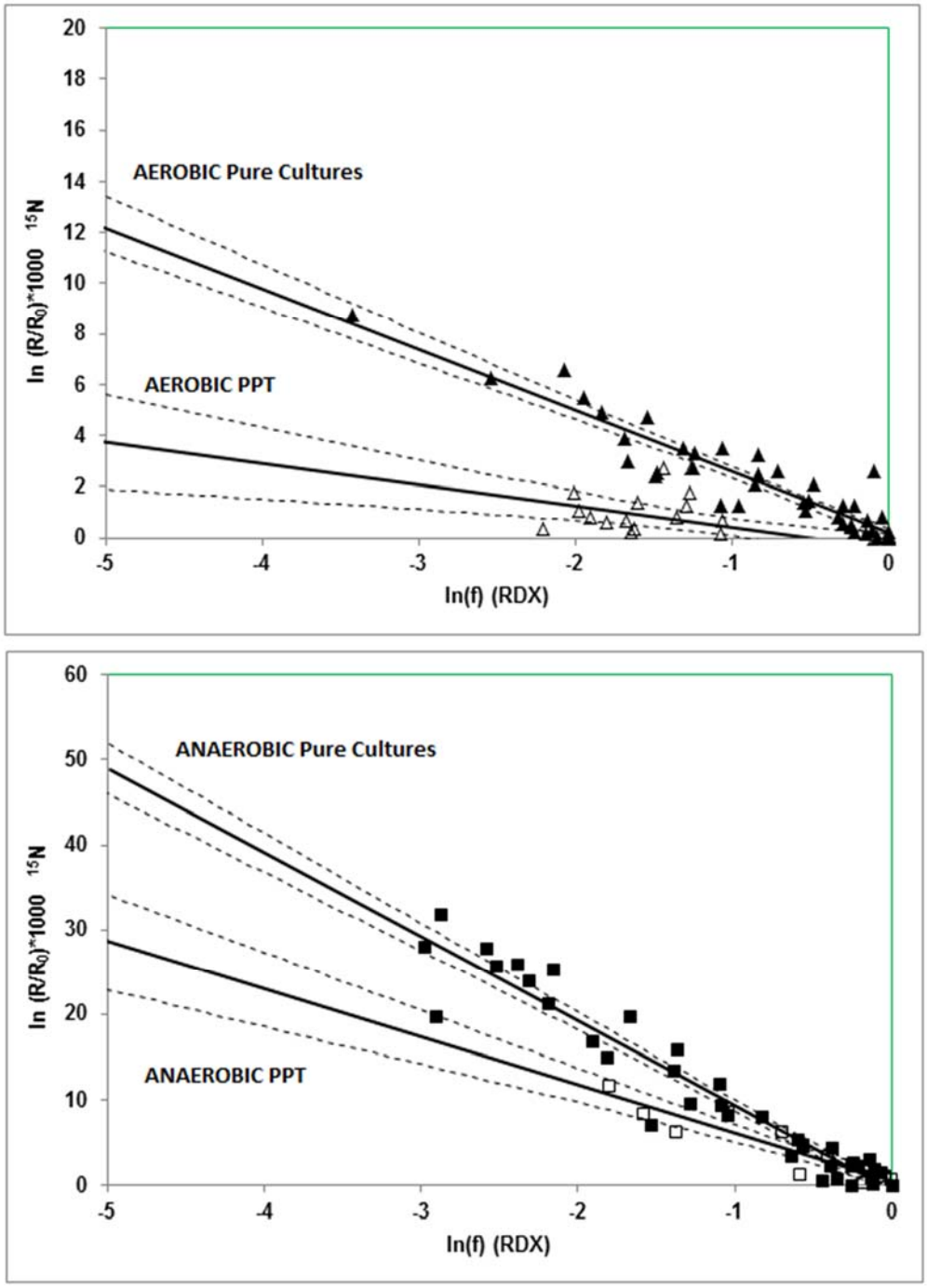

Figure 5.32. Fractionation of ^{15}N in RDX Degradation During Aerobic Bioaugmentation (top panel) and Anaerobic Biostimulation (bottom panel) Push Pull Testing at UMCD Compared with Pure Culture Data (Mixing During Sampling Scenario).

Solid lines represent best-fit linear regression of the data, and dashed lines represent 95 % confidence intervals around the best-fit line. Pure culture data are from (27).

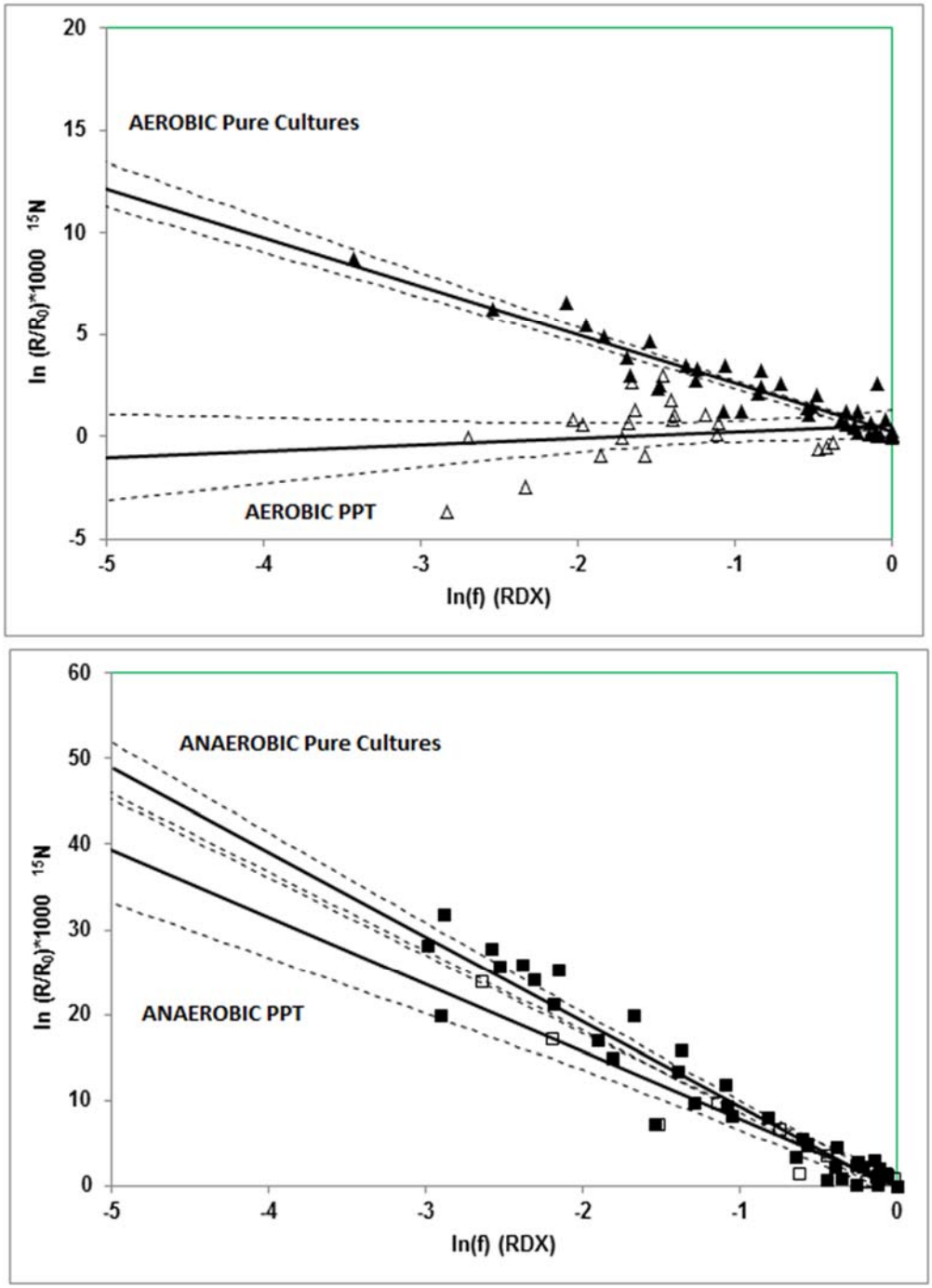

Table 5.15. Compiled ^{15}N Enrichment Factors (ε) from UMCD Push-Pull Testing (Mixing During Injection).

	ε ^{15}N		
	‰	±	P-value
UMCD Aerobic Bioaugmentation Push-Pull Testing			
EW2-PPT1	-1.5	1.9	1.0E-01
DW2-PPT1	-0.7	2.5	5.0E-01
4106-PPT1	-0.3	0.5	1.9E-01
DW2-PPT2	-1.0	4.1	5.5E-01
Composited Aerobic Push-Pull[a]	**-0.8**	**0.5**	**9.2E-04**
Aerobic Pure Cultures			
Rhodococcus sp. DN22	-2.8	0.5	7.1E-09
Rhodococcus rhodocrous 11Y	-2.6	0.3	2.3E-10
Rhodococcus sp. Strain A	-2.3	0.4	2.6E-06
Gordonia sp. KTR9	-2.3	0.5	2.0E-06
Composited Aerobic Pathway[a]	**-2.4**	**0.2**	**3.3E-25**
UMCD Anaerobic Bioaugmentation Push-Pull Testing			
DW1-PPT3	-7.8	1.2	5.3E-05
MW28-PPT3	-5.4	1.5	1.1E-04
Composited Anaerobic Push-Pull[a]	**-5.6**	**1.2**	**4.2E-07**
Anaerobic Pure Cultures			
Shewanella oneidensis MR-1	-9.6	1.3	5.6E-12
Klebsiella pneumoniae SCZ-1	-5.8	2.6	6.3E-04
Desulfovibrio sp.	-10.9	1.2	5.2E-10
Clostridium acetobutylicum ATCC 82	-8.0	5.5	1.9E-02
Composited Anaerobic Pathway[a]	**-9.9**	**0.7**	**1.8E-32**
Dahlgren NSWC Anaerobic Enrichment Cultures			
Mn Reducing	-4.0	0.0	4.0E-07
Fe Reducing	-5.8	3.3	1.2E-02
Sulfate Reducing	-6.4	0.7	2.5E-06
Methanogenic	-4.2	2.7	1.2E-02

[a] All data from the strains associated with designated pathway included in a single regression analysis.

Table 5.16. Compiled ^{15}N Enrichment Factors (ε) from UMCD Push-Pull Testing (Mixing During Sampling).

	ε ^{15}N		
	‰	±	P-value
UMCD Aerobic Bioaugmentation Push-Pull Testing			
EW2-PPT1	-1.6	1.8	7.8E-02
DW2-PPT1	-0.1	2.0	9.5E-01
4106-PPT1	1.1	1.7	1.6E-01
DW2-PPT2	1.4	0.5	7.8E-04
Composited Aerobic Push-Pull[a]	**0.3**	**0.5**	**2.2E-01**
Aerobic Pure Cultures			
Rhodococcus sp. DN22	-2.8	0.5	7.1E-09
Rhodococcus rhodocrous 11Y	-2.6	0.3	2.3E-10
Rhodococcus sp. Strain A	-2.3	0.4	2.6E-06
Gordonia sp. KTR9	-2.3	0.5	2.0E-06
Composited Aerobic Pathway[a]	**-2.4**	**0.2**	**3.3E-25**
UMCD Anaerobic Bioaugmentation Push-Pull Testing			
DW1-PPT3	-7.9	1.1	3.7E-05
MW28-PPT3	-8.0	2.3	1.4E-04
Composited Anaerobic Push-Pull[a]	**-7.9**	**1.4**	**2.9E-08**
Anaerobic Pure Cultures			
Shewanella oneidensis MR-1	-9.6	1.3	5.6E-12
Klebsiella pneumoniae SCZ-1	-5.8	2.6	6.3E-04
Desulfovibrio sp.	-10.9	1.2	5.2E-10
Clostridium acetobutylicum ATCC 82	-8.0	5.5	1.9E-02
Composited Anaerobic Pathway[a]	**-9.9**	**0.7**	**1.8E-32**
Dahlgren NSWC Anaerobic Enrichment Cultures			
Mn Reducing	-4.0	0.0	4.0E-07
Fe Reducing	-5.8	3.3	1.2E-02
Sulfate Reducing	-6.4	0.7	2.5E-06
Methanogenic	-4.2	2.7	1.2E-02

[a] All data from the strains associated with designated pathway included in a single regression analysis.

6.0 PERFORMANCE ASSESSMENT

6.1 MEASURE $\varepsilon^{15}N$ FOR RDX *IN SITU* UNDER AEROBIC CONDITIONS

6.1.1 Dahlgren NSWC

Over the course of the project, $\delta^{15}N$ in RDX was measured in groundwater samples collected (1) from the bulk aerobic aquifer at Dahlgren along the flowpath of two RDX plumes and (2) during a push-pull test in which a culture capable of aerobically degrading RDX was bioaugmented into an aquifer at UMCD along with a low dose of carbon substrate. The objective was considered to be met if (1) $\delta^{15}N$ values obtained from replicate measurements had an overall precision of ± 1‰ or better (1-sigma) and (2) if $\varepsilon^{15}N$ values could subsequently be calculated from those $\delta^{15}N$ values.

As described in Section 5.6.3, $\delta^{15}N$ values were obtained for RDX collected from 11 different wells at Dahlgren. As part of this study, two different collection techniques were tested: (1) passage of groundwater through SPE resin in the field to trap RDX and (2) passage of groundwater through SPE resin in the laboratory to trap RDX. The RDX was extracted and concentrated from both sets of SPE units in the laboratory by the same general procedures. For the lab-prepared samples, the standard deviation of $\delta^{15}N$ measurements for 6 of the 7 sampled wells was < 0.5‰, and the seventh well was 1.4‰. The mean of the standard deviations was ~ 0.4‰. Thus, using this technique, our initial goal of an overall precision of ± 1‰ was met. Interestingly, for the field-prepared samples, the standard deviation was somewhat higher. For the same set of 7 wells, the standard deviations ranged from 0.7 to 3.8 ‰, with a mean value of 1.8 ‰. There was, however, no appreciable difference in the actual $\delta^{15}N$ values for samples collected by the two methods. The reason for this difference is unclear, but may reflect the fact that fines in the ground water were trapped on the SPE column in the field but not in the lab (having settled before processing), causing some increased variability in measurement by the GC-IRMS technique.

The laboratory and field-collected $\delta^{15}N$ data along assumed transects through the RDX plume did not provide an indication of natural attenuation via aerobic RDX biodegradation. A previous investigation by our group revealed no detectable NDAB (an aerobic degradation product of RDX) or MNX, DNX, or TNX (common anaerobic degradation products) in groundwater from the Churchill Range. Taken together with the general low pH of the groundwater at this site (~ 4.5), the data may indicate a general lack of biological attenuation of the RDX plumes at this location.

6.1.2 UMCD

The measured RDX concentration data and stable isotope values obtained from aerobic push-pull tests were corrected using conservative tracer (Br^- or Cl^-) to account for mixing of the injected water and dilution with the background groundwater. Mixing was compared under two scenarios expected to bound the potential mixing with background RDX in the aquifer: 1) mixing during injection, and 2) mixing during sampling. AS noted previously, the fractionation of ^{15}N during one of the push-pull tests (EW2-PPT1) provided a consistent indication of aerobic RDX biodegradation with an $\varepsilon^{15}N$ values of -1.5 and -1.6 ‰ under the two different mixing scenarios. Results from the other three tests, however, were less conclusive and varied significantly with the mixing model employed.

With pure microbial cultures, the aerobic fractionation of N in RDX averaged -2.4 ‰ (27; Section 5.6.5). This is a relatively low ε value, making it difficult to clearly document aerobic RDX degradation by this process in the field unless the extent of RDX loss is high, variability in $\delta^{15}N$ measurements in the environmental samples is low, and a large number of samples across a range of fractionation values are available. The fractionation of ^{15}N during the push-pull testing was not consistent enough to clearly indicate RDX biodegradation among the four different tests. The relatively complex mixing scenarios with background RDX in groundwater provided further complication given the low overall $\varepsilon^{15}N$ value for this process. Theoretically, at an ε value of 2 ‰, approximately 75 % of a contaminant must be degraded to observe a shift of only 3 ‰ in the relevant δ value for an element (54). While this extent of RDX degradation is certainly feasible, and even likely at some RDX sites, the precision of N isotope measurement in RDX as well as effects of field heterogeneity (e.g., (37)), may limit the application of CSIA for measuring aerobic degradation of RDX in many instances, as appears to generally be the case for the push-pull testing, perhaps with the exception of EW2-PPT1, where a value of -1.5 to -1.6 ‰ was documented, irrespective of the mixing scenario. Further discussion concerning the measurement of degradation in environmental samples as a function of stable isotope enrichment factors can be found in Meckenstock et al. (2004).

6.2 MEASURE $\varepsilon^{15}N$ AND $\varepsilon^{13}C$ FOR RDX *IN SITU* UNDER ANAEROBIC CONDITIONS

6.2.1 Dahlgren NSWC

At Dahlgren NSWC, $\delta^{15}N$ and $\delta^{13}C$ in RDX were measured in a series of wells along a groundwater flow path at Dahlgren NSWC before and after injection of emulsified oil into a biobarrier (Section 5.6.4). The objective was considered to be met if (1) $\delta^{15}N$ and $\delta^{13}C$ values could be obtained from the wells with reproducibility of individual isotopic measurements at a precision of ± 1 ‰ or better (1-sigma) and $\varepsilon^{15}N$ and $\varepsilon^{13}C$ could subsequently be calculated from those values in order to clearly document anaerobic RDX biodegradation document. Both objectives were considered to be met in this case.

The calculated $\varepsilon\ ^{13}C$ and $\varepsilon\ ^{15}N$ values downgradient of the biobarrier in the plot were -2.2 ‰ and -6.8 ‰, respectively (Section 5.6.4). This compares favorably to pure culture data for strains degrading RDX under anaerobic conditions, averaging -4.7 ‰ and -9.9 ‰, respectively (Section 5.6.4.1; 27), and includes individual strains whose ε values were as low as -2.0 ‰ and -5.8 ‰, for C and N, respectfully. The marginal depression in the $\varepsilon\ ^{13}C$ and $\varepsilon\ ^{15}N$ values in the field compared to laboratory studies has been observed during the degradation of other compounds (58, 75), and is attributed abiotic effects (e.g., dispersion, dilution, incomplete mixing) during the testing (47, 75). The isotope fractionation factor ratio ($\varepsilon\ ^{15}N / \varepsilon\ ^{13}C$) for the samples was ~ 3.0 which falls well within the relatively wide range determined from anaerobic pure cultures (1.5-5.5), and most closely matches that determined for *Clostridium acetobutylicum* ATCC 824, at ~ 2.9. The range most likely reflects the differing or mixed anaerobic pathways of RDX degradation. **To our knowledge this study represents the first field study clearly showing dual-element CSIA can be utilized to clearly document RDX biodegradation under anaerobic conditions.**

6.2.2 UMCD

Push-pull testing was conducted at UCMD also to evaluate RDX biodegradation under bulk anaerobic conditions created by adding fructose to the aquifer at 15 – 24 mM at several different times (55). The mean $\varepsilon^{15}N$ values in RDX calculated from two push-pull tests under these conditions were -5.6 ‰ under the "mixing during injection" scenario and -7.9 ‰ under the "mixing during sampling" scenario with calculated confidence intervals of 1.2 and 1.4, respectively (see Section 5.6.5). Because of interference with other carbon-containing compounds, $\delta^{13}C$ for RDX could not be measured in these samples. Additional purification procedures are being evaluated to overcome this limitation. However, as noted for the Dahlgren NSWC test, the data from this site clearly showed that RDX biodegradation under anaerobic conditions can be documented via CSIA even if only N data are available.

6.3 MEASURE $\delta^{15}N$ AND/OR $\delta^{18}O$ IN NO_3^- OR NO_2^- *IN SITU* UNDER AEROBIC CONDITIONS

During this task, $\delta^{15}N$ and $\delta^{18}O$ were quantified in NO_3^- collected across the Dahlgren NSWC site during MNA sampling. NO_2^- was not detected in the Dahlgren aquifer. The core objective was to determine if $\delta^{15}N$ and $\delta^{18}O$ values could be utilized to distinguish NO_3^- (or NO_2^-) generated from aerobic RDX biodegradation from that generated from other processes, such as nitrification, *in situ.* Studies conducted previously with pure aerobic cultures suggested that RDX-derived NO_2^- or NO_3^- might be isotopically distinct from that generated from other processes such as nitrification (see **Figure 5.22** and 27).

With the exception of one sample, the combined $\delta^{15}N$ and $\delta^{18}O$ data from Dahlgren NSWC samples fell within the range of "biogenic NO_3^-" on a dual isotope plot, where N and O isotopes were compared (**Figure 5.22**). This is typically NO_3^- produced via nitrification in soils. The $\delta^{18}O$ values for most of the Dahlgren NSWC samples were in the general range of those of NO_2^- produced during aerobic degradation of RDX, but the $\delta^{15}N$ values were appreciably higher. The one sample that did not fall within this range from PZ-2 had a very high value of $\delta^{15}N$ (> + 30 ‰) and a somewhat elevated value of $\delta^{18}O$ (nearly + 20 ‰), which could be consistent with N isotope fraction during biological degradation of biogenic NO_3^-. Thus, it is likely that the NO_3^- that was analyzed from Dahlgren NSWC did not originate from RDX. This is consistent with the absence of MNA observed for RDX at this site as previously discussed from both metabolite analysis and N isotope analysis. It is also interesting to note that the $\delta^{15}N$ for NO_2^- generated by anaerobic degradation processes (particularly with *Pseudomonas* spp. employing Xen enzymes for the initial degradation; 27) has values ranging from 20 ‰ to nearly 40 ‰ lower than the lowest range for biogenic NO_3^-. Although natural attenuation of RDX was not detected in this case via either RDX or NO_2^-/NO_3^- stable isotope analysis, the data suggest that these combined analyses may be used to confirm natural degradation processes, particularly under anaerobic conditions.

6.4 VERIFICATION OF COLUMN COLLECTION METHOD FOR RDX STABLE ISOTOPE ANALYSIS

The main objective of this task was to develop an efficient means to collect RDX from groundwater where low concentrations exist (e.g., < 10 µg/L) to avoid needing to ship multiple liters of groundwater to the laboratory for processing. SPE columns were designed and evaluated for this purpose (Section 5.4). After several different tests, one of which revealed that the column collection process did not fractionate $\delta^{15}N$, a design was finalized for field validation. A comparison of $\delta^{15}N$ data from RDX derived from the field SPE columns vs the laboratory SPE columns indicated that there was no significant difference between the two methods given the variability in stable isotope data. When relevant samples were compared for the entire dataset, the $\delta^{15}N$ for RDX from the laboratory processed samples was 1.1 ± 1.2 ‰ (n = 8), while that for the field-processed samples was 1.1 ± 1.7 ‰ (n = 11). If the same 8 wells are taken into account for the field samples, the mean $\delta^{15}N$ was 1.4 ± 1.8 ‰. Interestingly, the variability in the $\delta^{15}N$ analyses on a well by well basis (i.e., replicate $\delta^{15}N$ measurements on the same sample) was somewhat higher in the field-processed samples than in the laboratory processed samples. With one exception, the laboratory samples had a standard deviation < 0.5 ‰, while the field samples were typically > 1 ‰. Further investigation would be required to determine the reason for this discrepancy, and potential solutions.

6.5 EFFICIENT SAMPLE COLLECTION

Small SPE columns were developed for field use as noted in Section 6.3. During the studies at Dahlgren NSWC, the SPE column design was used effectively to remove RDX from up to 4 liters of groundwater without plugging or other issues.

7.0 COST ASSESSMENT

The nature of this project does not allow for a traditional ESTCP cost assessment, where this technology is evaluated against traditional alternatives. However, this section is intended to provide a reasonable cost estimate for sampling and analysis of C and N isotopes in RDX for a typical natural attenuation assessment, similar to that detailed in Section 5.4.4.

For the cost assessment, we assume that a total of 20 groundwater wells will be sampled by a single field technician using low-flow sampling (62), and that the technician can sample 4 wells per day. For each well, basic field parameters (dissolved oxygen, oxidation-reduction potential, pH, conductivity) will be determined using a field meter, and samples will subsequently be collected for explosives concentration (EPA Method 8330), anions (EPA Method 300), C and N stable isotope analysis in RDX and N and O stable isotope analysis in NO_3^-. Packing and shipping of coolers for off-site analysis of explosives and anions will occur daily and shipping of samples for stable isotope analysis will occur one time at the end of the sample event. Based on this scenario, the following cost assumptions were made:

1) Rental of required sampling pumps and meters: 1 week ($400);
2) Field labor $70 per hr x 40 hrs ($ 2,800);
3) Vehicle rental: 1 week ($375);
4) Hotel (4 nights) and per diem (5 days), Maryland default rate $93/$51 ($627).
5) Coolers: $30 ea x 6 ($180)
6) Shipping samples to laboratories: $50 ea x 6 ($300)
7) Other miscellaneous materials including field column supplies ($300)
8) EPA Method 300 anions (5): 20 x $55 ($1,100)
9) EPA Method 8330 explosives: 20 x $131 ($2,620)
10) N and O stable isotope analysis in NO_3^- at USGS: 20 x $149 ($2,980)
11) C and N stable isotope analysis in RDX at EIGL: 20 x $500 ($10,000)

Analytical costs for EPA Method 300 ($55 per sample for analysis of 5 anions) and EPA Method 8330 ($131 per sample) represent GSA pricing from a national analytical laboratory. Stable isotope analysis of N and O in nitrate at $149 per sample is the external analysis price for 6 to 20 samples from the USGS Reston, VA Stable Isotope Laboratory and C and N isotope analysis in RDX at $500 per sample was the pricing provided by the University of Delaware EIGL Laboratory of Dr. Neil Sturchio, which is currently the only laboratory performing this method on a per-sample basis. Based on all assumptions provided above, the estimated cost of sampling and analysis of 20 wells in support of a natural attenuation evaluation of RDX is $21,682.

Page Intentionally Left Blank

8.0 IMPLEMENTATION ISSUES

The primary end-users of this technology are expected to be DoD site managers and their contractors, consultants and engineers. The general concerns of these end users are likely to include the following: (1) technology availability and cost; (2) appropriate application of the technology at DoD sites; and (3) interpretation of CSIA data. These implementation issues are addressed in the following sections.

8.1 TECHNOLOGY AVAILABILITY

The C and N stable isotope analyses described herein are not currently available in commercial laboratories to our knowledge. However, the analyses are currently being conducted at the University of Delaware, Environmental Isotope Geochemistry Laboratory (EIGL) under the supervision of Dr. Neil Sturchio on a per sample basis. Contact information for Dr. Sturchio is provided in Appendix A. The methodological information provided in this document and in (27) would allow a commercial laboratory to conduct the analyses described herein. Analyses of N and O stable isotopes in NO_3^- are available on a routine per sample basis from various laboratories including the USGS in Reston, VA. Isotopic analyses of NO_2^- may be available by special arrangement at some laboratories, as described (53).

8.2 APPROPRIATE APPLICATION OF THE TECHNOLOGY AT DOD SITES

The CSIA technology described herein is applicable for documenting the biological degradation of RDX in groundwater by both aerobic and anaerobic mechanisms. When RDX is degraded aerobically via the typical denitration pathway (see **Figure 2.1**), the extent of N fractionation is expected to be low ($\varepsilon = \sim -2.4$ ‰) and C is not expected to fractionate measurably based on pure culture studies. Thus, for the method to be useful for field samples, losses of RDX in groundwater either over distance (e.g., along a groundwater flowpath) or time (e.g., in an individual well) must be substantial, on the order of 80% or higher from initial concentrations. In many instances, and given the observed variability in this measurement, it is unlikely that aerobic biodegradation of RDX in the field will be definitively proven by N isotope fractionation. It is recommended that additional lines of evidence of RDX biodegradation under these conditions be assessed along with N isotope analysis of RDX, including (1) evaluation of NDAB as a possible degradation intermediate; (2) molecular analysis of aquifer samples for the presence of *xplA/xplB* genes, which encode key enzymes involved in aerobic RDX biodegradation (49, 66); (3) analysis of N and O stable isotopes in NO_2^- and/or NO_3^- that co-occur with RDX (particularly if initial RDX concentrations are in the mg/L range or higher); (3) laboratory microcosms or columns incubated aerobically to document RDX biodegradation under controlled conditions (e.g., (25)); and (4) application of stable isotope probing (SIP) in laboratory microcosms or mesocosms to identify organisms that aerobically degrade RDX (64). The combination of one or more of these techniques in conjunction with N stable isotope analysis of RDX at a field site is recommended to clearly document aerobic RDX biodegradation or confirm the absence of this process.

When RDX is biodegraded via anaerobic mechanisms (see **Figure 2.1**), C and N stable isotopes are both applicable to document this process due to relatively high fractionation factors based on culture studies ($\varepsilon = \sim -4.7$ ‰ for C and $\varepsilon = \sim -9.9$ ‰ for N; 27). Dual isotope plots can be utilized to confirm biodegradation, as was done for Dahlgren NSWC field samples downgradient of an emulsified oil biobarrier (see **Figure 5.26**). Many of the general lines of evidence previously suggested for evaluating aerobic RDX biodegradation are also applicable for anaerobic biodegradation, including (1) evaluation of degradation intermediates, but in this case MNX, DNX and TNX rather than NDAB (see **Figure 2.1**); (2) analysis of N and O stable isotopes in NO_2^- and/or NO_3^- that co-occur with RDX, as significant fractionation has been observed by some organisms that degrade RDX (**Figure 2.6, 2.7** and 27); (3) laboratory microcosms or columns incubated anaerobically to document RDX biodegradation under controlled conditions (e.g., Section 5.2.1 and (15)); and (4) application of stable isotope probing (SIP) in laboratory microcosms or mesocosms to identify organisms that anaerobically degrade RDX (15, 16). As previously noted for evaluating aerobic biodegradation, a combination of one or more of these techniques in conjunction with C and N stable isotope analysis of RDX is recommended to document anaerobic RDX biodegradation.

8.3 INTERPRETATION OF CSIA DATA

CSIA data gathered on environmental pollutants has been utilized to (1) document biological and abiotic contaminant degradation, (2) estimate or constrain rates of contaminant degradation; (3) identify dominant degradation mechanisms; and (4) forensically determine dominant sources of a specific contaminant in the environment, as well as various other specific applications for individual contaminants. The application and interpretation of CSIA data for the above purposes have been thoroughly reviewed in a US Environmental Protection Agency (EPA) document entitled "A Guide for Assessing Biodegradation and Source Identification of Organic Groundwater Contaminants Using Compound Specific Isotope Analysis (CSIA)" (46). This document is available online through the EPA NEPIS Site (https://nepis.epa.gov/Exe/ZyPDF.cgi/P1002VAI.PDF?Dockey=P1002VAI.PDF). The readers of this ESTCP report are referred to Chapter 4 in this document entitled "Interpretation of Stable Isotope Data from Field Sites" which clearly describes and provides examples of how CSIA data can be utilized to document and quantify the biodegradation of organic contaminants in groundwater aquifers. The RDX isotope data gathered during this project do not allow source discrimination, as this was not an objective, but the reported fractionation factors for C and N stable isotope analysis can be used in conjunction with field samples/data to quantify RDX degradation, constrain field rates, and potentially distinguish aerobic from anaerobic degradation mechanisms using the general methods provided in the EPA document.

9.0 REFERENCES

1. **Bateman, A. S., and S. D. Kelly**. 2007. Fertilizer nitrogen isotope signatures. Isotopes in Environmental and Health Studies **43(3):** 237-247.
2. **Bell, C. F.** 1996. Hydrogeology and Water Quality of the Shallow Aquifer System at the Explosive Experimental Area, Naval Surface Warfare Center, Dahlgren Site, Dahlgren, Virginia. U.S. Geological Survey Water-Resources Investigation Report 96-4209.
3. **Bernstein, A., E. Adar, Z. Ronen, H. Lowag, W. Stichler, and R. U. Meckenstock**. 2010. Quantifying RDX biodegradation in groundwater using δ15N isotope analysis. Journal Of Contaminant Hydrology
4. **Bernstein, A., Z. Ronen, E. Adar, R. Nativ, H. Lowag, W. Stichler, and R. U. Meckenstock**. 2008. Compound-specific isotope analysis of RDX and stable isotope fractionation during aerobic and anaerobic biodegradation. Environmental Science & Technology **42(21):** 7772–7777.
5. **Bernstein, A., Z. Ronen, and F. Gelman**. 2013. Insight on RDX degradation mechanism by *Rhodococcus* strains using ^{13}C and ^{15}N kinetic isotope effects. Environmental Science & Technology **47(1):** 479-484.
6. **Bhushan, B., A. Halasz, J. C. Spain, and J. Hawari**. 2002. Diaphorase catalyzed biotransformation of RDX via N-denitration mechanism. Biochemical And Biophysical Research Communications **296(4):** 779-784.
7. **Böhlke, J. K., S. J. Mroczkowski, and T. B. Coplen**. 2003. Oxygen isotopes in nitrate: new reference materials for ^{18}O:^{17}O:^{16}O measurements and observations on nitrate-water equilibration. Rapid Communications in Mass Spectrometry **17(16):** 1835-1846.
8. **Böhlke, J. K., R. L. Smith, and J. E. Hannon**. 2007. Isotopic analysis of N and O in nitrite and nitrate by sequential selective bacterial reduction to N_2O. Analytical Chemistry **79(15):** 5888-5895.
9. **Boparai, H. K., S. D. Comfort, T. Satapanajaru, J. E. Szecsody, P. R. Grossl, and P. J. Shea**. 2010. Abiotic transformation of high explosives by freshly precipitated iron minerals in aqueous FeII solutions. Chemosphere **79(8):** 865-872.
10. **Bordeleau, G., R. Martel, G. Ampleman, and S. Thiboutot**. 2008. Environmental impacts of training activities at an air weapons range. Journal Of Environmental Quality **37(2):** 308-317.
11. **Buchwald, C., and K. L. Casciotti**. 2013. Isotopic ratios of nitrite as tracers of the sources and age of oceanic nitrite. Nature Geosci **6(4):** 308-313.
12. **Casciotti, K. L.** 2009. Inverse kinetic isotope fractionation during bacterial nitrite oxidation. Geochimica Et Cosmochimica Acta **73(7):** 2061-2076.
13. **Casciotti, K. L., J. K. Böhlke, M. R. McIlvin, S. J. Mroczkowski, and J. E. Hannon**. 2007. Oxygen isotopes in nitrite: analysis, calibration, and equilibration. Analytical Chemistry **79(6):** 2427-2436.
14. **Casciotti, K. L., D. M. Sigman, M. Garanter Hastings, J. K. Böhlke, and A. Hilkert**. 2002. Measurement of the oxygen isotopic composition of nitrate in seawater and freshwater using the denitrifier method. Analytical Chemistry **74(19):** 4905-4912.
15. **Cho, K.-C., D. G. Lee, M. E. Fuller, P. B. Hatzinger, and K.-H. Chu**. 2015. Application of ^{13}C and ^{15}N stable isotope probing to characterize RDX degrading microbial communities under different electron-accepting conditions. Journal Of Hazardous Materials **297:** 42-51.

16. **Cho, K.-C., D. G. Lee, H. K. Roh, M. E. Fuller, P. B. Hatzinger, and K.-H. Chu**. 2013. Application of ^{13}C-stable isotope probing to identify RDX-degrading microorganisms in groundwater. Environmental Pollution **178:** 350-360.
17. **Clausen, J., J. Robb, D. Curry, and N. Korte**. 2004. A case study of contamination on military ranges: Camp Edwards, Massachusetts, USA. Environmental Pollution **129(1):** 13-21.
18. **Coffin, R. B., P. H. Miyares, C. A. Kelley, L. A. Cifuentes, and C. M. Reynolds**. 2001. Stable carbon and nitrogen isotope analysis of TNT: Two-dimensional source identification. Environmental Toxicology And Chemistry **20(12):** 2676-2680.
19. **Comfort, S. D., P. J. Shea, T. A. Machacek, and T. Satapanajaru**. 2003. Pilot-scale treatment of RDX-contaminated soil with zerovalent iron. Journal Of Environmental Quality **32(5):** 1717-1725.
20. **Coplen, T.B., J.K. Böhlke, and K.L. Casciotti.** 2004. Using dual bacterial denitrification to improve δ^{15}N determinations of nitrates containing mass independent ^{17}O. Rapid Communications in Mass Spectrometry **18:**245-250.
21. **Crocker, F. H., K. J. Indest, C. M. Jung, D. E. Hancock, M. E. Fuller, P. B. Hatzinger, S. Vainberg, J. D. Istok, E. Wilson, and M. M. Michalsen**. 2015. Evaluation of microbial transport during aerobic bioaugmentation of an RDX-contaminated aquifer. Biodegradation **26(6):** 443-451.
22. **DiGnazio, F. J., N. C. Krothe, S. J. Baedke, and R. F. Spalding**. 1998. d15N of nitrate derived from explosive sources in a karst aquifer beneath the Ammunition Burning Ground, Crane Naval Surface Warfare Center, Indiana, USA. Journal Of Hydrology **206(3-4):** 164-175.
23. **EPA**. 2004. Performance monitoring of MNA remedies for VOCs in groundwater. USEPA National Risk Management Research Laboratory, Office of Research and Development, Cincinnati, OH. Report# EPA/600/R-04/027.
24. **Fournier, D., A. Halasz, J. Spain, P. Fiurasek, and J. Hawari**. 2002. Determination of key metabolites during biodegradation of hexahydro-1,3,5-trinitro-1,3,5-triazine with *Rhodococcus* sp. strain DN22. Applied And Environmental Microbiology **68(1):** 166-172.
25. **Fuller, M. E., P. B. Hatzinger, C. W. Condee, C. Andaya, M. M. Michalsen, F. H. Crocker, K. J. Indest, C. M. Jung, H. Eaton, and J. D. Istok**. 2015. Laboratory evaluation of bioaugmentation for aerobic treatment of RDX in groundwater. Biodegradation **26(1):** 77-89.
26. **Fuller, M. E., J. Hawari, and N. Perreault**. 2010. Microaerophilic degradation of hexahydro-1,3,5-trinitro-1,3,5-triazine (RDX) by three *Rhodococcus* strains. Letters In Applied Microbiology **51(3):** 313-318.
27. **Fuller, M. E., L. Heraty, C. W. Condee, S. Vainberg, N. C. Sturchio, J. K. Böhlke, and P. B. Hatzinger**. 2016. Relating carbon and nitrogen isotope effects to reaction mechanisms during aerobic or anaerobic degradation of RDX (hexahydro-1,3,5-trinitro-1,3,5-triazine) by pure bacterial cultures. Applied And Environmental Microbiology **82(11):** 3297-3309.
28. **Fuller, M. E., J. Kruczek, R. L. Schuster, P. L. Sheehan, and P. M. Ariente**. 2003. Bioslurry treatment for soils contaminated with very high concentrations of 2,4,6-trinitrophenylmethylnitramine (tetryl). Journal of Hazardous Materials B **100(1-3):** 245-257.

29. **Fuller, M. E., K. McClay, J. Hawari, L. Paquet, T. E. Malone, B. G. Fox, and R. J. Steffan**. 2009. Transformation of RDX and other energetic compounds by xenobiotic reductases XenA and XenB. Applied Microbiology And Biotechnology **84(3):** 535-544.
30. **Fuller, M. E., K. McClay, M. Higham, P. B. Hatzinger, and R. J. Steffan**. 2010. Hexahydro-1,3,5-trinitro-1,3,5-triazine (RDX) bioremediation in groundwater: Are known RDX-degrading bacteria the dominant players? Bioremediation Journal **14(3):** 121-134.
31. **Gelman, F., A. Kotlyar, D. Chiguala, and Z. Ronen**. 2011. Precise and accurate compound-specific carbon and nitrogen isotope analysis of RDX by GC-IRMS. International Journal Of Environmental Analytical Chemistry **91(14):** 1392-1400.
32. **Gregory, K. B., P. Larese-Casanova, G. F. Parkin, and M. M. Scherer**. 2004. Abiotic transformation of hexahydro-1,3,5-trinitro-1,3,5-triazine by Fe^{II} bound to magnetite. Environmental Science & Technology **38(5):** 1408-1414.
33. **Griest, W. H., A. J. Stewart, R. L. Tyndall, J. E. Caton, C. H. Ho, K. S. Ironside, W. M. Caldwell, and E. Tan**. 1993. Chemical and toxicological testing of composted explosives-contaminated soil. Environmental Toxicology And Chemistry **12(6):** 1105-1116.
34. **Halasz, A., and J. Hawari**. 2011. Degradation routes of RDX in various redox systems. p. 441-462. *In* Aquatic Redox Chemistry, American Chemical Society,
35. **Harkins, V. R., M. T., C. Heintz, and K. Rainwater**. 1999. Aerobic biodegradation of high explosives, Phase I - HMX. Bioremediation Journal **3(4):** 285-290.
36. **Hartenbach, A., T. B. Hofstetter, M. Berg, J. Bolotin, and R. P. Schwarzenbach**. 2006. Using nitrogen isotope fractionation to assess abiotic reduction of nitroaromatic compounds. Environmental Science & Technology **40(24):** 7710-7716.
37. **Hatzinger, P., and J. Diebold**. 2009. In Situ Bioremediation of Perchlorate in Groundwater. Environmental Security Technology Certification Program (ESTCP). Report# ER-200224.
38. **Hatzinger, P. B., J. K. Bohlke, and N. C. Sturchio**. 2013. Application of stable isotope ratio analysis for biodegradation monitoring in groundwater. Current Opinion In Biotechnology **24:** 542-549.
39. **Hatzinger, P. B., J. K. Böhlke, N. C. Sturchio, B. Gu, L. J. Heraty, and R. C. Borden**. 2009. Fractionation of stable isotopes in perchlorate and nitrate during in situ biodegradation in a sandy aquifer. Environmental Chemistry **6(1):** 44-52.
40. **Hatzinger, P. B., and M. E. Fuller**. 2016. Passive Biobarrier for Treating Co-mingled Perchlorate and RDX in Groundwater at an Active Range. Environmental Security Technology Certification Program (ESTCP). Report# ER-201028.
41. **Hatzinger, P. B., and D. Lippincott**. 2012. In Situ Bioremediation of Energetic Compounds in Groundwater Environmental Security Technology Certification Program (ESTCP). Report# ER-200425.
42. **Hawari, J., A. Halasz, T. Sheremata, S. Beaudet, C. Groom, L. Paquet, C. Rhofir, G. Ampleman, and S. Thiboutot**. 2000. Characterization of metabolites during biodegradation of hexahydro-1,3,5-trinitro-1,3,5-triazine (RDX) with municipal anaerobic sludge. Applied And Environmental Microbiology **66(6):** 2652-2657.
43. **Heaton, T. H. E.** 1986. Isotopic studies of nitrogen pollution in the hydrosphere and atmosphere: A review. Chemical Geology: Isotope Geoscience section **59(0):** 87-102.

44. **Howa, J. D., M. J. Lott, L. A. Chesson, and J. R. Ehleringer**. 2014. Carbon and nitrogen isotope ratios of factory-produced RDX and HMX. Forensic Science International **240:** 80-87.
45. **Hübner, H.** 1986. Isotope effects of nitrogen in the soil and biosphere. p. 361-425. *In* P. Fritz and J. C. Fontes (ed.), Handbook of Environmental Geochemistry, Volume 2, The Terrestrial Environment B:, Elsevier, Amsterdam.
46. **Hunkeler, D., R. U. Meckenstock, B. Lollar, T. C. Schmidt, and J. T. Wilson**. 2009. A Guide for Assessing Biodegradation and Source Identification of Organic Groundwater Contaminants Using Compound Specific Isotope Analysis (CSIA). US EPA. Report# EPA/600/R-08/148.
47. **Hunkeler, D., R. U. Meckenstock, B. Sherwood Loller, T. C. Schmidt, and J. T. Wilson**. 2008. A Guide for Asessing Biodegradation and Source Identification of Organic Groundwater Contaminants using Compound Specific Isotope Analysis (CSIA). . USEPA Office of Research and Development, National Risk Management Research Laboratory, ADA, OK. Report# EPA 600/R-08/148.
48. **Hyer, K. E., J. M. Denver, M. J. Langland, J. S. Webber, J. K. Böhlke, W. D. Hively, and J. W. Clune**. 2016. Spatial and temporal variation of stream chemistry associated with contrasting geology and land-use patterns in the Chesapeake Bay watershed—Summary of results from Smith Creek, Virginia; Upper Chester River, Maryland; Conewago Creek, Pennsylvania; and Difficult Run, Virginia, 2010–2013. U.S. Geological Survey Scientific Investigations Report 2016-5093.
49. **Jackson, R. G., E. L. Rylott, D. Fournier, J. Hawari, and N. C. Bruce**. 2007. Exploring the biochemical properties and remediation applications of the unusual explosive-degrading P450 system XplA/B. Proceedings of the National Academy of Sciences **104(43):** 16822-16827.
50. **Jackson, W. A., J. K. Böhlke, B. Gu, P. B. Hatzinger, and N. C. Sturchio**. 2010. Isotopic composition and origin of indigenous natural perchlorate and co-occurring nitrate in the southwestern United States. Environmental Science & Technology **44(13):** 4869-4876.
51. **Kim, J. S., P. J. Shea, J. E. Yang, and J.-E. Kim**. 2007. Halide salts accelerate degradation of high explosives by zerovalent iron. Environmental Pollution **147(3):** 634-641.
52. **Kuder, T., J. T. Wilson, P. Kaiser, R. Kolhatkar, P. Philp, and J. Allen**. 2005. Enrichment of stable carbon and hydrogen isotopes during anaerobic biodegradation of MTBE: Microcosm and field evidence. Environmental Science & Technology **39:** 213-220.
53. **McIlvin, M. R., and M. A. Altabet**. 2005. Chemical conversion of nitrate and nitrite to nitrous oxide for nitrogen and oxygen isotopic analysis in freshwater and seawater. Analytical Chemistry **77(17):** 5589-5595.
54. **Meckenstock, R. U., B. Morasch, C. Griebler, and H. H. Richnow**. 2004. Stable isotope fractionation analysis as a tool to monitor biodegradation in contaminated aquifers. Journal of Contaminant Hydrology **75(3–4):** 215-255.
55. **Michalsen, M. M., A. S. King, R. A. Rule, M. E. Fuller, P. B. Hatzinger, C. W. Condee, F. H. Crocker, K. J. Indest, C. M. Jung, and J. D. Istok**. 2016. Evaluation of biostimulation and bioaugmentation to stimulate hexahydro-1,3,5-trinitro-1,3,5,-triazine

degradation in an aerobic groundwater aquifer. Environmental Science & Technology **50(14):** 7625-7632.

56. **Michalsen, M. M., R. Weiss, A. King, D. Gent, V. F. Medina, and J. D. Istok**. 2013. Push-pull tests for estimating RDX and TNT degradation rates in groundwater. Groundwater Monitoring & Remediation **33(3):** 61-68.
57. **Michalski, G., J. K. Böhlke, and M. Thiemens**. 2004. Long term atmospheric deposition as the source of nitrate and other salts in the Atacama Desert, Chile: New evidence from mass-independent oxygen isotopic compositions. Geochimica et Cosmochimica Acta **68(20):** 4023-4038.
58. **Miller, L. G., K. L. Warner, S. M. Baesman, R. S. Oremland, I. R. McDonald, S. Radajewski, and J. C. Murrell**. 2004. Degradation of methyl bromide and methyl chloride in soil microcosms: Use of stable C isotope fractionation and stable isotope probing to identify reactions and the responsible microorganisms1. Geochimica et Cosmochimica Acta **68(15):** 3271-3283.
59. **Oh, S. K., P. C. Chiu, and D. K. Cha**. 2008. Reductive transformation of 2,4,6-trinitrotoluene, hexahydro-1,3,5-trinitro-1,3,5-triazine, and nitroglycerin by pyrite and magnetite. Journal Of Hazardous Materials **58(2-3):** 652-655.
60. **Oregon_DEQ**. 2003. Lower Umatilla Basin Groundwater Management Area Synoptic Sampling Area Event Report. State of Oregon, Department of Environmental Quality, Water Quality Division.
Report# http://www.deq.state.or.us/wq/groundwa/LUBGWMgmtArea.htm.
61. **Paquet, L., F. Monteil-Rivera, P. B. Hatzinger, M. Fuller, and J. Hawari**. 2011. Analysis of the key intermediates of RDX (hexahydro-1,3,5-trinitro-1,3,5-triazine) in groundwater: Occurrence, stability and preservation. Journal Of Environmental Monitoring **13(8):** 2304-2311.
62. **Puls, R. W., and M. J. Barcelona**. 1996. Low-Flow (Minimal Drawdown) Ground-Water Sampling Procedures. USEPA, Office of Research and Development, Office of Solid Waste and Emergency Response. Report# EPA/540/S-95/504.
63. **Qi, H., T. B. Coplen, H. Geilmann, W. A. Brand, and J. K. Böhlke**. 2003. Two new organic reference materials for δ13C and δ15N measurements and a new value for the δ13C of NBS 22 oil. Rapid Communications in Mass Spectrometry **17(22):** 2483-2487.
64. **Roh, H., C.-P. Yu, M. E. Fuller, and K.-H. Chu**. 2009. Identification of hexahydro-1,3,5-trinitro-1,3,5-triazine (RDX)-degrading microorganisms via ^{15}N-stable isotope probing. Environmental Science and Technology **43(7):** 2505–2511.
65. **Schaefer, C. E., M. E. Fuller, C. W. Condee, J. M. Lowey, and P. B. Hatzinger**. 2007. Comparison of biotic and abiotic treatment approaches for co-mingled perchlorate, nitrate, and nitramine explosives in groundwater. Journal Of Contaminant Hydrology **89(3-4):** 231-250.
66. **Seth-Smith, H. M. B., J. Edwards, S. J. Rosser, D. A. Rathbone, and N. C. Bruce**. 2008. The explosive-degrading cytochrome P450 system is highly conserved among strains of *Rhodococcus* spp. Applied And Environmental Microbiology **74(14):** 4550-4552.
67. **Sigman, D. M., K. L. Casciotti, M. Andreani, C. Barford, M. Galanter, and J. K. Böhlke**. 2001. A bacterial method for the nitrogen isotopic analysis of nitrate in seawater and freshwater. Analytical Chemistry **73(17):** 4145-4153.

68. **Song, D. L., M. E. Conrad, K. S. Sorenson, and L. Alvarez-Cohen**. 2002. Stable carbon isotope fractionation during enhanced *in situ* bioremediation of trichloroethene. Environmental Science & Technology **36:** 2262-2268.
69. **Sturchio, N. C., J. K. Böhlke, A. D. Beloso, S. H. Streger, L. J. Heraty, and P. B. Hatzinger**. 2007. Oxygen and chlorine isotopic fractionation during perchlorate biodegradation: Laboratory results and implications for forensics and natural attenuation studies. Environmental Science & Technology **41(8):** 2796-2802.
70. **Sturchio, N. C., P. B. Hatzinger, M. D. Arkins, C. Suh, and L. J. Heraty**. 2003. Chlorine isotope fractionation during microbial reduction of perchlorate. Environmental Science and Technology **37:** 3859-3863.
71. **URS**. 2007. Spring 2007 Groundwater Monitoring Report for the Open Burn/Open Detonation Unit, Naval Surface Warfare Division Dahlgren, Dahlgren, Virginia. URS Group Inc., Oak Ridge, TN.
72. **URS**. 2010. Groundwater Flow and Transport Modeling Report, Explosives Experimental Area, Naval Surface Warfare Center Dahlgren (Draft Report). URS Group Inc., Oak Ridge, TN.
73. **USACE**. 2010. Final Third Five-Year Review Report for Umatilla Chemical Depot. US Army Corps of Engineers Seattle District. Report# http://www.epa.gov/region10/pdf/sites/umatilla/umatilla_3rd_fyr_073010.pdf.
74. **Van Aken, B., J. M. Yoon, and J. L. Schnoor**. 2004. Biodegradation of nitro-substituted explosives 2,4,6-trinitrotoluene, hexahydro-1,3,5-trinitro-1,3,5-triazine, and octahydro-1,3,5,7-tetranitro-1,3,5-tetrazocine by a phytosymbiotic *Methylobacterium* sp. associated with poplar tissues (*Populus deltoides* x *nigra* DN34). Applied and Environmental Microbiology **70(1):** 508-517.
75. **Vieth, A., M. Kästner, M. Schirmer, H. Weiß, S. Gödeke, R. U. Meckenstock, and H. H. Richnow**. 2005. Monitoring in situ biodegradation of benzene and toluene by stable carbon isotope fractionation. Environmental Toxicology and Chemistry **24(1):** 51-60.
76. **Wani, A. H., D. R. Felt, and J. L. Davis**. August 2003. Biologically Active Zone Enhancement (BAZE) Supplemental Study: Mass Balance of RDX Biotransformation and Influence of Aquifer Temperature on RDX Biodegradation in Groundwater. U.S. Army Corps of Engineers. Report# ERDC/EL TR-03-11.
77. **Wiedemeier, T. H., M. A. Swanson, D. A. Moutoux, E. K. Gordon, J. T. Wilson, B. H. Wilson, D. H. Kampbell, J. E. Hansen, P. Haas, and F. H. Chapelle**. 1996. Technical Protocol For Evaluating Natural Attenuation Of Chlorinated Solvents In Groundwater. Air Force Center for Environmental Excellence, San Antonio, TX.
78. **Wozniak, K. C.** 1995. Hydrogeology. p. *In* G. H. Grondin, K. C. Wozniak, D. O. Nelson, and I. Camacho (ed.), Hydrogeology, Groundwater Chemistry and Land Uses in the Lower Umatilla Basin, http://www.deq.state.or.us/wq/groundwater/lubgwma.htm.
79. **Xue, D., J. Botte, B. De Baets, F. Accoe, A. Nestler, P. Taylor, O. Van Cleemput, M. Berglund, and P. Boeckx**. 2009. Present limitations and future prospects of stable isotope methods for nitrate source identification in surface- and groundwater. Water Research **43(5):** 1159-1170.
80. **Yamamoto, H., M. C. Morley, G. E. Speitel, Jr., and J. Clausen**. 2004. Fate and transport of high explosives in a sandy soil: Adsorption and desorption. Soil & Sediment Contamination **13(3):** 459-477.

81. **Zakikhani, M., J. C. Pennington, D. W. Harrelson, and D. Gunnison**. 2000. Monitored natural attenuation of explosives at the Louisiana Army Ammunition Plant. Land Contamination and Reclamation **8(3):** 233-239.
82. **Zhang, C., R. C. Daprato, S. F. Nishino, J. C. Spain, and J. B. Hughes**. 2001. Remediation of dinitrotoluene contaminated soils from former ammunition plants: soil washing efficiency and effective process monitoring in bioslurry reactors. Journal Of Hazardous Materials **87(1-3):** 139-154.
83. **Zhao, J.-S., A. Halasz, L. Paquet, C. Beaulieu, and J. Hawari**. 2002. Biodegradation of hexahydro-1,3,5-trinitro-1,3,5-triazine and its mononitroso derivative hexahydro-1-nitroso-3,5-dinitro-1,3,5-triazine by *Klebsiella pneumoniae* strain SCZ-1 isolated from an anaerobic sludge. Applied And Environmental Microbiology **68(11):** 5336-5341.

Page Intentionally Left Blank

APPENDIX A POINTS OF CONTACT

Point of Contact Name	Organization Name Address	Phone Fax Email
Dr. Paul B. Hatzinger	APTIM Federal Services 17 Princess Road Lawrenceville, NJ 08648	609-895-5356 (phone) Paul.hatzinger@APTIM.com
Dr. Mark E. Fuller	APTIM Federal Services 17 Princess Road Lawrenceville, NJ 08648	609-895-5348 (phone) Mark.fuller@APTIM.com
Dr. Neil C. Sturchio	Department of Geological Sciences University of Delaware 255 Academy Street/103 Penny Hall Newark, DE 19716	302-831-8706 (phone) sturchio@udel.edu
Dr. J.K. Böhlke	U.S. Geological Survey 431 National Center 12201 Sunrise Valley Drive Reston, VA 20192	703-648-6325 (phone) jkbohlke@usgs.gov
Dr. Andrea Leeson	SERDP/ESTCP 4800 Mark Center Drive, Suite 17D03, Alexandria, VA 22350-3605	571-372-6398 (phone) Leeson.Andrea@gmail.com

Page Intentionally Left Blank

APPENDIX B SELECTED DATA FOR NITRATE AND NITRITE ISOTOPIC STUDIES

Table B.1. Concentrations and Isotopic Compositions of RDX, Nitrate+Nitrite ($NO_{[3+2]}$), and Nitrite (NO_2^-) from Selected RDX Degradation Experiments (data used in Figures 2.6, 2.7, and 5.23).

See (27) for explanation. HPLC = RDX concentrations by EPA Method 8260; IRMS1 = isotope-ratio mass spectrometry of RDX following GC separation; IRMS2 = isotope-ratio mass spectrometry of N_2O produced by bacterial reduction (8, 14, 67), with estimated uncertainties (1 sd) listed in the bottom row.

Strain	Sample	APTIM HPLC RDX µmol/L	UIC IRMS1 RDX $\delta^{15}N$ ‰	USGS IRMS2 $NO_{[3+2]}^-$ µmol/L	USGS IRMS2 $NO_{[3+2]}^-$ $\delta^{15}N$ ‰	USGS IRMS2 NO_2^- µmol/L	USGS IRMS2 NO_2^- $\delta^{15}N$ ‰	USGS IRMS2 NO_2^- $\delta^{18}O$ ‰
Aerobic								
DN22	B-1	97.8	8.2					
	B-2	97.4	8.3					
	B-3	89.2	10.9			12.4	*-5.6*	9.8
	B-4	73.1	9.5	26.9	5.2	29.4	*-2.9*	10.2
	B-5	60.4	10.3	51.4	3.9	41.6	*-7.0*	10.0
	B-6	48.2	10.9	53.1	-0.3	49.8	*-7.0*	9.6
	B-7	33.9	11.8	68.6	4.3	60.3	*-4.1*	10.5
	B-8	20.9	13.0	71.0	7.1	56.3	*-3.8*	10.8
	B-9	12.3	14.9	71.5	13.8	45.9	*2.3*	13.0
11Y	D-1	96.8	8.5					
	D-2	96.4	9.0					
	D-3	83.5	8.9	18.0	0.7	20.0	*-5.5*	9.5
	D-4	76.3	9.1	31.5	0.7	29.1	*-5.9*	9.7
	D-5	56.9	9.8	59.7	5.1	46.3	*-3.2*	10.9
	D-6	41.8	11.2	68.0	7.6	54.2	*-1.2*	12.2
	D-7	27.6	11.5	52.4	12.4	35.6	*0.0*	14.5
Anoxic								
Ps. putida	P2-1	85.3	8.3					
	P2-2	81.9	8.9	2.3		3.6		
	P2-3	77.4	11.1	7.1		12.3	-34.4	-8.7
	P2-4	70.4	11.1	19.1	-35.9	20.9	-36.2	-10.4
	P2-5	51.7	15.1	38.9	-34.4	42.7	-35.5	-9.5
	P2-6	26.7	24.2	59.6	-32.4	65.1	-32.4	-7.3
	P2-7	11.3	33.4	69.3	-29.7	77.1	-29.6	-5.2
	P2-8	8.7	41.5	76.7	-27.8	79.5	-27.5	-3.5
	P2-9	6.8	50.8	66.4	-24.6	75.0	-24.3	1.0
Ps. fluorescens	F1-1	87.5	12.1	2.2				
	F1-2	59.8	14.2	30.0	-40.1	31.3	-41.8	-16.6
	F1-3	50.0	17.4	38.9	-39.6	40.8	-41.2	-16.5
	F1-4	20.6	32.1	66.1	-35.6	69.8	-36.7	-12.5
	F1-5	16.8	33.5	64.7	-35.1	69.9	-36.0	-11.9
	F1-6	10.0	34.7	71.7	-32.7	74.4	-33.6	-10.1
	F1-7	4.2	50.1	85.4	-30.8	86.7	-31.4	-8.7
	F1-8	0.3	82.8	86.9	-29.0	88.9	-29.5	-6.7
Average Reproducibility				5-10%	0.6	5-10%	0.3	0.6

Italics indicate relatively large uncertainties for the aerobic $\delta^{15}N[NO_2^-]$ values (averaging ± 1.4 ‰).

Table B.2. Concentration and Isotopic Composition of Nitrate in Groundwater Samples from the Dahlgren Site (data used in Figure 5.23).

IC = nitrate concentrations by EPA Method 300; IRMS2 = isotope-ratio mass spectrometry of N_2O produced by bacterial reduction (14, 67), with estimated uncertainties (1 sd) listed in the bottom row.

Site ID	Collection date	APTIM IC NO_3^- µmol/L	USGS IRMS2 $NO_{[3+2]}^-$ µmol/L	USGS IRMS2 $NO_{[3+2]}^-$ $\delta^{15}N$ ‰	USGS IRMS2 $NO_{[3+2]}^-$ $\delta^{18}O$ ‰
CMOBOD02	10/10/2012	223	217	9.0	6.4
CMOBOD07	10/10/2012	38	38	11.2	6.5
Dahlgren-01	10/10/2012	188	196	12.8	8.2
Dahlgren-04	10/10/2012	201	204	9.8	9.3
EEA-17	10/11/2012	32	34	4.5	1.1
IW-1	10/12/2012	217	215	9.0	9.8
IW-8	10/10/2012	232	241	8.8	6.5
IW-15	10/12/2012	218	241	8.1	4.0
MW-1	10/12/2012	227	234	8.3	6.4
MW-2	10/12/2012	228	234	8.2	6.4
MW-3	10/12/2012	230	242	8.4	6.4
MW-4	10/12/2012	241	252	8.4	6.4
MW-5	10/12/2012	238	262	8.5	7.2
MW-6	10/12/2012	231	236	8.3	7.6
MW-7	10/12/2012	210	211	9.2	10.0
MW-8	10/12/2012	266	287	7.3	9.7
MW-9	10/12/2012	303	297	7.2	4.7
MW-10	10/12/2012	226	219	7.8	5.9
PZ-02	10/11/2012	70	69	31.9	18.5
PZ-17	10/11/2012	168	169	10.1	9.0
PZ-19	10/12/2012	265	287	8.0	5.0
PZ-20	10/11/2012	148	189	10.3	6.5
PZ-22	10/11/2012	236	237	8.5	5.9
PZ-30	10/12/2012	339	330	7.1	4.0
PZ-28	10/11/2012	403	392	7.0	4.5
Average Reproducibility			5-10 %	0.3	0.6